SCUOLA DI DOTTORATO
TERRA, AMBIENTE E BIODIVERSITÀ

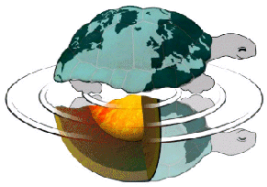

Dottorato di Ricerca in Scienze della Terra
Ciclo XXV

Contribution to the comprehension of climate change towards cryosphere and atmospheric analysis: the cases study of Changri Nup Glacier, Nepal Himalayas and of Forni Glacier, Italian Alps

Ph.D. Thesis

Elisa Maria Vuillermoz
Matricola R08741

Tutore	**Anno Accademico**	*Coordinatore*
Prof. Claudio Smiraglia	**2011-2012**	**Prof. Elisabetta Erba**

Co- Tutore
Prof. Guglielmina Diolaiuti
Dott. Paolo Bonasoni

Index

Abstract

In this PhD Thesis are reported the main results from an interdisciplinary research focused on evaluating impacts and effects of black carbon (BC) on glacier snow and ice melting. With this purpose we selected two glaciers: the Changri Nup glacier (Nepal, Himalaya) and the Forni glacier (Italian Alps). The glaciers have been chosen due to their representativity (geographical setting, size, morphology) and the availability of meteorological and energy data collected at the glacier surface through Automatic Weather Stations (AWSs).

In fact on both the glaciers AWSs have been installed in the recent years and they have been running without meaningful interruptions thus permitting to analyze glacier micrometeorology and to evaluate glacier surface energy balance and its variability (data are sampled with a hourly frequency all over the year). Moreover we planned and performed field campaigns to collect snow samples for describing chemical and physical features of soot and dust present in the glacier snow.

More precisely, since the Autumn 2005 and AWS has been running at the melting surface of the Forni Glacier (Italian Alps). The AWS is property of UNIMI and it attends the international network SHARE (Stations at High Altitude for Research on the Environment) promoted and managed by EVK2CNR Committee. Within the Ev-K2-CNR Project SHARE on February 2010 an AWS has been installed on the debris-free surface of the Changri Nup Glacier (Nepal, Himalayas, Sagarmatha Nationa Park) at 5,700 m asl to acquire meteorological data and energy fluxes (incoming and outgoing) at the glacier surface. The AWS is property of EvK2CNR Committee. The acquired data permit the calculation of glacier energy balance and high resolution analysis of glacier albedo. In the present study more than 85.000 meteorological parameters, related to the time window 2010-2012 and collected by The Changri Nup AWS, have been analyzed, processed and validated. Average daily parameters estimated at glacier surface have been: temperature: -4.61 °C, relative humidity: 78.47%, atmospheric pressure: 505.6 hPa, SWin: 220 W m^{-2}, SWout:136 W m^{-2}, LWin: 240 W m^{-2}, LWout: 280 W m^{-2}, wind speed: 1.48 m s^{-1}, prevalent wind direction: 183°.

Yearly albedo, deriving from SWout/SWin was 0.7, with an average of 0.75 for snow and 0.26 for glacier ice. Instead data from Forni AWS were already available thanks to another PhD research presently on line at the University of Milan.

Ablation season at the Changri Nup glacier occurred in summer period, in the monsoon season, when the temperature conditions (T>0°C) and radiation and rain precipitation increase the melting process. Results have been compared with the Alpine site of Forni glacier, the largest Italian valley glacier, located in the Stelvio National Park and characterized by a “strategic” location on the Central-Eastern Alpine sector, able to be reached by southern fluxes and close to the northern Alpine

Italian boundary. This part of the research was performed within the SHARE STELVIO project aiming at detecting and quantifying climate change evidences and effects on a sensible area located in the Stelvio National Park – Lombardy sector (600 km^2 of area). This project will permit to evaluate composition, quality and variability of high elevation atmosphere and effects on the alpine water resource (i.e. snow, glaciers and meltwater rivers).
In both sites the main component deterring melting are positive temperature and shortwave radiation, this latter higher in the Himalaya due to the difference of latitude, altitude and incident direction. Melting season in the Alps is longer than in the Himalaya and in both sites the effect of latent and sensible heat fluxes have a minor effect in driving melting processes. Both sites are characterized by a typical katabatic wind regime.

At the Changri Nup glacier surface some ablation stakes have been positioned in the debris free part of the glacier and two of these stakes were located nearby the AWS. Glacier ablation was evaluated through field campaigns twice: February-May 2010 and May-November 2012. The field data allowed to compare measured glacier ablation with melting amount derived from energy balance measurements and to evaluate the reliability of our computations.

It was found by previous authors that absorbing aerosols and dust play a key role in varying snow and ice albedo and in driving glacier ablation on several high elevation glaciers. In this study, by coupling energy data (from the AWS) with the atmospheric measurement of BC concentration allow the investigation of the relations among atmosphere and cryosphere and to quantify impacts of atmospheric black carbon deposition on glacial ablation rates.

In Himalaya atmospheric observations are carried out at the Nepal Climate Observatory-Pyramid (NCO-P) located at 5,079 m asl near the Pyramid Laboratory Observatory, while at Forni glacier a summer campaign has been held in 2012 at Guasti Hut (c. 3200 m asl).

Results at Changri Nup glacier were consistent with the typical estimation available in literature of BC deposition and % of albedo reduction in premonsoon season, where the atmospheric concentration are high. Experimental results reports that at Changri Nup the % of albedo reduction has been 4.26% for an estimated BC deposition in snow of 49 μg kg^{-1} consistent with the concentration range of BCC in snow of 26.0–68.2 μg kg−1 due to snow density variations between 195–512 kg m^{-3} as reported in literature.

The same estimation has been done at Forni Glacier too, but results were different because the summer BC monitoring campaign detected BC concentrations in the atmosphere typical of free troposphere background conditions, thus in the analyzed period, their deposition didn't have a predominant effect in driving melting process.

To compare the estimated BC deposition in snow deriving from atmospheric measurements, snow samples has been done at the Changri Nup glaciers and the chemical analysis allow to determine a typical premonsoon concentration consistent with literature data and with the experimental estimation done at Changri Nup glaciers.

Future step will foresee a further analysis of these results, thanks also to the availability of long term dataset, moreover, in order to improve the knowledge of the effect of dust and aerosol deposition on glacier, more samples will be collected and analyzed.

Chapter 1

Introduction

Significant orographic features occupy close to 25% of continental surfaces (Kapos et al., 2000) and although only about 26% of the world's population resides within mountains or in the foothills of the mountains (Meybeck et al., 2001), mountain-based resources indirectly provide sustenance for overhalf. Moreover, 40% of global population lives in the watersheds of rivers originating in various mountains of the world. Although mountains differ considerably from one region to another, one common characteristic is the complexity of their topography. Orographic features include some of the sharpest gradients found in continental areas. Related characteristics include rapid and systematic changes in climatic parameters, in particular temperature and precipitation, over very short distances (Becker &Bugmann, 1997). Since climate changes rapidly with height over relatively short horizontal distances, so do hydrology and vegetation (Whiteman, 2000). As a consequence, mountains exhibit high geo and bio diversities. As climate exerts a fundamental control on many biological, physical and chemical systems in mountains, it is of interest to assess here the climate-induced effects (Beniston, 2003). Since June 1992 the United Nations Environment and Development Conference (UNCED, Riode Janeiro) has included mountainous areas among the systems most sensible to climatic changes, and Chapter 13 of Agenda 21 states the importance of mountains in the global ecosystem.

The Alps, in particular, due to their geographical location and configuration, are interesting regions form any climate and environmental studies; these mountains, in fact, are at a “climatic crossroads" that include oceanic, continental, polar, Mediterranean and, on occasion, Saharan influences. Moreover the temperature change in the Alps is more marked than on a global or hemispheric scale. The warming experienced on the Alps since the early 1980s, while synchronous with warming at the global scale, is however of far greater amplitude, which represents roughly a two-fold amplification of the global climate signal (Diaz & Bradley, 1997).

Concerning Himalaya, glaciers therein represent, with the Karakoram and Pamir-Tian Shan ones, the largest ice masses outside the Polar regions (c. 33.000 km², Dyurgerov and Meier, 2005). Their runoff feeds major rivers (e.g. Indus, Ganges, Brahmaputra) whose tributaries deliver precious water for several hundred million people. Recent studies indicate that glaciers of south-eastern Tibet have negative mass balances (Aizen and Aizen, 1994), witnessing overall degradation of these glaciers as well. Ageta and Kadota (1992) suggested that small glaciers in the Nepal Himalaya and Tibetan Plateau would disappear in a few decades if air temperature persistently exceeds a few degrees above that required for an equilibrium state of mass balance. However, global warming should intensify the summer monsoon with consequent increased moisture fluxes, precipitation and cloudiness therein, which could end the rise of local air temperature, so still raising questions about the mechanism of air temperature-precipitation and glacier interaction, which requires further

scientific efforts (e.g. Aizen et al., 2002). Bethier et al. (2007), monitoring mass balances in the Spiti/Lahaul region (Himachal Pradesh, Western Himalaya) for the window 1999-2004, found on most glaciers clear thinning at low elevations, even on debris-covered tongues. They obtained a specific mass balance of -0.7 to -0.85m/year of water equivalent, twice as much as the long-term (1977 to 1999) mass balance record for Himalaya, with higher losses for glaciers larger than 30 km^2. The hydrological regimes of Himalayan rivers and potential impact of climate change therein have been hitherto assessed in a number of contribution in the scientific available literature (e.g. Aizen et al., 2002; Hannah et al, 2005). Economy of Himalayan regions is relying upon agriculture, and thus is highly dependent on water availability and irrigation systems (e.g. Snow and ice hydrology project, 1990; Akhtar et al., 2008). Over the last 30 years, a 10-25% increase in agricultural cover of the middle mountain area of Nepal has occurred (Collins et al., 1999). Consequently, water supply systems went under increasing pressure to meet the\rising demands of irrigation. Therefore, local authorities witness an upwelling need of tools for water resources management to effectively sustain agricultural politics (Chalise et al., 2003; Rees et al., 2006)and adaptation of food production and water allocation strategies to climate change. However, long term measurements of hydrological and climatological data of highest glacierized areas are seldom available (see Chalise et al., 2003), thus making assessment of hydro-climatic trends difficult to say the least. Seasonal snow cover dynamics in Himalaya is also tremendously important in regulating monsoonal season precipitation (e.g. Robock et al., 2003). Albeit such, comprehensive studies of snow cover patterns on Himalaya chain are still lacking (e.g. Immerzeel et al., 2009). Due to lack of long term series of climatic data, proxy data are used in some cases for identification of historical series, including e.g. dendro-chronological analysis of tree rings (e.g. Yadav et al., 2002), and modified frozen ground signature (e.g. Fukui et al., 2007 for an application on Khumbu glacier) for temperature and snow cores, for seasonal snow cover depth and chemistry estimation (e.g. Polesello et al., 2007, for a case study in Khumbu Valley).

As such, evaluation of the present conditions is important for assessment of water resource distribution, while future scenarios need to be worked out to develop new water management strategies. For this purpose, local evaluation of climatic trends coupled with scenarios from climatic models is used (e.g.Drogue et al., 2004; Kang & Ramirez, 2007) to provide the climatic input for medium to long term impact analysis on water resources (e.g. Beniston et al., 2003; Hagg and Braun, 2005) and hydrological extremes (e.g. Boroneant et al., 2006). Schneeberger et al. (2004) investigated mass balance for 11glaciers and 6 small glacierized areas worldwide, two of which in Swiss Alps (Arolla and Griesglaciers). In all cases, they found a strong decrease (i.e. water loss) in the net mass balance, due to decrease of snowfall precipitation, snow cover duration and, more importantly, to temperature rise. Bavay et al. (2009) preliminarily used climate change scenarios and a sophisticated model ALPINE 3Dto investigate the consequences of climate change (A2 and B2 scenarios of IPCC until year 2100) on the runoff of two snow fed watersheds of different size (Dischma Catchment, 43 km^2, Inn catchment,1945 km^2) in Swiss Alps, and found strong decrease of water storage in snow and shortening of snow cover in the whole range of altitude (1500 to 3200 m asl), with no continuous snow cover predicted. Also, they found considerably high winter runoff (up to twice as much as presently) and shortened spring flow seasons. Bultot et al. (1994) studied the Broye catchment (CH, 400 to 1500 m asl),predicting that, even for a rise in air temperature of about 1°C, snow cover duration and mean snow water equivalent on the ground during the first and last months of the snow season may sensibly decrease, while

trading of snow for rainfall due to temperature rise may generate additional floods during the winter season. Recently Akhtar et al. (2008) investigated hydrological conditions pending different climate change scenario for three glacierized watersheds in the Hindukush-Karakorum-Himalaya (Hunza, 13925 km^2, glacierized 4688 km^2; Gilgit, 12800 km^2, glacierized 915 km^2; Astore, 3750 km^2, glacierized 612 km^2). Future climate SRES A2 scenario (2071-2100) are simulated by a regional climate model (PRECIS, 25 by 25 km). Hydrological simulation of future conditions for three fixed stages of glacier coverage (100%, 50%, 0% of glacier area) is carried out in view of the largely unknown extent of glacier area and especially volume. Results indicate temperature and precipitation increase towards the end of 21st century, with discharges increasing for 100% and 50% glacier scenarios, whereas noticeable decrease is conjectured for 0% scenario, i.e. for depletion of ice caps. The authors suggest that transfer of climate change signals into hydrological changes is likely consistent. Immerzeel et al. (2009) studied the strongly snow fed Indus watershed (NW Himalaya, 200.677 km^2, including the Hunza and Gilgit basins) and found warming in all seasons, and greater at the highest altitudes, giving diminished snow fall, whereas total precipitation increases of 20% or so. Flow wise, they found snow melt peaks shifted up to one month earlier, increased glacial flow due to driving of temperature, and significant increase of rainfall runoff.

Observations on atmospheric composition and physico-chemical processes carried out at high altitude research stations are in fact being considered representative of a wide spatial area. These stations have a fundamental role in the detection of changing and damages of terrestrial ecosystem and environmental conditions (Wathne et al., 1993; Bonasoni, 2008). The analysis of atmospheric and cryospheric recent variations (last decade and present) in high altitude glacial areas allow to identify the connections between the to systems (atmosphere and cryosphere), contributing to the comprehension of recent atmospheric dynamics an their effects on glacier and water resources at local scale in the Himalayas, comparing the results with the Italian Alps.

1.1 Area of study

1.1.1 Sagarmatha National Park (SNP), Nepal

SNP (Fig .1) is located in the northeastern part of Nepal, amidst the world's highest peaks. The park encompasses extremely rugged terrain, deeply incised valleys, and glaciers; the elevation ranges from 2300 m (Surke villagein the Buffer Zone) to the summit of Mount Sagarmatha (Nepaliname of Mount Everest) at 8848 m. It spreads over a total area of about 1400 km^2, including the upper catchment of the Dudh Kosi River basin. Byers (2005) and Salerno et al (2008) have described the climatic and physical–chemical features of SNP, which are determined by the monsoon regime with most precipitation (70–80%) occurring between June and September. Although relatively small in size, SNP has abroad range of bioclimatic conditions, with 4 bioclimatic zones: a forested lower zone; a zone of alpine scrub; the upper alpine zone, which includes the upper limit of vegetation growth, and the Arctic zone, where no plant scan grow (United Nations Environment Programme [UNEP] and World Conservation Monitoring Centre[WCMC] 2008).

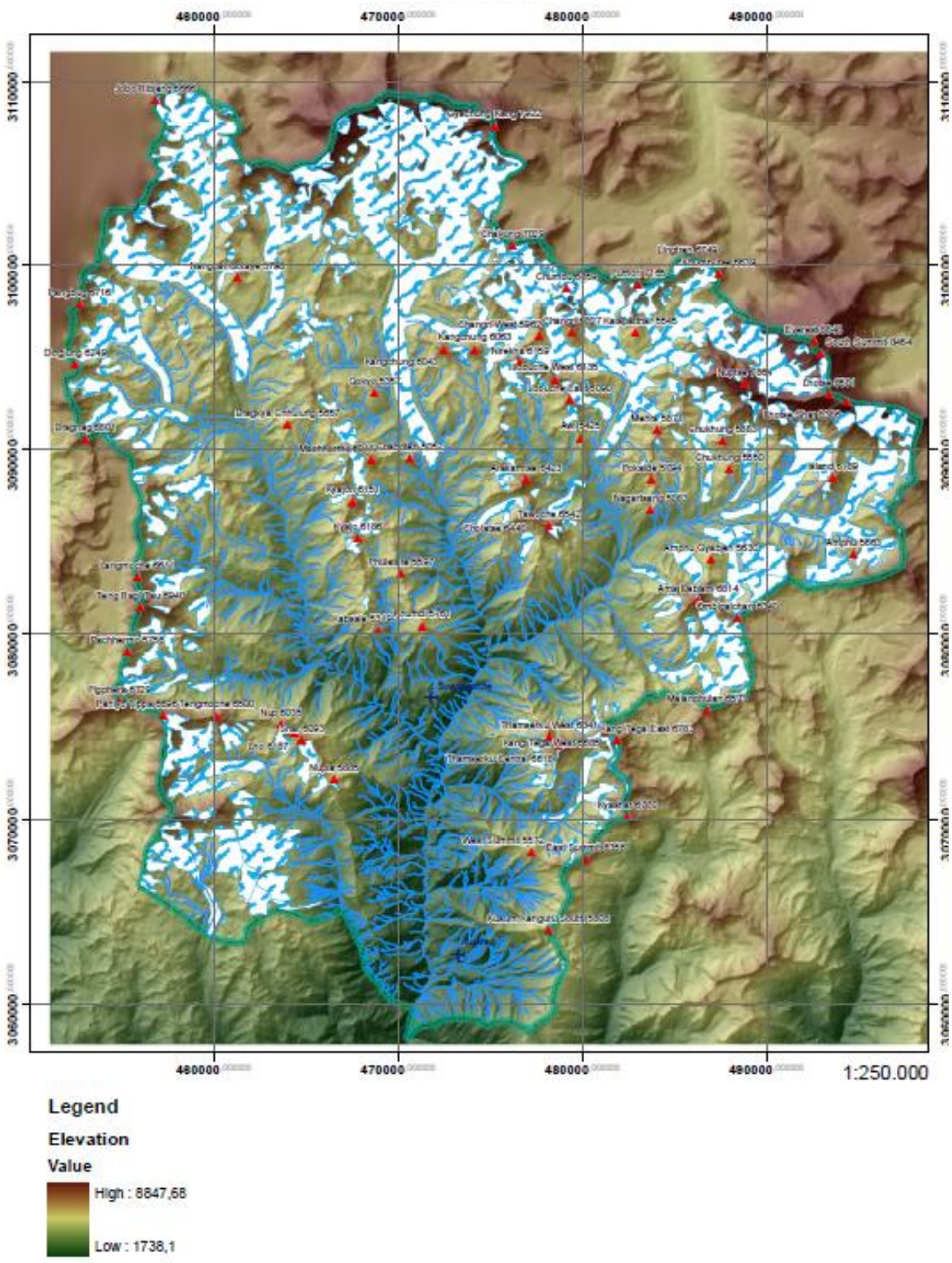

Figure 2. Sagarmatha National Park land Cover Map

Land cover (Fig. 2) classes for elevation ranges in SNP are summarized in Table 1, which shows that almost one third of the territory is characterized by snow and glaciers, while less than 10% of the park area is forested. In 2008, the park included about 100 settlements with 6221 local residents, mostly of the Sherpa people, with over 1892 head of livestock. Although in many villages, traditional agriculture and animal husbandry are still the main sources of livelihood, more recently the local economy has become dependent upon tourism and tourism-related activities (climbing, portering, guiding, and lodge management), which represent increasingly important employment sources for local communities (Department of National Park and Wildlife Conservation[DNPWC] 2003). Exceptional natural beauty and diversity in cultural and biological endowment dominated by Mount Everest make SNP a prime destination for nature- and adventure-loving tourists. The growth of mountaineering and trekking tourism since the 1970s has had a major influence on the social –economical system, often with a positive economic impact, providing tourism-related employment opportunities, but also causing landscape and cultural changes (Daconto and Sherpa 2010; DNPWC 2003). The number of international visitors reached 28,800 people in 2008 (Caroli 2008). The high influx of tourism puts an additional pressure on precious local resources, such as fuel wood, which remains the predominant source of energy for the majority of people in the park for cooking, boiling, and heating (DNPWC 2003) because it is relatively accessible and affordable, especially at lower altitudes. Overexploitation of forest resources is omnipresent in the region currently, but fuel wood is not produced adequately to meet the increasing demand for energy caused by a booming tourist industry and growing local population (UNEP and WCMC 2008). The limited supply of reliable and efficient energy has compelled a majority of the population to burn fuelwood, resulting in deforestation as well as indoor and ambient air pollution and health hazards (Pandey and Basnet 1987; Nepal 2008) (Salerno et al., 2010).

Table 1 Land cover classification by elevation zones in SNP. (Source: Bajracharya et al 2010)

Land cover (ASTER 2006)	Area per elevation zone (10^4 m^2)				Total area (10^4 m^2)	%
Class name	2000–3000	3000–4000	4000–5000	>5000		
Forest	2716	6677	386	0	9779	7.0
Shrub	353	3990	12,248	96	16,687	11.8
Grass	34	685	5800	1696	8215	5.8
Bare soil	210	567	19,714	41,094	61,585	43.7
Built-up area (including cultivated area)	308	375	259	0	942	0.7
Glacial lakes	0	0	429	393	822	0.6
Snow and glaciers	0	0	4600	38,189	42,789	30.4
Total					**140,819**	**100.0**

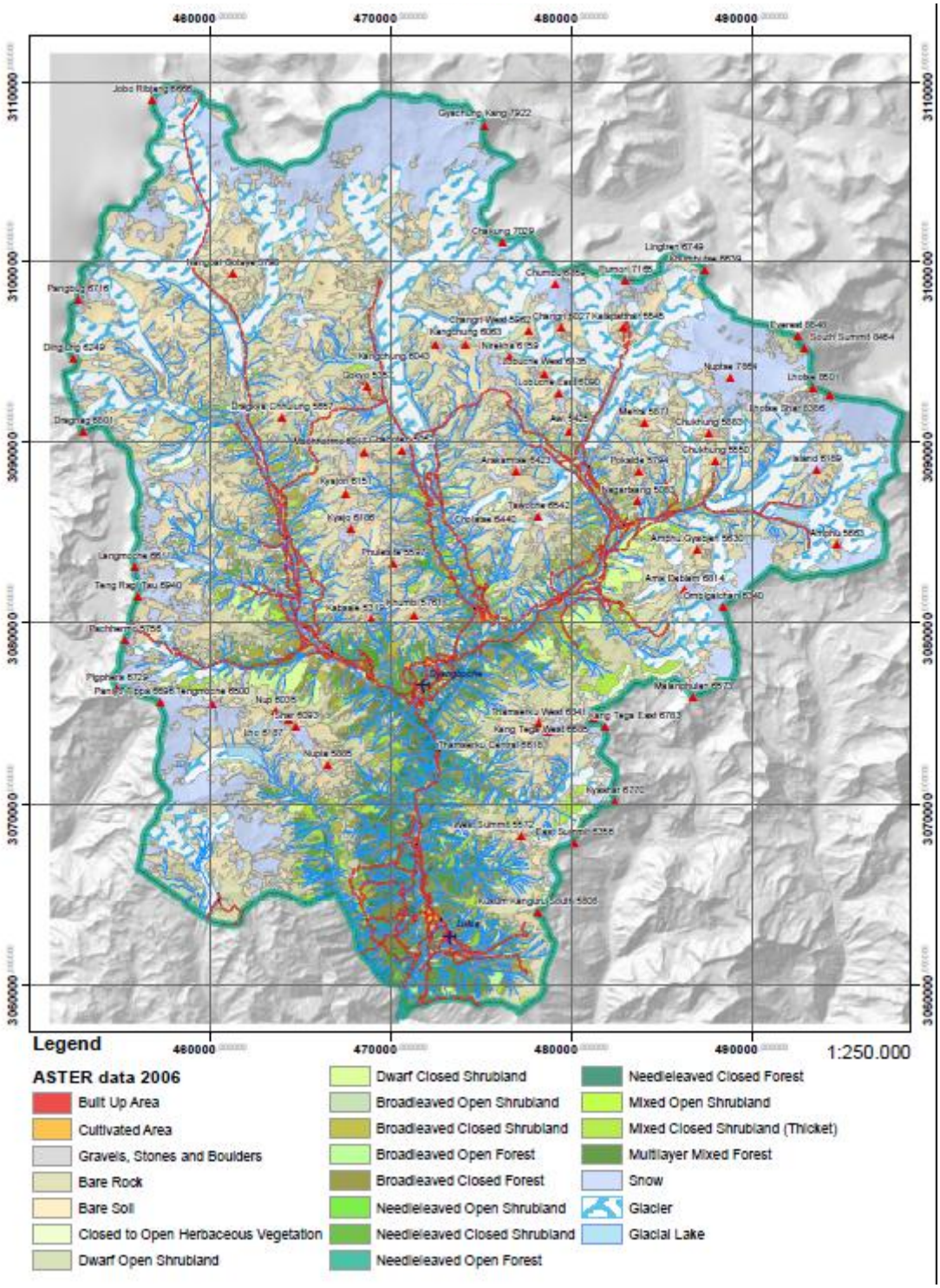

Figure 2. Sagarmatha National Park land Cover Map

1.1.2 Changri Nup Glacier

The Changri Nup Glacier is one of the tributaries of the larger Khumbu Glacier. It is located in the Sagarmatha National Park, in the Nepal Himalaya (Fig. 3). The glacier is oriented E-W (Fig. 4) and it is partially debris covered from the terminus until it reaches an altitude of about 5350 ma.s.l. From that elevation to the highest parts (5700 ma.s.l.) its surface is debris free. The debris cover on the glacier tongue varies in thickness between a few cm to 1-2 m. The glacier terminus is at an elevation of about 5200 m a.s.l. not far from the tongue of Khumbu glacier, on its right lateral side. The glacier area is about 8 km^2, whereas the mean glacier width is approximately 800 m. The accumulation area starts at an elevation of around 5400 m which leads to two separate accumulation basins. Only the north one resulted nowadays still contribution to the glacier flow .

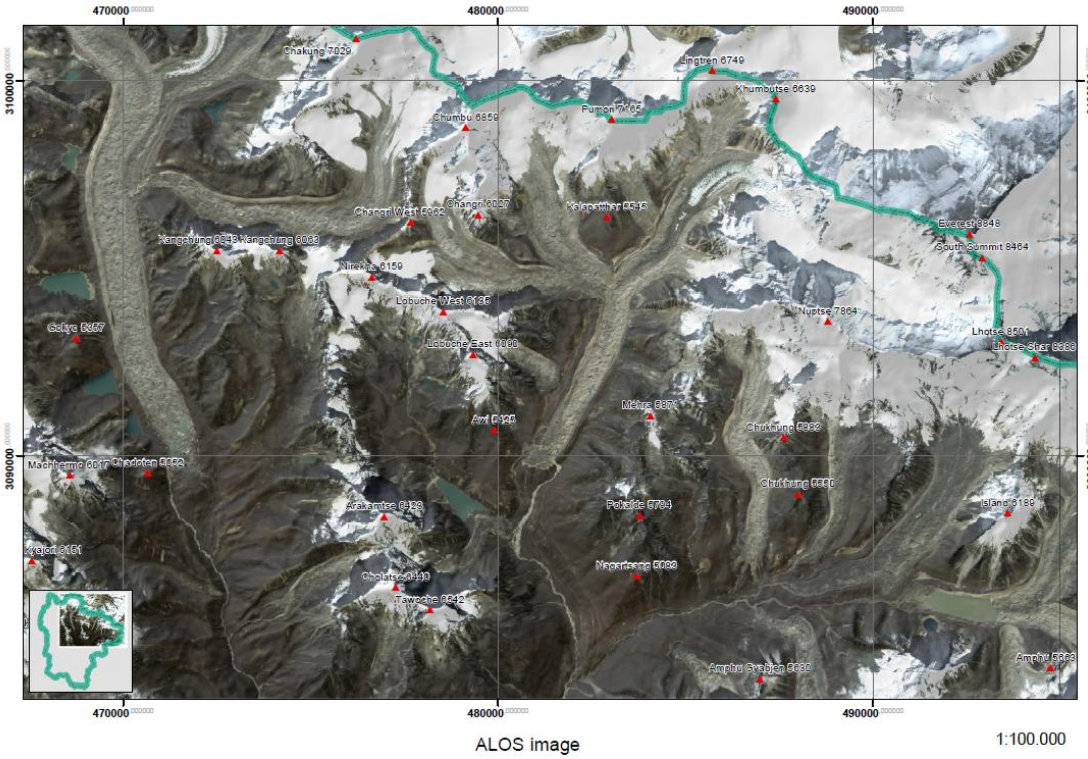

Figure 3. Location of Changri Nup respect to the SNP boarder

On its debris covered tongue several supraglacial lakes exist and the roughness is rather high (with elevation changes of 30-40 m on small distances due to differential ablation). .
Changri Nup Glacier is located not far away from the Ev-K2-CNR Pyramid Laboratory-Observatory (5050 m a.s.l.) (fig. 5) which allows frequent investigations and the rather easy implementation of different experiments (Smiraglia et al.; 2007).

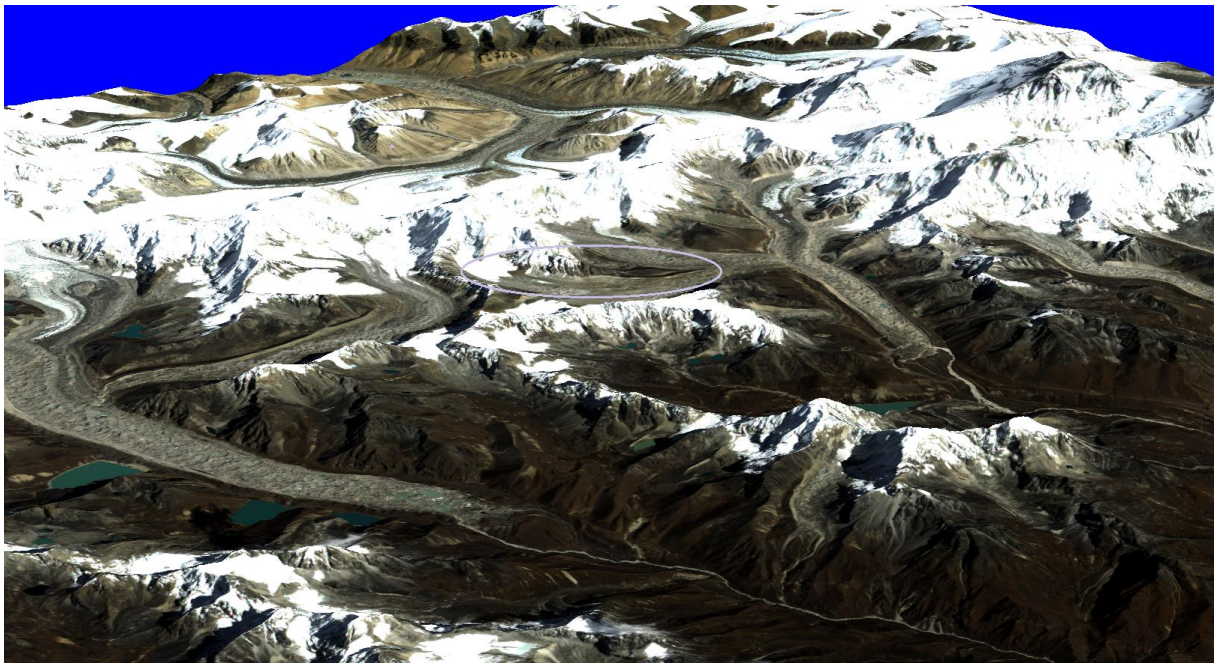

Figure 4; DEM of the Changri Nup Glacier area

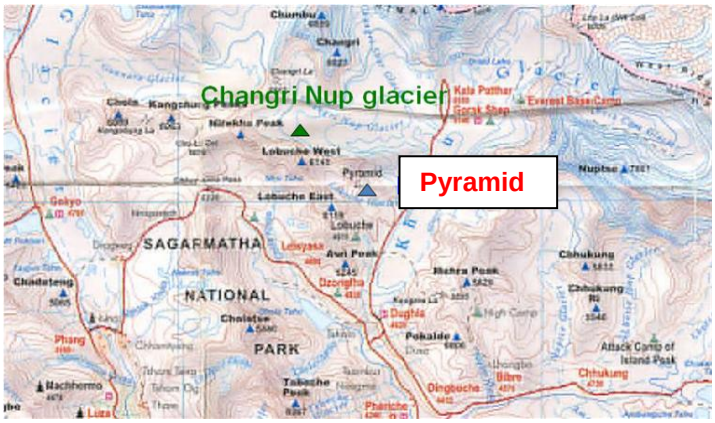

Figure 5. Location of the Changri Nup Glacier and the Ev-K2-CNR Pyramid Laboratory

1.1.3 The Forni Valley and the Forni Glacier

The Forni Valley (46_25N, 10_34E), is located in Upper Valtellina (Lombardy Alps, Italy) (Fig. 6).

Figure 6. Location of the Forni Glacier

The valley is dominated by the Forni Glacier, the largest Italian valley glacier (ca.12 km2 of surface area), in the Ortles-Cevedale group. The Forni Glacier is also located in a protected area, the Stelvio National Park, one of most important Italian protected area. The Forni Glacier lies on the northern slopes below Mt. S Matteo, at an elevation range between 3,670 and 2,600 m a.s.l. The glacier and the glacierized basin are identified as ‘‘Sites of Community Importance’’ (SCI) under directive 92/43/EEC and managed by the Stelvio National Park. The Forni Glacier has been visited for scientific and tourist purposes (e.g. Smiraglia 1984, 1985, 1989; Guglielmin and others1995; Diolaiuti and Smiraglia 2001b, 2010; Pelfini and Gobbi 2005; Pelfini 1987, 1996) since the middle of the 19th century, thus representing a strong element of the mountain landscape and environment for people at local and national level. More recently, the first supraglacial Automatic Weather Station (AWS) in the Italian Alps (Citterio and others 2007b; Senese and others 2012) was installed on its surface, thereby increasing the scientific value of the glacier.

The Forni Glacier is also included in the list of glaciers monitored by the Italian Glaciological Committee to evaluate changes in length (Comitato Glaciologico Italiano – CGI- 1914–1977, 1978–2011); moreover, from historic maps and aerial photos, its area coverage has been calculated for the last 150 years. The results show that the Forni Glacier has experienced a marked decrease in length and area: from 17.80 km^2 at the end of the Little Ice Age (LIA *1860) to 11.36 km2 in 2007 (-36.2 %). In the same time frame its tongue retreated by about 2 km (Fig. 7).

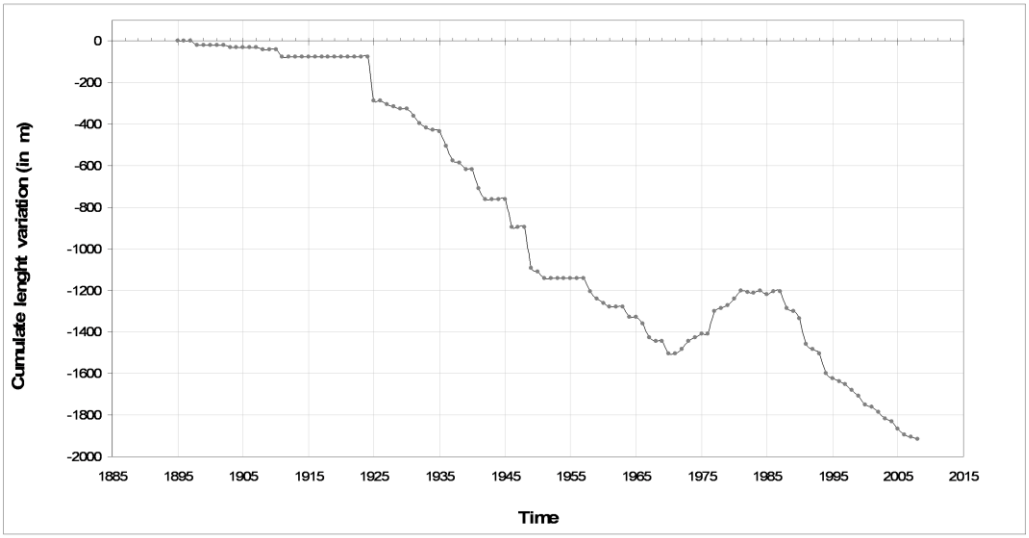

Figure 7: Cumulated length variations of the Forni Glacier (data from CGI data base)

Records for length variations in the Forni Glacier are among the longest standing in the Italian Alps, making Forni a benchmark glacier of primary importance. Fluctuation data for the glacier terminus show a basic retreating trend from 1895 to the present. A more detailed analysis of the front reveals a more complex picture, showing a strong retreat from the end of the LIA up to the seventies, then a small advancing phase up to the second half of the eighties, when glacier decrease again became dominant (Diolaiuti and Smiraglia 2010). The Forni glacier was also the scene of an important event in Italian history during the First World War, when battles were fought on the glacier surface and on the mountain ridges overlooking the glacier valley. These events and the remaining evidence, now revealed by the large quantity of ruins and finds present at the glacier surface, add a cultural value to the glacier. For all of the above reasons the Forni glacier was included in the Lombardy Region official Geosite List (Regione Lombardia 2009).

The Forni valley is characterized by easy accessibility, several climbing routes areavailable for climbers and expert alpinists. The huts are open in summer for tourists, trekkers and alpinists visiting the glacier area and in spring for skiers who enjoy the glacier snow and can reach the main peaks surrounding the Forni Glacier (Garavaglia et al., 2012).

1.2 Microclimate of glaciers

In spite of the oldest series of direct mass balance measurements in the world was from the Clariden firnin Switzerland (Vincent &*alii*, 2004) where observations have been carried out since 1914, the first studies performed to describe and analyze glacier microclimate started later, only after the second world war. At the end of the forties Ahlmann (1948) studied processes and mechanisms involved in the strong glacier reduction he observed around the North Atlantic Ocean. Moreover in the same period, a comprehensive study of water, ice and energy budgets was started on several glaciers in Oetztal, Austria, and greatly expanded during the International Hydrological Decade in the 1950s (Hoinkes&Untersteiner, 1952; Hoinkes,1955), during which several long-term mass balance series were initiated (Hoinkes&Steinacker, 1975; Reinwarth& Escher-Vetter, 1999).

Actual systematic investigations of the meteorological parameters on melting glaciers were performed only from the 1960s (Capello, 1959-1960; Björnsson, 1972; Wendler& Weller, 1974; Munro & Davies, 1978; Hogg &*alii*, 1982; Munro, 1989; Ohata&*alii*, 1989; Ishikawa &*alii*, 1992). These studies provided supraglacial meteorological data and energy fluxes measurements only for short periods (one or more ablation seasons) and only on accumulation basins: Hintereisferner, Austria (Van deWal et al, 1991), West-Greenland (Oerlemans&Vugts,1993), Pasterze, Austria (Greuell et al, 1997), Vatnajökull, Iceland (Oerlemans at al, 1999). The data obtained in these experiments have made clear that longer series of measurements from ablation zones are also needed.

Especially on larger glaciers, melting on the lower parts is not restricted to the summer season. A better calibration of mass balance models could be achieved if data over longer time periods would be available. Thus from 1987longer dataset are recorded on the melting zones of the Greenland ice-sheet, of Hardangerjokulen (Norway) and of Morteratschgletscher (Switzerland) (Oerlemans, 2000;Oerlemans&Klok, 2002; Klok&Oerlemans, 2004). Up to now the longest glacier data series is obtained from the Automatic Weather Station (from here AWS) located on the Morteratsch gletscher; due to the possibility of regular visits and to the favorable atmospheric conditions (little icing) a good quality meteorological data set is obtained during the last 2 decades (Oerlemans, 2001; 2009).

On short period melting areas also of debris covered glaciers were analyzed through AWS for evaluating energy fluxes and supraglacial meteorology features (see the experiment on the Miage debris covered glacier, Mont Blanc, Italian Alps, further details in Brock &*alii*, 2010).

After the recognizing of AWS importance, these stations have been deployed over a wide variety of glaciated surfaces (e.g. continental ice sheets, valley glaciers, sea ice and icebergs) and have a variety of applications, including climate variability assessment, in support of operational weather forecasting, model validation and in avalanche information support. AWS applications share a common challenge of obtaining continuous and reliable measurements both unattended and often in extreme environments. AWSs have facilitated growth in the branch of glacio-meteorology.

The collection of meteorological data recorded by permanent AWSs, in fact, is essential for measuring energy fluxes at the glacier-atmosphere interface and snow accumulation, for calculating the energy available for snow/ice melt, for the validation of mass balance models,

meteorological models (regional/mesoscale) and satellite products, for constructing parameterizations for energy balance models (Oerlemans&Vugts, 1993; Greuell&*alii*, 1997;Oerlemans & *alii*, 1999; Oerlemans, 2000; Klok&Oerlemans,2002; Oerlemans&Klok, 2002; De Ruyter de Wildt & *alii*, 2003; Klok & Oerlemans, 2004; Senese & *alii*, 2012).

The meteorological parameters are also fundamental to characterize glacier surface and sky conditions. For example albedo and cloudiness are the most important parameters that determine the amount of solar radiation adsorbed at the surface (apart from geometric effects like shading): at the glacier surface the solar radiation mainly drives ice and snow melt. From the incoming radiation the cloud conditions can normally be inferred qualitatively: days with overcast conditions are marked by lower values of incoming solar radiation and higher ones of incoming longwave radiation. In fact, clouds and water vapor make the atmospheric emissivity larger. On the contrary glacier outgoing longwave radiation shows less pronounced variations.

1.3 Atmospheric Black Carbon and its deposition on snow/ice surface

The transport of atmospheric pollutants can significantly impact high mountain areas and glaciers, which are generally considered "clean" regions. An important component of such atmospheric pollution is black carbon (BC), also called "soot",an aerosol produced by the incomplete combustion of biomass (e.g. wood, dung, crop residue, wild fire,etc.), coal and fossil fuels (e.g. petroleum, diesel, charcoal, and etc.) and able to contribute to climate change by altering the Earth's radiative balance (Andreae and Crutzen,1997). Atmospheric BC has a significant impact on the earth's climate (IPCC, 2007), scattering and absorbing the incoming and outcoming solar radiation. Once deposited onto snow-surface in the cryosphere, BC can considerably reduce the surface albedo, (e.g., Warren and Wiscombe, 1980; Aoki et al., 2006, 2007). The impurity effect on snow albedo reduction is more important for visible wavelength than that for near infrared radiation (e.g., Warren and Wiscombe, 1980; Flanner et al., 2009). possibly resulting in increased glacier retreat and earlier seasonal snowpack melt and therefore impacting water re-sources, agriculture, and human health. Knowledge of BC concentrations and variability in high mountain regions and deposition on glaciers is therefore essential to evaluate the impacts of pollutants on the environment.

Due to the large amount of absorbing aerosols present in the Atmospheric Brown Cloud (Ramanathan et al., 2008), these aerosols may be directly warming the atmosphere in the Indian-monsoon region. Lau et al. (2006, 2008), proposed the so-called Elevated Heat Pump (EHP) effect, whereby heating of the atmosphere by elevated absorbing aerosols strengthens local atmospheric circulation, leading to a northward shift of the monsoon rain belt, resulting in increased rainfall in northern Indian and the foothills of the Himalayas in the late boreal spring and early summer season. More recently, Lau et al. (2010) showed that the EHP effect can also lead to accelerated melting of snow cover in the Himalayas and Tibetan Plateau, by a transfer of energy from the upper troposphere to the land surface over Tibetan Plateau.

In recent years, a highlight on BC's climatic effects is drawing more and more attention from scientists, i.e. BC deposited in the surfaces of snow and ice (e.g. snowpack, glacier, ice sheet, sea ice, and etc.) (Fig. 10) could enhance solar radiation absorption, reduce the albedos intensively, and thus accelerate the melting of ice (Ming et al., 2009). It was found that a concentration of 15 μg kg−1 of BC in snow may reduce the snow albedo by ~1% (Light et al. 1998) calculated that 150 μg kg^{-1} of BC embedded in sea ice could reduce the albedo of sea ice by ~30% at its maximum. Hansen and Nazarenko (2004) used a model (GISSE) to simulate the solar absorption of BC in snow and ice, suggesting it may be responsible for ~0.17 °C of the observed global warming in the past century (accounting for ~25% of the 20th-centurywarming); for the same purpose, Jacobson (2004) used a different model (GATOR-GCMOM) to calculate the global warming caused by BC in snow and ice, suggesting the global mean of BC concentrations in snow and ice was ~5 μg kg^{-1} and this level of concentration could reduce the albedos of snow and sea ice by ~0.4% and thus could contribute the global warmingby +0.06 °C per decade. IPCC Fourth Assessment Report: Climate Change (IPCC AR4, 2007) reported the radiative forcing caused by BC in snow and ice was 0.10±0.10 W m^{-2} of global mean. And a new result from another model (SNICAR)revealed from1906 to 1910 when the maximum BC concentration appeared in an Arctic ice core, estimated surface climate forcing in early summer from BC in Arctic snow was ~3Wm^{-2},whichwas eight times of the typical preindustrial forcing value (McConnell et

al., 2007). Using the same model, a north hemisphere-based simulation suggested the greatest instantaneous forcing by BC in snow appeared on the Tibetan Plateau (TP), exceeding 20Wm^{-2} in some places during spring (Flanneret al., 2009); in particular, the mean forcing by BC deposited in the ice of the middle Himalayas exceeded 2 W m^{-2} after 2000(Ming et al., 2008). These results indicated the solar absorption by BC in snow and ice on the Tibetan Plateau might have significant impact on the mass balance of the glaciers. Neighboring west China, there are two strong BC-emitting regions, South Asia and East Asia, respectively (Bond et al., 2007).This effect increases heating of the snow and ice surface, thus accelerating melting, shortening snow duration, altering mass balance and causing the retreat of mountain glaciers. These physical activities change the amount of available water resource in the region (e.g., Hansen and Nazarenko, 2004;IPCC, 2007; Flanner et al., 2007, 2009).

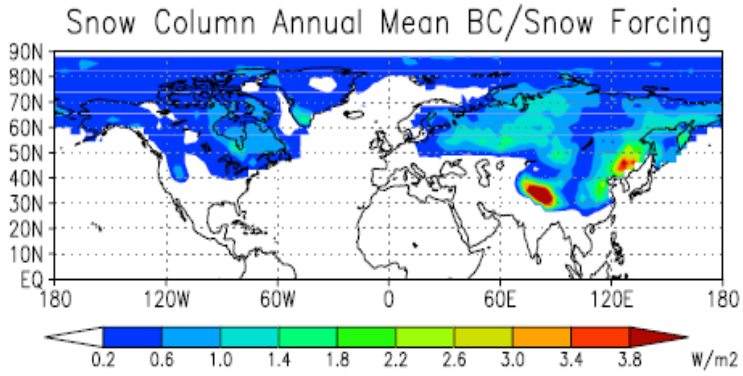

Figure 9: Surface forcing (W m^{-2}) from BC in snow

The southern slope of the Himalaya is directly exposed to Indian emissions and more likely to be impacted by BC than the northern slope. However, the available data of black carbon concentrations in atmosphere and BC deposition (BCD), for studying snow albedo reduction at the southern slopes in Himalayan regions, are still very scarce. Moreover, only a few BC concentrations (BCC) and morphological properties in the snow and ice cores, in the northernslopes of the Himalayan and Tibetan Plateau regions, have been measured thus far (Ming et al.,2008, 2009). Studies on BC concentration in snowpack at the southern slope in Himalayas are less. In addition, glaciers in Himalayas are located in severe topography. Consequently, logistic constraints have severely limited data availability on snow and ice composition, as wellas atmospheric composition observations. Hence, an alternative approach to estimating BCD over Himalayan glaciers is necessary for understanding the impact of BCD on melting glaciers (Yasunari at al., 2010).

Atmospheric data of equivalent BC concentration(eq BCC), aerosol particle number concentration and size distribution, as well as meteorological parameters, are continuously measured at the Nepal Climate Observatory– Pyramid (NCO-P, 5079 a.s.l.) on Southern slope of the Himalayans since 2006 (Bonasoni et al., 2008, 2010) (Fig. 9). The NCO-P is the highest aerosol observatory managed within the Ev-K2-CNR Stations at High Altitude for Research on the Environment (SHARE) and the United Nations Environmental Program (UNEP) Atmospheric Brown Clouds (ABC) projects. This station was established in March 2006 for atmospheric research in the Khumbu Valley, Sagarmatha National Park, near the base of the Nepalese side of Mt. Everest (5079 ma.s.l.) (http://evk2.isac.cnr.it/).In July 2010 the NCO-P was upgraded to Global Atmospheric Watch Global Station in the framework of WMO program. Because high altitude measurement sites are relatively clean and far from

anthropogenic emission sources, they offer an opportunity to study the influence of anthropogenic pollution transported from remote areas. The Indian sub-continent, especially the Indo-Gangetic Plain is one of the largest BC emission sources in the world (Ramanathan et al., 2007) and it is in the vicinity of the Himalayan glaciers. Preliminary work of Bonasoni et al. (2008)has found very elevated eq BCC under different meteorological conditions, with well defined seasonality showing a maximum in pre-monsoon season (Marinoni et al., 2010).

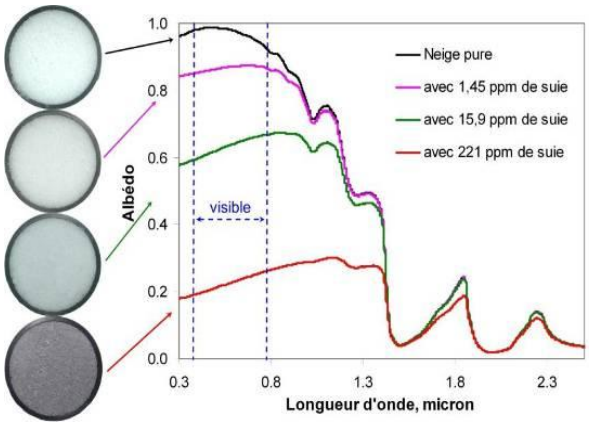

Figure10: Albedo variability as a function of BC (Courtesy of F. Dominé, LGGE)

Chapter 2

Material & Methods

2.1 Meterology

On February 2010 an Automatic Weather Stations (AWS) (Tab. 2) has been installed on the debris-free surface of the Changri Nup Glacier (Nepal, Himalayas) at 5,700 m asl (N 27°58'54''.5 ; E 86°45'53''.8) (Smiraglia et al.; 2007). During the field campaign, ablation stakes have been positioned and snow sampling have been carried out. The AWS is acquiring continuously meteorological data and energy fluxes (incoming and outgoing) at the glacier surface. The data will permit the calculation of the glacier energy balance and the high resolution analysis of surface albedo (snow or ice). Obtained results would be correlated with the atmospheric observations carried out at the Nepal Climate Observatory-Pyramid (NCO-P) located at 5,079 m asl, 5.7 km away, near the Pyramid Laboratory Observatory and part of UNEP-ABC and WMO-GAW networks.

The first Italian permanent glacial AWS (Tab.2) , installed in 2005 by the University of Milan, in collaboration with Ev-K2-CNR is fundamental to analyze the atmospheric boundary layer characteristics to quantify energy fluxes on the ice-atmospheric interface and to calculate energy and mass balance. The AWS1 Forni (46°23'56.0" N,10°35'25.2" E), ca. 2700 m, is located on the lower glacier sector, about 800 m far from the glacier front (Citterio et al., 2007). From 2009 the AWS was inserted in the CEOP network in the frame of the GEWEX project. Data analyses permitted to characterise the glacier surface conditions, the calculation of the energy balance and the evaluation of the ablation amount; moreover snow accumulation was considered thus permitting to estimate the glacier mass balance. Both stations measure continuously every 30 minutes temperature, relative humidity, atmospheric pressure, wind speed and direction, solar radiation and at present only in the Italian site, snow level too.

Table 2: measurements at Forni and Changri Nup AWSs

PARAMETER	AWS FORNI	AWS CHANGRI NUP
Air temperature		
Relative humidity		
Wind speed		
Wind direction		
Atmospheric pressure		*To be installed*
Incoming Shortwave Radiation		
Outgoing Shortwave Radiation		
Incoming Longwave Radiation		
Outgoing Longwave Radiation		
Total precipitation		
Snow level		*To be installed*

Data points, sampled at 60-second intervals and averaged over a 30-minute time period for most of the sensors, are recorded in the flash memory card, together with basic distribution parameters (maximum, minimum and standard deviation values). Wind data are sampled every 5 seconds, and then processed by the data-logger software, which produces an hourly set of information, including minimum, maximum and average speed, dominant wind direction and statistics on the azimuth sectors. This information is stored in the flash memory. Prior to storage in the memory, the raw analog and digital signals are converted by the data logger into the corresponding physical values by applying programmed calibration factors or tables. Basic validation checks such as out-of-range values and cable connection defects are also run by the data logger, and any error codes are saved in the flash memory card. However, most calculations involving data from more than one sensor, such as sound speed corrections for air temperature in snow level measurements or radiometer temperatures for infrared radiation must be carried out later through the following equation:

$$LW+5{,}67*(10^{-8})*(T_{CNR1}+273{,}15)^4$$

Where LW is the raw measured data and T_{CNR1} is the net radiometer sensor temperature

At Forni Glacier, snow accumulation on the sky facing radiometers has been detected in the recorded data, which needs to be carefully filtered for such occurrences.

Pressure sensor was not available at Changri Nup AWS, thus Atmospheric Pressure data have been derived from Kala Patther AWS, located at 5.600 m asl,near the Everest Base Camp according to the following ipsometric formula (Wallace and Hobbs, 2006):

$$p2=p1\ exp\text{-}(Z2\text{-}Z1/H)$$

Where :
p2=Pressure Changri
p1= Pressure Kala Patthar

Z2=Elevation Changri AWS
Z1= Elevation Khala Pattar AWS

H=scale height (29.3 Tv)

Tv= Virtual temperature → *tv=t/(1-(e/p)*0.622);*

t= Kala Pattar AWS temperature
e=water vapour pressure estimated as → *e=exp(20.386-5132(kelvin)/t);*

Kala Patther temperature has been used as Tv for a major accuracy. Normally Tv should be integrated in the whole atmospheric layer dividing Kalpatthar AWS from Changri Nup AWS, but in this case Tv has been approximated and considered as constant in the atmospheric layer dividing Kala Patthar and Chanfri Nup AWS.

2.2 Radiation

To calculate the surface energy balance, the 30-min radiation data were analyzed. At the glacier surface, solar radiation is the most important energy balance component driving ice and snow melt. Therefore the albedo (from here α) is an important and noteworthy parameter of glacier surface to be analyzed in terms of temporal variability.

Firstly we filtered the incoming and outgoing shortwave radiation data (SWin and SWout, respectively) in order to remove erroneous values (e.g.: after a snow fall event, values showing SWout exceeding SWin due to the presence of fresh snow on the top pyranometer); then the following relation was applied:

$$\alpha = SW_{out} * SW_{in}^{-1}$$

The incoming and outgoing longwave radiation (LWin and LWout, respectively), were measured by the CNR1 pyrgeometers. The acquired data represent the flux at each sensor surface, and the values have been converted to the ground and atmospheric (upward and downward) directional flux by Stephan-Boltzmann's law.

2.3 Turbulent fluxes

Because measurements are available for one level only, no attempt was made to use sophisticated schemes for the calculation of the turbulent heat fluxes. Instead the well-known bulk aerodynamic formulas were used according to the methods introduced by Oerlemans (2000):

$$SH = r_a * c_p * C_h * V_{2m} * (T_{2m} - T_S)$$

$$LE = 0.622 * r_a * L_v * C_h * V_{2m} * (e_{2m} - e_S) * p^{-1}$$

where ra is air density (0.87 kg m-3), cp is the specific heat of dry air (1.006 kJ kg-1 °C-1), Ch is the turbulent exchange coefficient (0.00127 ± 0.00030; from Oerlemans, 2000), V2m is wind speed value at 2 m, T2m is air temperature value at 2 m, TS is the surface temperature, Lv is the latent heat of vaporization (Harrison, 1963), e2m is vapor pressure value at 2 m, eS is vapor pressure value at the surface (calculated using the Wexler formula; Wexler, 1976) and p is air pressure value at sensor level. The TS is calculated by using the Stephan-Boltzmann law: TS=4√(LWout * σ-1 * ε-1), where σ is the Stephan-Boltzmann constant, 5.67 * 10-8 W m-2 K-4 and ε is the emissivity of the snow/ice surface, assumed to be equal to the unity. Wind speed is measured at 5 m thus it has been calculated at 2 m (following the method introduced by Oerlemans, 2000). At this stage the Ch is assumed to be constant, (Oerlemans and Klok, 2002).

2.4 Surface energy balance

To calculate the glacier energy balance components, we applied the following methods by considering the 30-min meteorological values.

The energy balance at the glacier surface (RS) determines the net energy available for heating and melting. RS was calculated as

$$RS = SWnet + LWnet + SH + LE$$

All the fluxes (W m^{-2}) were defined positive when directed towards the surface. The conductive heat flux at the surface was neglected since no temperature sensors were located in the snowpack and in the ice surface layer. During the ablation season, when melting occurs and surface ice temperature is ~0°C, at the glacier surface all the energy is used to melt the ice. Consequently the conductive heat flux at the surface is equal to zero thus permitting to calculate RS without considering the conductive heat flux. Differently, when the glacier surface is not at the melting point and RS is lower than 0 W m^{-2}, the surface cools and the conductive heat flux value is not equal to zero and has to be evaluated. In our study, neglecting the conductive heat flux at the surface, is resulting in a slight overestimation of ice melting.

2.5 Monitoring of Black Carbon (BC) concentrations in the atmosphere

BC concentration are monitored continuously at NCO-P (Nepal Climate Observatory at Pyramid) station, the UNEP-ABC and WMO-GAW observatory installed in February 2006 (Fig. 11).

The station measured aerosol concentration and size distribution, aerosol optical properties, ozone, halogenated compounds. BC concentration in particular are monitored through the Multi Angle Absorption Photometer (MAAP). Collected data are sent to the CNR-Institute of Atmospheric Science and Climate of Bologna in real time through satellite connection.

Figure 11: The NCO-P Station and the aethalometer for BC monitoring

2.5 Snow sampling procedure at Changri Nup Glacier

Snow samples, which are planned to be acquired periodically, to understand seasonal behaviour and through intensive field campaign to estimate aerosol deposition rate, will be analyzed to quantify the presence of atmospheric absorbing aerosols (e.g. black carbon, soil dust). In fact, this latter was found to play a key role in varying snow and ice albedo and in driving glacier ablations on several high elevation Himalayan and Alpine glaciers. In this experiment, by coupling energy data (from the AWS) with the results from snow sample chemical analysis, will be possible to investigate the relations between atmosphere and cryosphere and to quantify the impacts, if any, of atmospheric dust and/or black carbon deposition on the Changri Nup and Forni Glaciers ablation rates.

Snow sampling should take place at each snow fall and durng each periodical fiels visit to the monitoring sites. 3 samples should be collected (2 glass jars (Schott) of 100mL and 1 glass jar of 500 ml).

The bottles have been preconditioned at the Laboratoire di Glaciologie et Géophysique de l'Environnemenmt - LGGE - in Grenoble (cleaned and dried) and packed into sealed plastic bags. The snow collection is very very sensitive to contamination, and the following procedure should be followed very attentively:

Needed equipments:

- One bag with a 500mL bottle
- One bag with 2 bottles of 100mL
- One-Two pair(s) of gloves
- Two ziplocks to place the label papers inside
- One large bag (sealed on one side)
- Some rubber bands
- The Teflon scraper

Arriving at one site, the operator should:

- Put on the pair of new disposable plastic gloves
- Open the bags of the individual bottles (using a knife) (1 bottle of 500 mL and 2 bottles of 100mL)
- Collect the snow sample with the operator always staying with the wind coming from face. The collection of the snow should take place by scraping de surface with the teflon scraper. The depth of collection should only be on the first 5 cm of the upper snow layer, and care should be taken to collect a single layer. Try to take as much snow as possible by knocking the back of the bottle to compact the snow in it. Recap the bottle tightly.
- Write the date and place of collect on the label, and place the label in a ziplock. Does that twice.
- After sampling, put the bottles back in their original bags and place in each bag a ziplock with the label; close each one with one of the rubber bands.

» Place the 3 bottles in the large bag, and close it also with a rubber band. Remove your gloves and dispose them.

Samples are preserved frozen until their arrival to the analytical laboratory (Kaspari, et al. in press). Chemical analysis will allow the determination of the contents of aerosol derived absorbing material through SP2 (Single Particle Soot Photometer).

2.5 Debris cover quantification

The quantification of presence and coverage of supraglacial sparse fine debris was performed by acquiring high resolution digital photos at each site we analyzed and processing them with a freeware software following the method proposed by Irvine-Fynn et al. (2010) who quantified cryoconite features. Digital imagines were taken, after the albedo measurements, in the central hours of the two days of surveys, when the sun was at its Zenith. At the studied parcels, 1 x 1 m wide, digital RGB (red-green-blue) imagines were acquired using a digital camera (Nikon D40, 6.1 megapixel). Image analysis was carried out with the public domain image-processing software ImageJ (http://rsbweb.nih.gov/ij/index.html). Firstly, in each image the area enclosed in a parcel 1 m^2 wide was blanked. After converting the pictures to 8 bit greyscale for highlighting the contrast between glacier ice and debris/dust, a characteristic threshold was fixed to discriminate between the debris-covered and debris-free ice surfaces. An 8 bit image is composed by 254 grey's tone included from 0 (i.e., black) to 255 (i.e., white) and ice surface could be isolated by selecting the pixels with brightness values higher than a specified threshold level; for instance, if the threshold is fixed at 100, pixels with a grey's tone from 0 to 100 represent debris, vice versa pixels with a grey's tone from 101 to 255 represent ice. Finally, for each image the number of pixels with a value lower than the threshold was calculated with the *measure* function of the software obtaining the percentage of the surface covered by debris.

Chapter 3

Results

3.1 Meteorological characterization

The Himalayan high-altitude climate is intensely characterized by its relationship with large scale circulation, and strongly dominated by the diurnal cycle of thermal parameters. In fact, at the Nepal Climate Observatory – Pyramid (NCO-P), the seasonal variation of atmospheric conditions is influenced both by the local mountain wind system (with a strong diurnal valley wind and a weak mountain night-breeze), and by the large-scale Asian monsoon circulation. In particular, besides determining the seasonal variations of the meteorological parameters, the annual variations of the main synoptic circulation can also modulate their diurnal cycles characterizing the local mountain weather regime (Bonasoni et al., 2010).

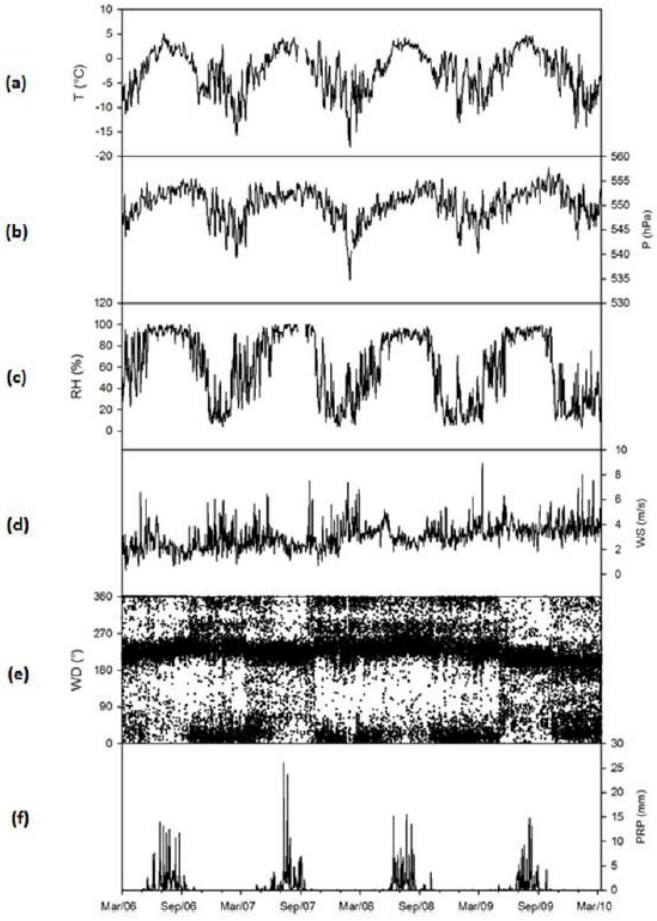

Figure 11: Daily mean values of the main meteorological parameters registered at NCO-P from March 2006 to March 2010: Temperature (a), Atmospheric Pressure(b), Relative Humidity (c), Wind Speed (d), wind direction (e), total precipitation (f) (Bonasoni et al., 2010)

The temperature behaviour registered at NCO-P in the four year period 2006-2010 (Fig. 11a, average value = -2.6°C) is characterized by lower values during the pre-monsoon period (daily average value: −5.5 °C) than those recorded during the summer monsoon season (daily average value of 1.5 °C) that is also characterized by a lower diurnal variation due to the frequently cloudy conditions occurring at the measurement site (Bollasina et al., 2002).Atmospheric pressure (Fig. 11b) is characterized by higher values(daily mean: 552.3 hPa) between June and July and lower values (daily mean:548.1hPa) between November and March. During pre-monsoon pressure showed a much greater variability with some rapid variations recorded in connection with the passage of synoptic. Relative humidity (Fig, 11c) shows a seasonal cycle with higher value (daily mean: 91.7%)between the end of May and the end of September and lower values (daily mean: 22.5%)from the end of November and January/February while during pre-monsoon, can decreased to a small percent. Relative humidity data allow the determination of the seasonal transition period.

Wind speed (Fig. 11d) shows mean values in the period of 3.0 m s-1 while wind direction (Fig. 11e) is characterized by a bimodal distribution due to the configuration of the Valley, oriented in North East – South West direction and by the presence of an evident mountain – valley breeze regime (Bollasina et al., 2002).From October to May valley wind prevail during the day, while mountain wind during the night. In summer monsoon period, due to the effect of South-East Asian monsoon synoptic circulation (Ueno et al., 2008),valley wind are predominant during nighttime too.

Total precipitation at NCO-P (Fig. 11e) is governed by the Himalayan monsoon regime, and precipitation days are concentrated from June to September, reaching the maximum values in August. Monsoon precipitations were characterized by light showers or drizzles while only sporadic events with heavier rain(>10 mm/day) were detected even if such values could be underestimated due to the loss of snowfall that would also explain the absence of any signal of precipitation from November to April, when air temperatures below 0 °C characterized the 92% of observations. The identification of the onset and decay of monsoon season at NCO-P (Tab. 3) has been defined taking in account the meteorological regime variation (Bonasoni et al., 2010),considering in particular relative humidity and wind direction data at NCO-P station. The monsoon season has been identified as the period characterized by high persistent humidity levels (never under 70%) and the presence at the measurement site of southerly wind, also during night-time (Ueno et al., 2008).In fact, in the Southern Himalayas significant changes in mountain weather regime, due to the summer onset of the large scale southern monsoon circulation, strongly anticipate the precipitation onset, as showed by Ueno et al. (2008) and Barros and Lang (2003). Winter season has been identified when daily relative humidity values never exceeded 70%, and northerly mountain winds were well established during night-time. The two remaining period of the year are defined on the basis of the monsoon season and are indicated as pre-monsoon and post-monsoon period.

Table 3: Onset and decay of monsoon season in the period 2010-2012 from NCO-P station data

Year	Starting Date	Ending Date
2010	May 6	September 24
2011	June 14	September 27
2012	June 17	September 20

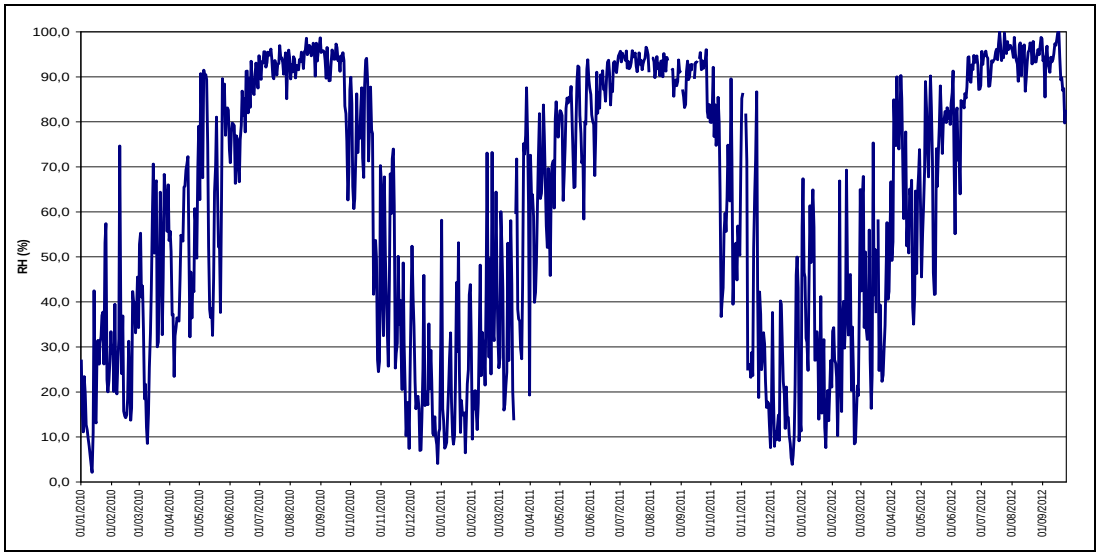

Figure 12:Relative Humidity at the Nepal Climate Observatory at Pyramid in the period 2010-2012

Monsoon onset and decay, as reported in table 3, are shown in figure 12 where the trend of relative humidity is characterized by a marked seasonality with lowest values in winter (dry period) and higher values in summer (monsoon season).

Relative humidity sensor at Changri Nup AWS show a malfunctioning from September 2010, for this reason Changri Nup relative Humidity data from February to September 2010 have been correlated with the AWS installed at 5.600 at Kala Patthar, close to the Mt. Everest Base Camp and located at similar altitude of Changri Nup station.

The correlation is reported in figure 13, and has been done considering the data from 0 to 85%, in order to minimize the instrumental problem in measuring relative humidity levels close to the saturation (instrument data sheet, LSI Lastem 2010)

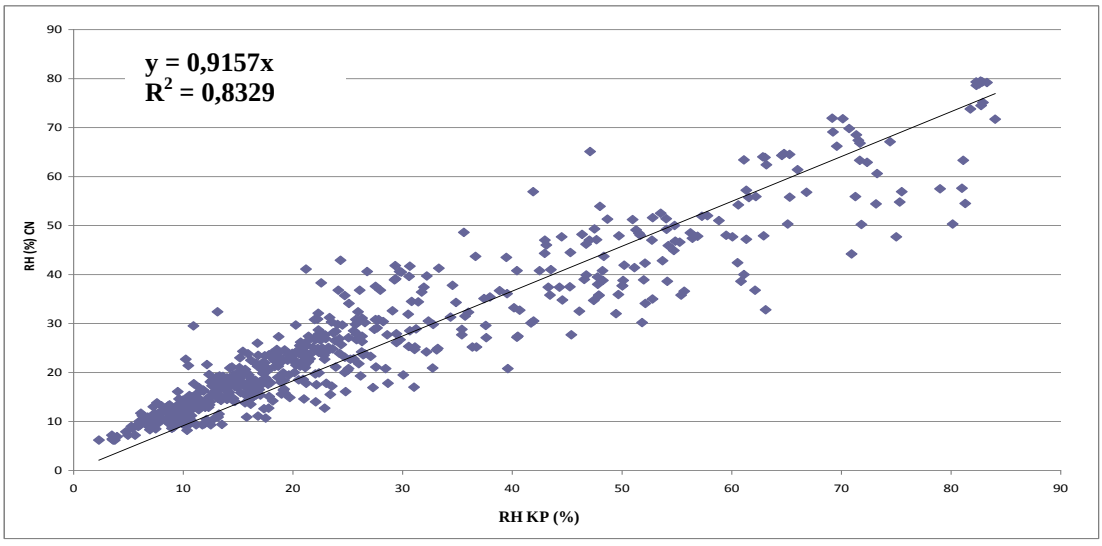

Figure 13: Correlation between relative humidity data of Changri Nup and Kala Patther AWSs from February to September 2010

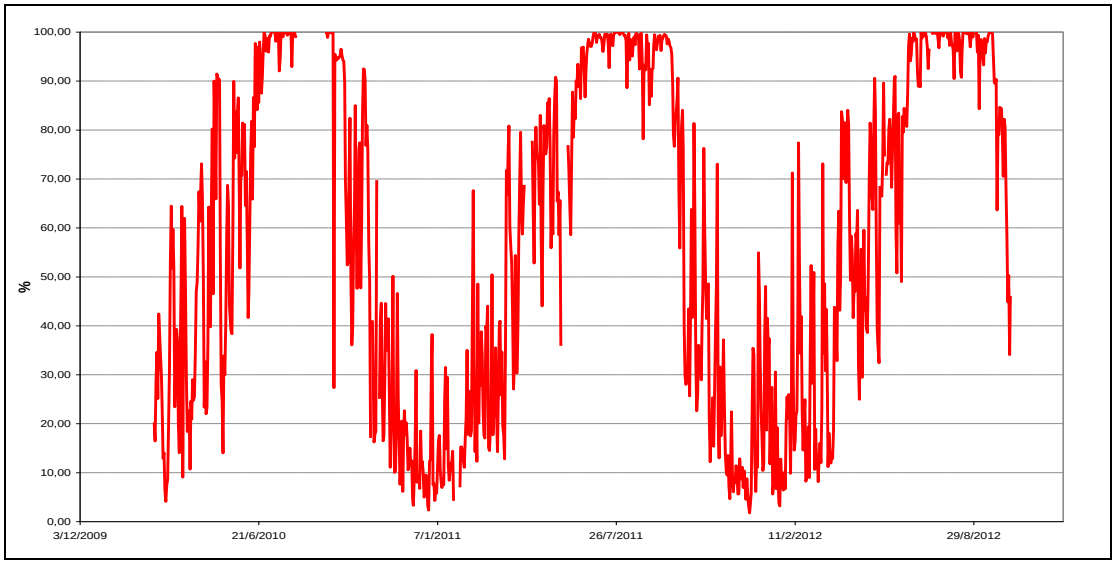

Figure 14: Relative humidity daily mean values from Kala Patther station in the period 2010-2012.

Daily mean relative humidity of Kala Patthar (Fig. 14) is consistent with the trend registered at Pyramid station with minimum values of 5% and maximum values of 100%.

Considering data availability at Changri Nup station compare to the 2010-2012 dataset of Pyramid station, the number of data registered at Changri Nup correspond to the 82% of the Pyramid station dataset, which represent a good number of measurement for an extreme remote site.

The following graphs describe the trend of both stations in the period 2010-2012 in order to have a complete vision of their behavior in the analyzed period.

Daily mean temperature data at Changri Nup and Pyramid AWS are reported in figures 15 and 16.

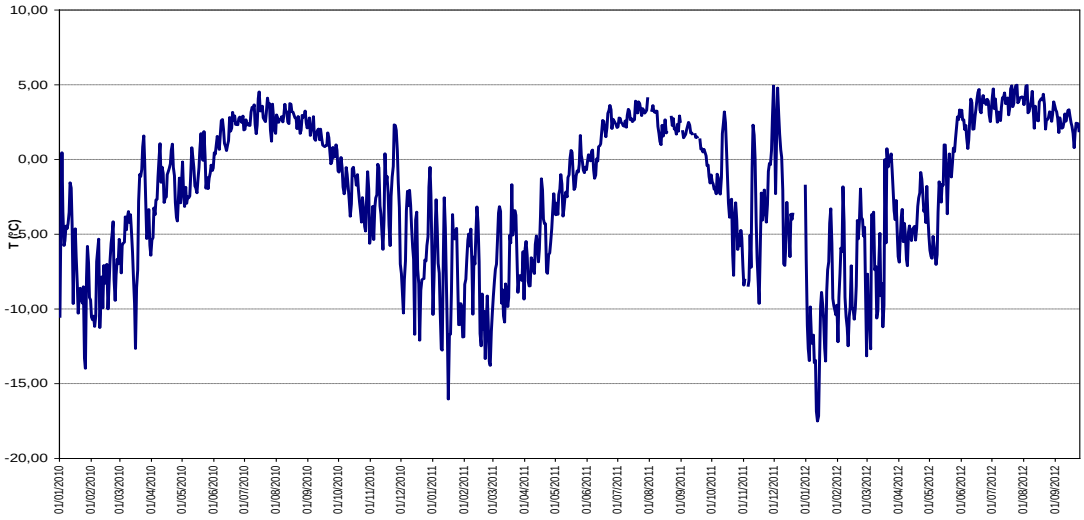

Figure 15: Daily mean temperature at Pyramid AWS in the period 2010-2012

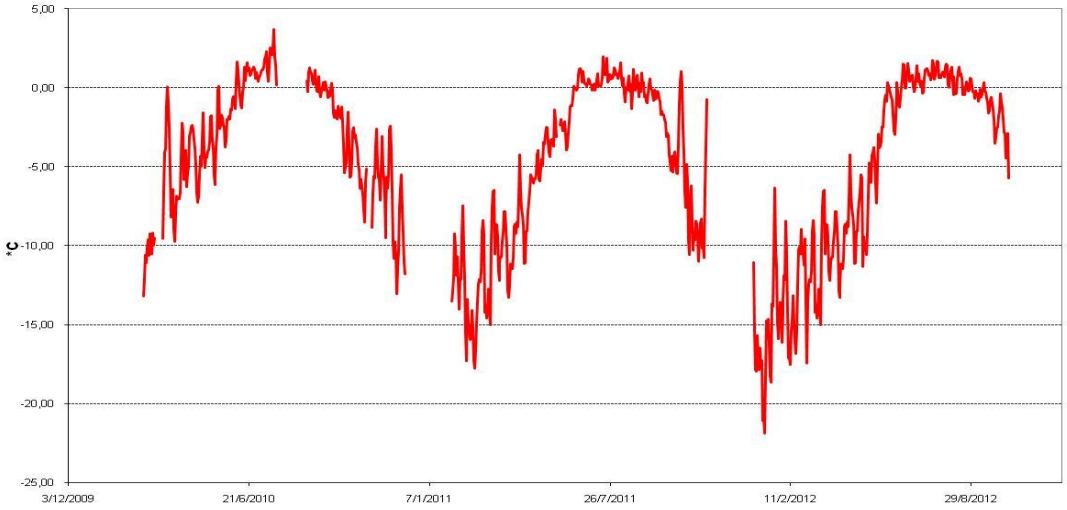

Figure 16: Daily mean temperature at Changri Nup AWS in the period 2010-2012

Daily mean values of air temperature at Changri Nup show an annual cycle with maxima value during summer period (monsoon), the only season on which temperature reaches value above 0 °C, and minimum value in winter. In the period 2010-2012 the average period has been -4.75 °C and the temperature range was between 3.69 °C and -21.87 °C.

Wind speed daily average at Changri Nup AWS (Fig. 17) is 1.46 m s^{-1}, lowest that the average value registered at NCO-P, due both to the effect of the orographic barrier but also to the fact that, due to the lowest temperature in winter time, the anemometer could become frozen and as a consequence underestimate wind speed in winter time. Maximum values are lower than the values registered at the Pyramid (Fig. 18).

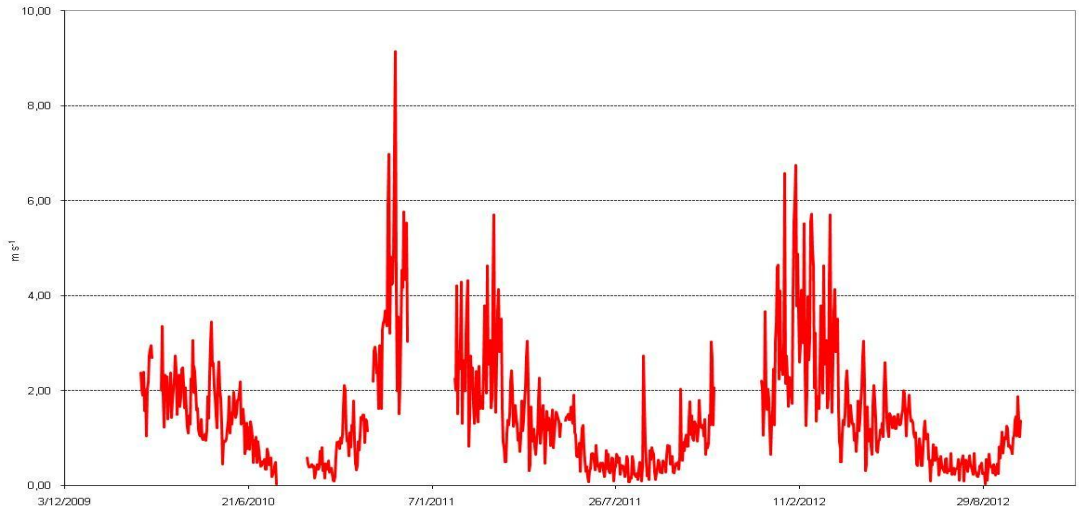

Figure 17: Daily mean wind speed at Changri Nup AWS in the period 2010-2012

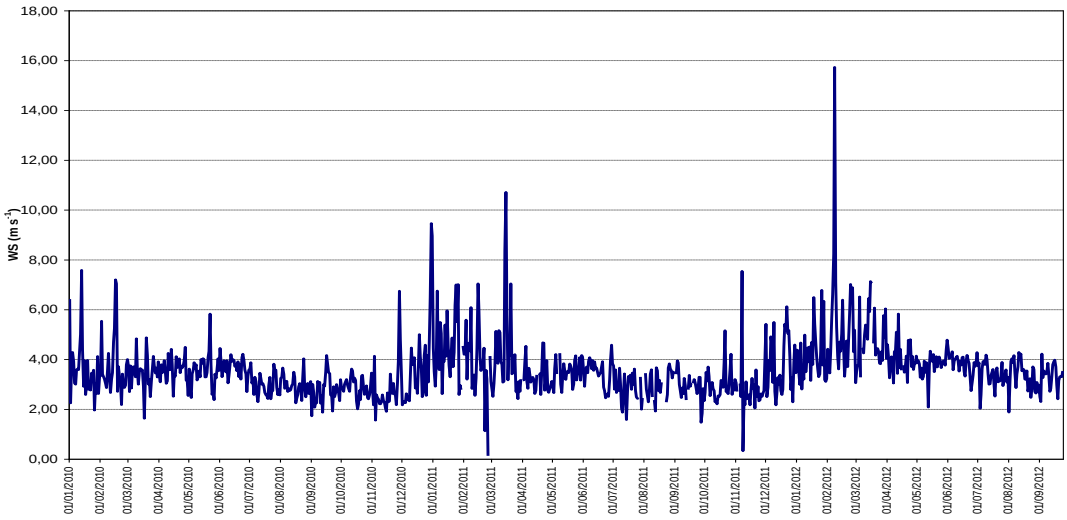

Figure 18. Daily mean wind speed at Pyramid AWS in the period 2010-2012

Prevailing wind direction (Fig. 19) is NNO, indicating a strong influence of mountain breeze circulation. Changri Nup glacier is exposed to East and the presence of the Shangri-La pass, affect the local circulation.

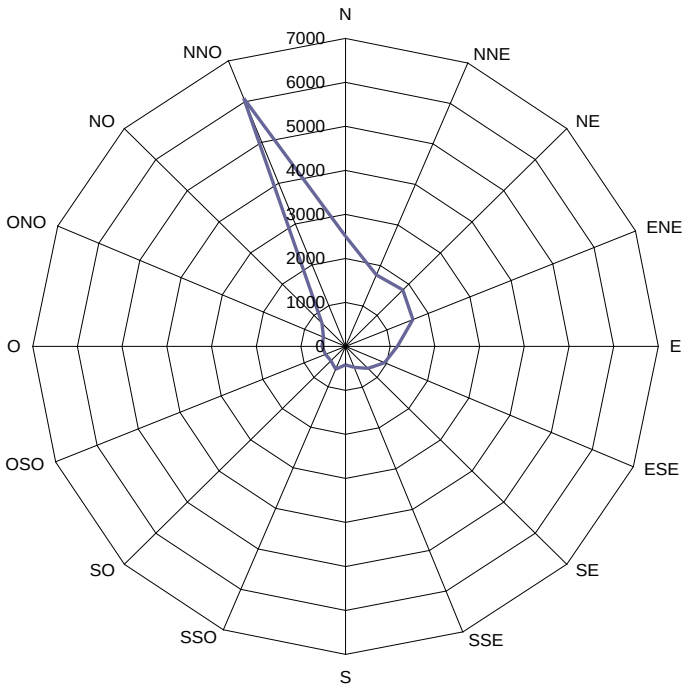

Figure 19: Daily mean wind direction at Changri Nup AWS in the period 2010-2012

The wind regime in the near surface glacier layer can be better understood with scatter plots of wind speed and wind direction, (30 minutes values) (Oerlemans & Grisogono, 2002).

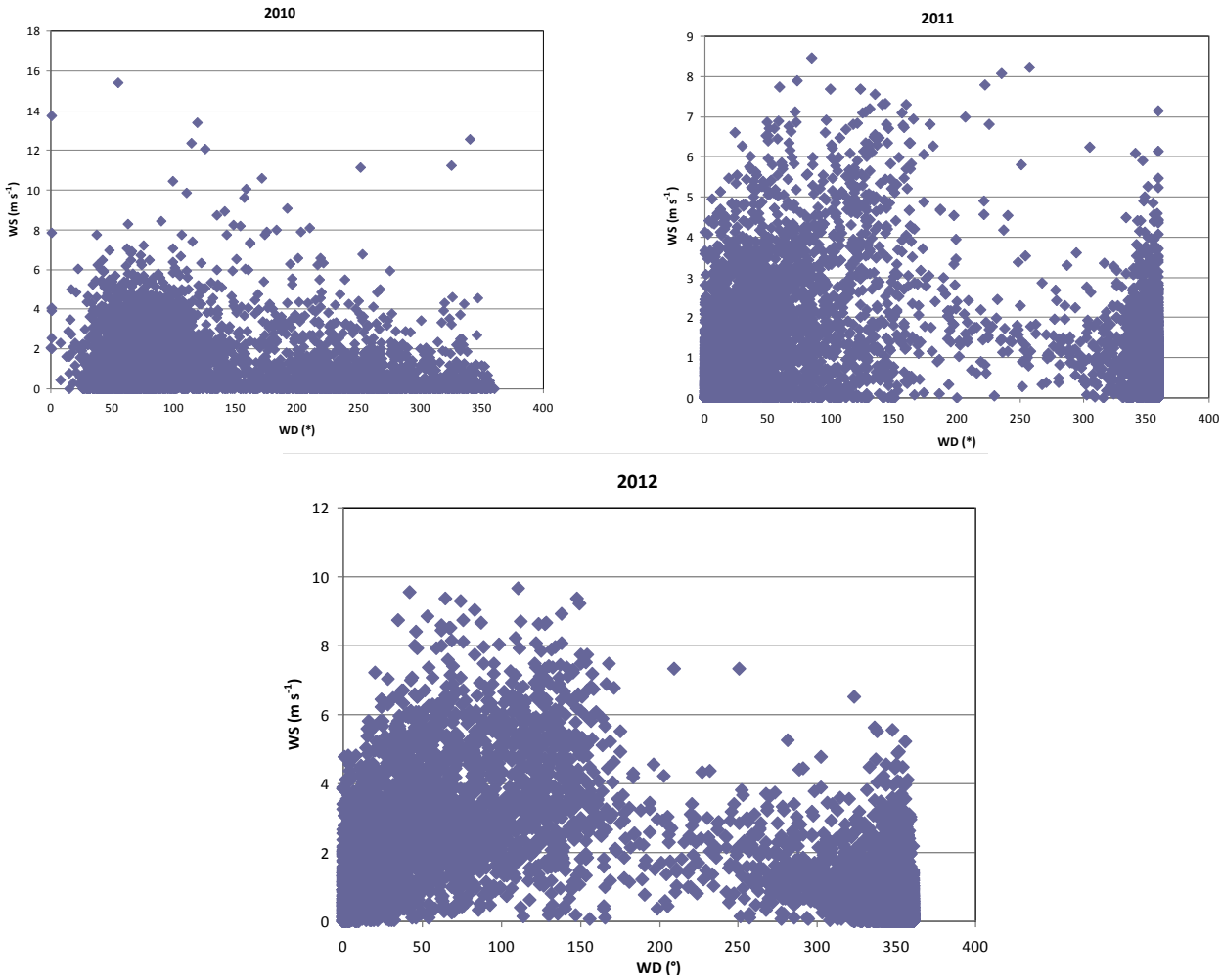

Figure 20: 30-min mean wind direction vs wind speed at Changri Nup AWS in the period 2010-2012

In yearly wind direction vs wind speed (Fig. 20), the more frequent wind directions (cluster around a provenance (from ca. 70°) occur with higher wind speed of around 8 m s-1. These features of direction and speed are characteristics of the katabatic regime (Oerlemans, 2010). Wind directions around 200° occur in correspondence of lowest wind speed values.

3.2 Surface energy fluxes

The effect of clouds on the shortwave and longwave radiation budgets is just the opposite. More clouds simply less shortwave radiation and more longwave radiation. The net effect depends on the surface albedo and on cloud transmissivity (Ambach, 1974; Bintanja & Broeke, 1996, Oerlemans, 1996, Oerlemans, 2005a). In the case of high surface albedo (e.g. fresh snow), the net change in longwave radiation for a given increase in cloudiness is greater than the net change in the solar radiation. Then, an increase in the net radiation balance occurs. In the case of lower albedo (e.g. ice), the solar radiation effect dominates and the net radiation budget decreases with cloudiness.

Figure 21 shows the global radiation (SWin) behavior measured at the Changri Nup glacier during 2010-2012 period together with those calculated with birds model (bleu). Daily variability of SWin is high and maxima values are present in winter season while minima values are evident during monsoon season which is characterized by a higher number of cloudy days compare to clear sky days. This feature seems to be enhanced by the disappearance of snow cover, reducing the effect of multiple reflection over the glacier surface too (Oerlemans, 2000).

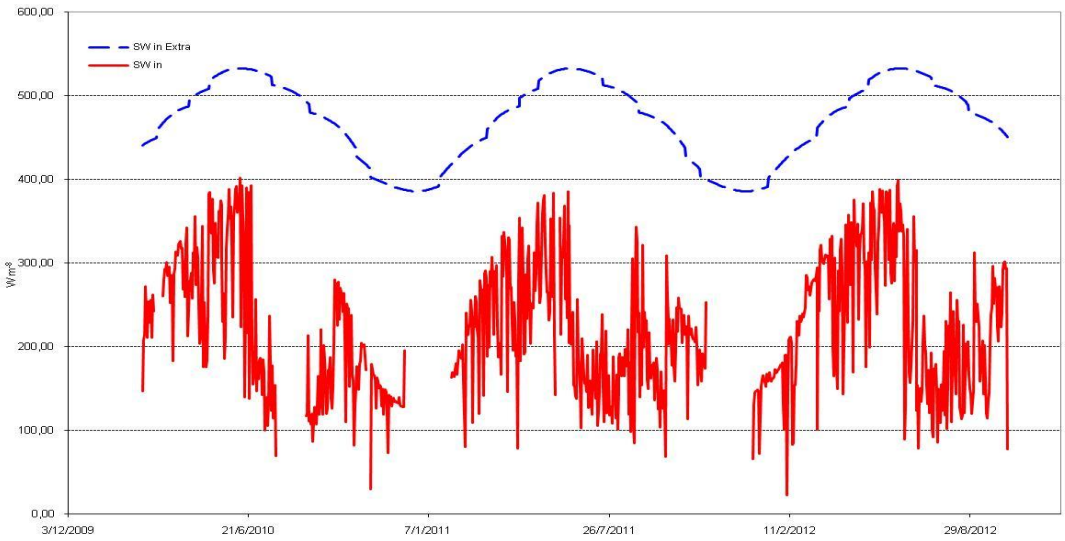

Fig. 21. Daily mean SWin measured at Changri Nup AWS in the period 2010-2012 and SWextra calculated with Bird models in the period 2010-2012.

Clear sky and cloudy days conditions at Changri Nup, seen in Fig. 22, are consistent with the seasonal behavior analyzed at NCO-P station in the period 2006-2008 and reported in Bonasoni et al., 2010.

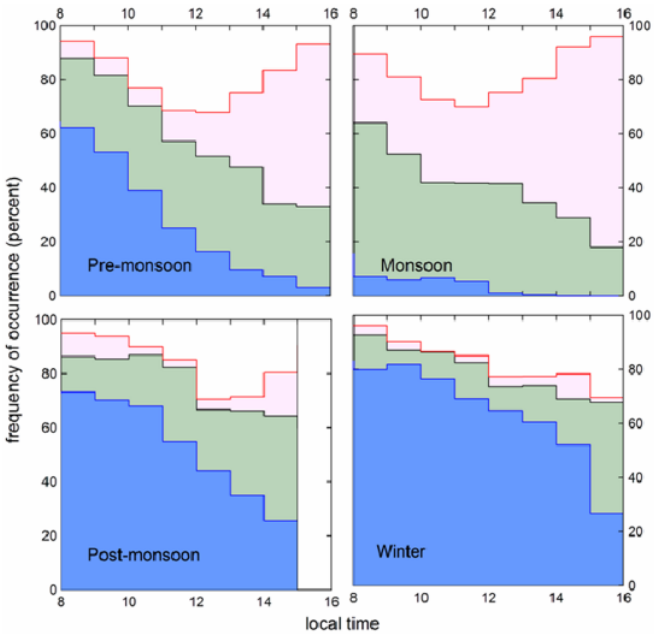

Figure 22: Frequency of occurrence of clear skies (light blue),thin/moderate clouds (grey), thick clouds (pink), and scattered clouds (white) versus time of day for the different seasons, as derived from the NCO-P observations (Bonasoni et al., 2010)

Daily mean global radiation measured at Changri Nup station in the period 2010-2012 has been 220 W m^{-2}. Measured daily mean values has been compared with the annual mean extraterrestrial irradiance calculated for the same latitude and elevation and estimated as 465 W m-2 using Bird method (Tab 4) which permit to produces estimates of clear sky direct beam, hemispherical diffuse, and total hemispherical solar radiation on a surface (Bird and Hulstrom, 1981). The comparison between the two values put in evidence that shading and clouds strongly decrease the amount of solar energy at the earth surface and in our case at the glacier surface. The reduction is ca. 53% excluding the processes of scattering and absorption of the clear atmosphere.

Table 4: Input parameter for the calculation of solar position based on NOAA's functions and clear-sky solar radiation based on Bird and Hulstrom's model at Changri Nup AWS

Site data and time info	
latitude in decimal degrees (positive in northern hemisphere)	28,800
longitude in decimal degrees (negative for western hemisphere)	86,800
Ground surface elevation (m)	5700,0
time zone in hours relative to GMT/UTC (PST= -8, MST= -7, CST= -6, EST= -5)	5,45
daylight savings time (no= 0, yes= 1)	0
start date to calculate solar position and radiation	23-Feb-10
start time	12:00 AM
time step (hours)	1
number of days to calculate solar position and radiation	1042
Bird model parameters	
barometric pressure (mb, sea level = 1013)	506
ozone thickness of atmosphere (cm, typical 0.05 to 0.4 cm)	0,27
water vapor thickness of atmosphere (cm, typical 0.01 to 6.5 cm)	0,27
aerosol optical depth at 500 nm (typical 0.02 to 0.5)	0,08
aerosol optical depth at 380 nm (typical 0.1 to 0.5)	0,08
forward scattering of incoming radiation (typical 0.85)	0,85

surface albedo (typical 0.2 for land, 0.25 for vegetation, 0.9 for snow)	0,7

The mean 3-years albedo value (Fig. 23, part a) is 0.65. During the accumulation season the 3-years mean annual albedo was 0.75 while during the ablation season was 0.26.

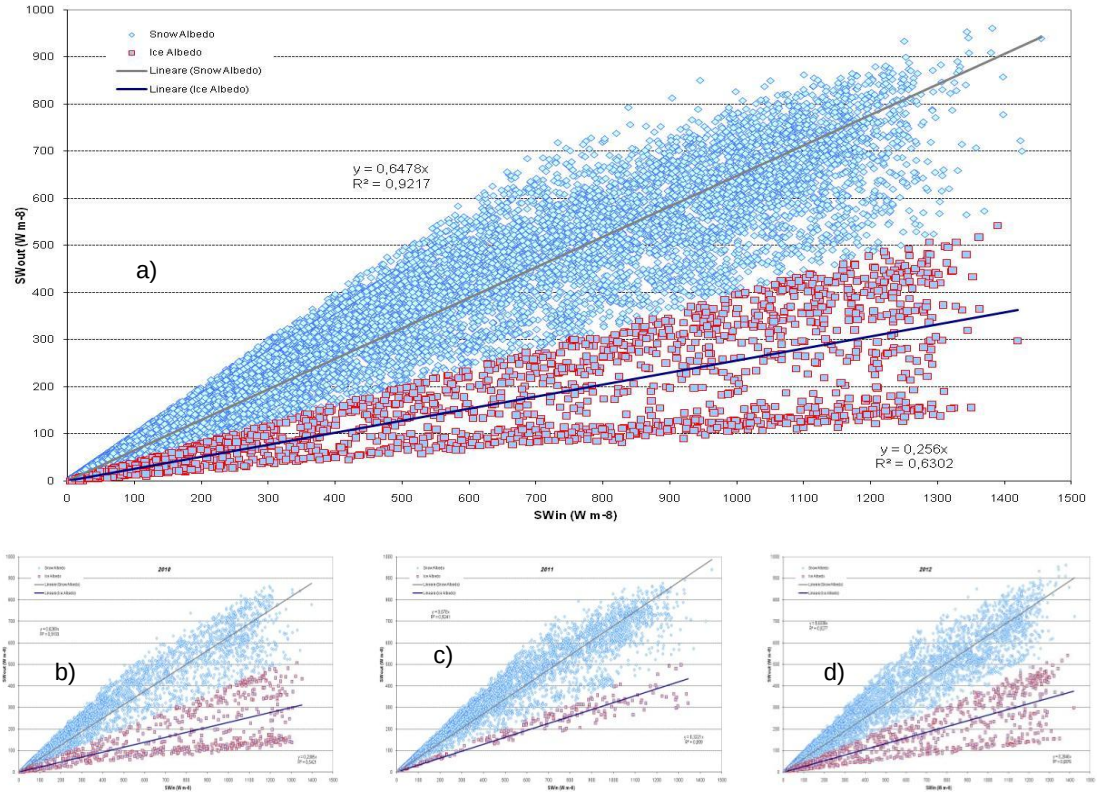

Figure 23: Daily albedo values characterizing exposed ice and snow covered surface in the period 2010-2012 (a) and per year (b, c, d)

Table 5:Snow and ice albedo values at Changri Nup Glacier

Period	Ice Albedo	Snow Albedo
2010-2012	0.26	0.65
2010	0.23	0.63
2011	0.32	0.68
2012	0.26	0.63

Yearly mean annual accumulation and ablation albedo are reported in table 5. Yearly values in 2010 and 2012 are almost the same, while in 2011 the snow and ice ablation values are higher. This is consistent with the duration of the ablation season which has been shorten in 2011, as reported in the table below. In general snowfall implies higher albedo, increasing outgoing radiation and less energy available for melting (Senese at al., 2012).

The ice-albedo correlation in figure 23a clearly put in evidence two group of data related to exposed ice (lower values) and snow covered ice (highest values).

In order to understand if this characteristics were related to a particular year, yearly albedo has been analyzed. The graphs in figure 23b and c shows the same situation and the evident

presence of both exposed and snow covered ice in the 2010 and 2012 melting season (see violet points in the graphs showing two different tendencies), while in 2011 (Fig. 23c) the line interpolating the violet plotted data reveals the presence of snow covered ice only (i.e.: highest mean albedo). As highlighted from the other results, ablation season in 2011 has been shortened and glacier melting was less compared to the results of 2010 and 2012. Table 7 summarize the length of the ice ablation period at Changri Nup Glacier.

Table: 7: Snow and ice days at ChangriNup Glacier

Ice ablation period	Tot days	Tot snow days	Tot ice days	N°of snowfalls
2010 (17-5/19-7)	64	24	40	1
2011 (4-6/23-6)	19	1	18	1
2012 (24-5/1-7)	38	3	35	1

The four components of energy balance (SH, LE, SWnet and LWnet) are reported in figures 24 and 26 shows a comparable trend of the annual cycle in the period, consistently with the ablation seasons, values entity are more similar in 2010 and 2012 then in 2011.

Higher values of net shortwave radiation (Fig. 24) are present in June, while lowest in July-August daily mean values have a similar behavior in the whole period, coherent with increase and decrease during the June peaks. Net longwave radiation increase up to values close to 0 W m^{-2} during monsoon season, confirming the higher presence of cloudy days. Negative values, up to -85 W m^{-2} are constantly present in the whole period. Generally LWnet up to -100 W m-2 are due to the 0°C glacier surface temperature (Oerlemans, 2001). During the transition from snow to ice, the lowering of the albedo (Fig. 25) occurs when the flux of SWin is large, determining a very steep increase in the net solar radiation.

On glacier surfaces, solar radiation contributes to the surface energy flux most when melting occurs. This makes surface albedo a particularly important parameter worthy of special attention. Albedo, the reflection coefficient, depends, in a complicated way, on crystal structure, surface morphology, dust and soot concentrations, moraine material, the presence of liquid water in veins and at the surface, solar elevation, cloudiness, etc. (Oerlemans, 2001; Citterio et al, 2007).

The incoming SW radiation could reach high value (higher then 1000 W m^{-2}), typical of a glacier surface on days with few clouds, when the multiple reflections between clouds, snow-covered valley slopes and the glacier surface lead to a peak value comparable to the extraterrestrial irradiance.

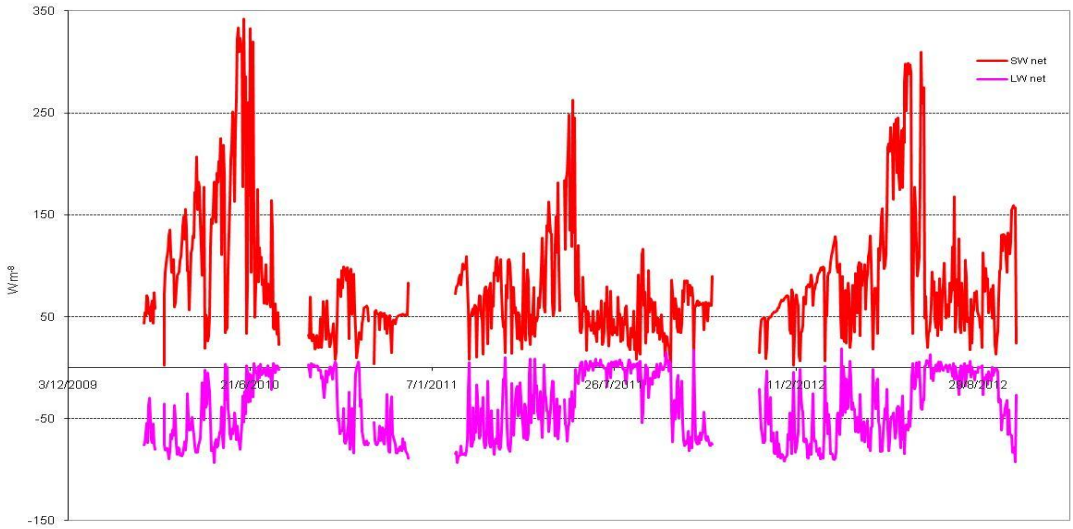

Figure 24: Daily mean SWnet and LWnet at ChangriNup AWS in the period 2010-2012.

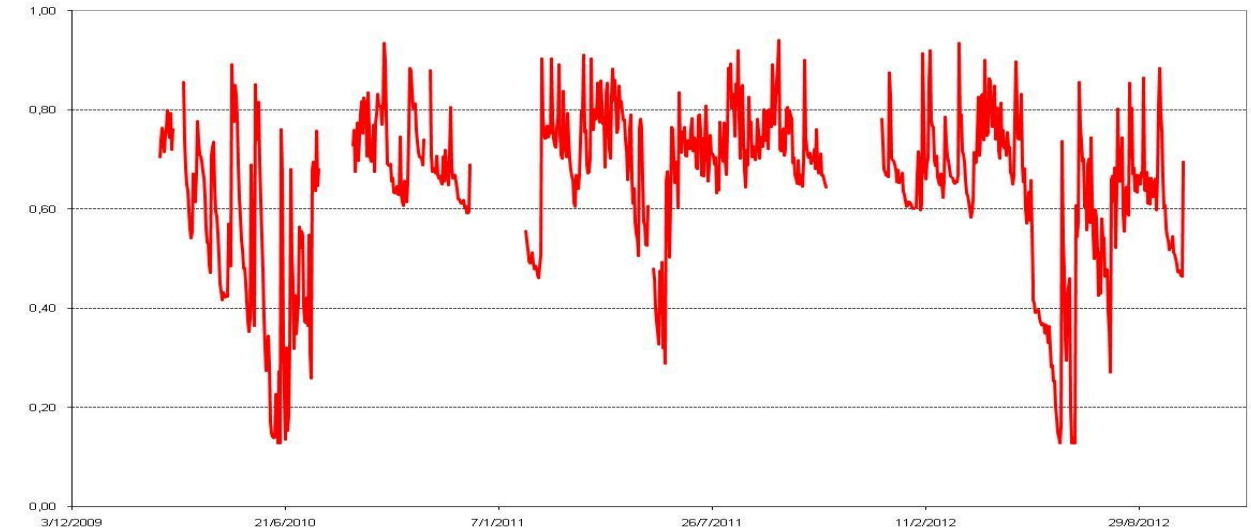

Figure 25: Daily mean albedo at ChangriNup AWS in the period 2010-2012.

During the ablation season, the latent heat flux (LE) (Fig. 26) is generally positive or close to zero, while in the rest of the year, the negative values correspond to low humidity combined with a minimal temperature difference between the glacier surface and the air (Oerlemans, 2000). Consequently sensible heat flux is higher in correspondence of negative LE values and lower or close to zero during the ablation season.

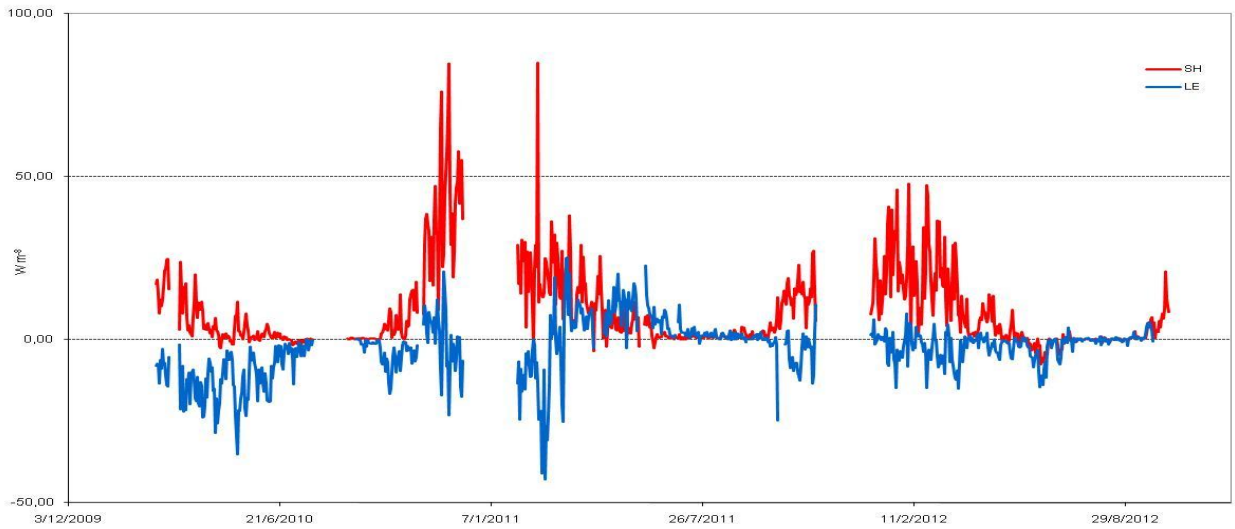

Figure26: Daily mean SH and LE at Changri Nup AWS in the period 2010-2012.

Net energy values (Rs) in figure 27 characterize non-monsoon/winter season, when snow/ice melting is absent, showing high values during the ablation monsoon season.

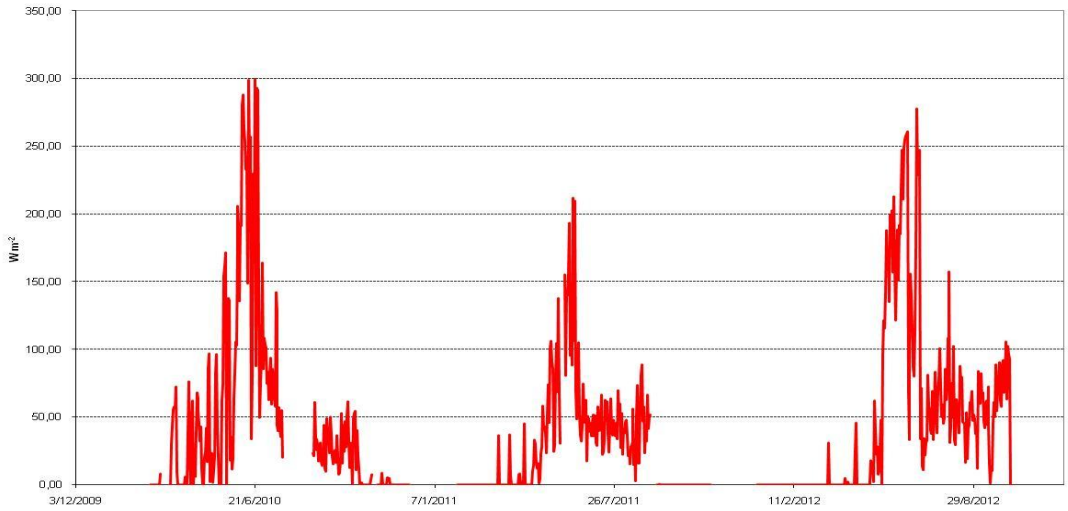

Figure 27: Daily mean RS at ChangriNup AWS in the period 2010-2012.

Cumulative daily melt in the three years period is reported in figure 28. In accordance with previous data, glacier melting has been more high in 2010/2012 then in 2011.

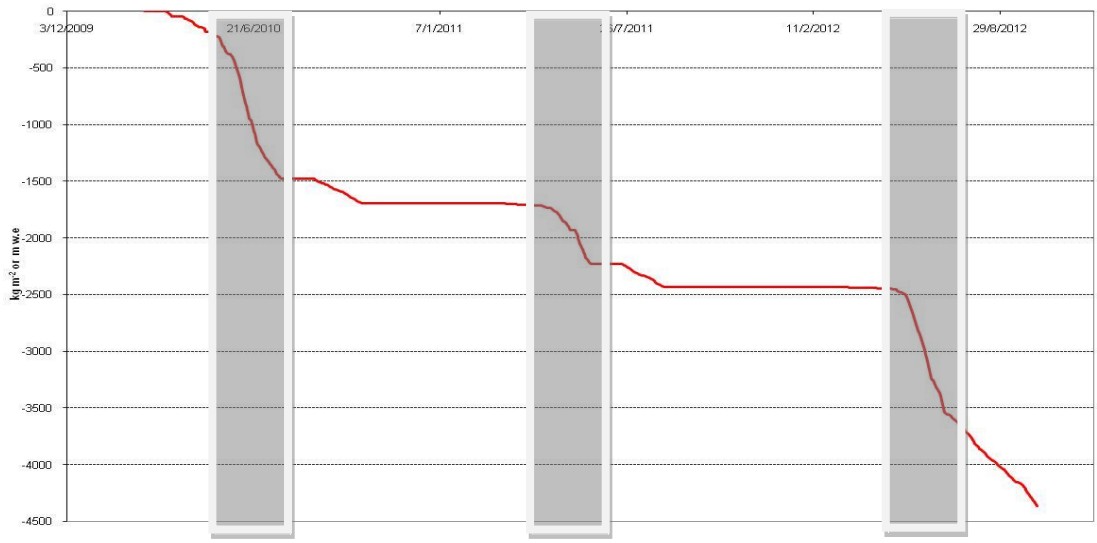

Figure 28: Cumulative daily melt at Changri Nup AWS in the period 2010-2012. Ice ablation is highlighted in grey.

3.3 Ablation measurements

To validate the melting computation, these results have been compared to field measurements in two periods: February 24-May 28, 2010 and May 5-November 25, 2012, periods in which ablation stakes was installed on glacier surface.
In 2010, three stakes have been positioned nearby the AWS. Location and field data are reported in the tables below (8 and 9).

Table 8: Location of the ablation stakes positioned nearby Changri Nup AWS in 2010 and related field measurement.

DATE	LOCAL TIME	STAKE No	Stake height from SNOW LEVEL (cm)	LOCATION		
				ALTITUDE (m asl)	LAT N	LONG E
24/02/2010	11:00	Stake 1	88	5.643	27 58.908	86 45.896
	11:00	Stake 2	80	5.673	27 58.913	86 45.886
	11:00	Stake 3	100	5.660	27 58.922	86 45.893
16/04/2010	11:23	Stake 1	146	5.646	27°58'922"	86° 45'862"
	11:24	Stake 2	157	5.646	27° 58'928"	86° 45'848"
	11:25	Stake 3	128	5.644	27° 58'937"	86° 45'856"
10/05/2010	12.15	Stake 1	184	5.649	27°58'54.2"	86°45'54.0"
	12.25	Stake 2	190	5.649	27°58'54.4"	86°45'53.0"
	12.28	Stake 3	170	5.648	27°58'55.8"	86°45'53.5"
28/05/2010	12:30	Stake 1	200	5.648	27°58'52.2"	86° 45'46.2"
	12:35	Stake 2	200	5.648	27° 58'52.6"	86° 45'54.8"
	12:45	Stake 3	195	5.647	27° 58'53.7"	86° 45'55.6"

No measurement from June 2010 due to the melting of glacier surface. Ablation stake network has been repositioned on May 2012

Table 9: Snow ablation data from stake measurements. The time frame covered by our survey is 93 days long. data are reported as cm of snow.

Snow ablation (cm)	stake	period	lenght
-58	Stake 1	from 24-02-2010 to 16-04-2010	51
-77	Stake2	from 24-02-2010 to 16-04-2010	51
-28	Stake3	from 24-02-2010 to 16-04-2010	51
-38	Stake1	from 16-04-2010 to 10-05-2010	24
-33	Stake2	from 16-04-2010 to 10-05-2010	24
-42	Stake3	from 16-04-2010 to 10-05-2010	24
-16	Stake1	from 10-05-2010 to 28/05/2010	18
-10	Stake2	from 10-05-2010 to 28/05/2010	18
-25	Stake3	from 10-05-2010 to 28/05/2010	18

Snow ablation (cm)	stake	period	lenght
-112	Stake1	from 24-02-2010 to 28/05/2010	93
-120	Stake2	from 24-02-2010 to 28/05/2010	93
-95	Stake3	from 24-02-2010 to 28/05/2010	93

In 2012, three stakes have been positioned nearby the AWS. Location and field data are reported in figure 29 and in the tables below (10 and 11).

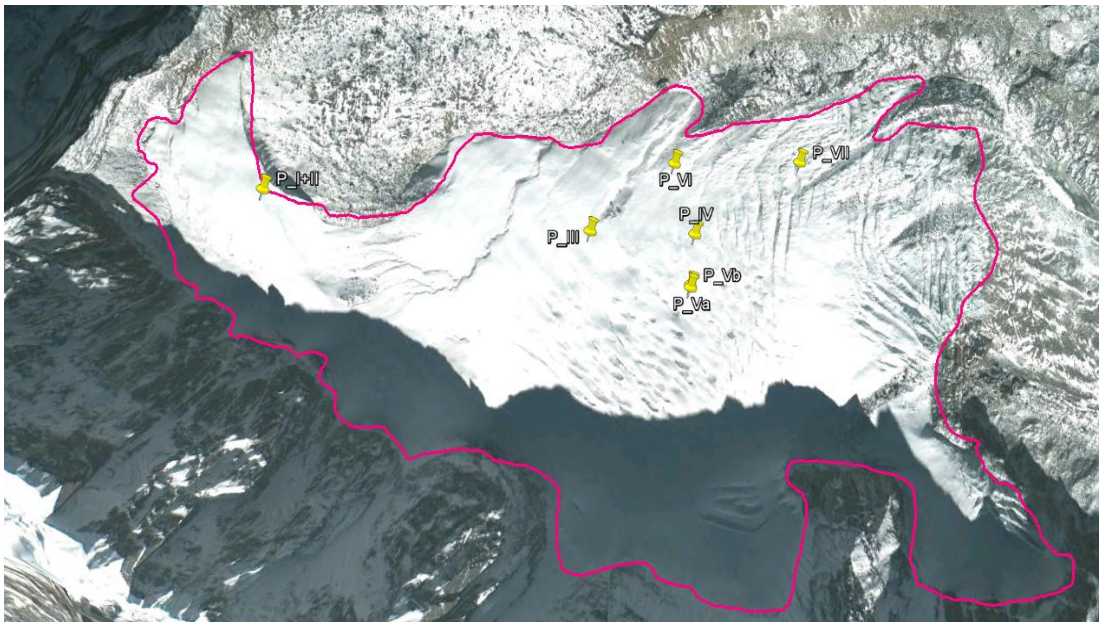

Figure 29.Ablation Stakes at Changri Nup Glacier in 2012

Table 10: Location of the ablation stakes positioned at Changri Nup glacier in 2012 and related field measurement.

DATE	STAKE No	Stake length (cm(	Stake height from SNOW LEVEL (cm)	Snowdepth (cm)	LOCATION		
					ALTITUDE (m asl)	LAT N	LONG E
03/05/2012	Stake 1	550	82	148	5.602	27°58'54.35"	86°45'53.82"
	Stake 2	550	92	157	5.602	27°58'54.35	86°45'53.82"
	Stake 3	605	185	80	5.497	27°58'51.93"	86°46'17.42"
	Stake 4	590	75	60	5.486	27°58'51.75"	86°46'25.32"
	Stake 5	549	80	75	5.493	27°58'48.48"	86°46'24.97"
	Stake 6	580	108	45	5.462	27°58'56.13"	86°46'23.77"
	Stake 7	580	124	35	5.442	27°58'56.27"	86°46'33.44"
23/11/2012	Stake 1	550	Stake not found	-	5.602	27°58'54.35"	86°45'53.82"
	Stake 2	550	Stake not found	-	5.602	27°58'54.35	86°45'53.82"
	Stake 3	605	30	50	5.497	27°58'51.93"	86°46'17.42"
	Stake 4	590	Stake not found	-	5.486	27°58'51.75"	86°46'25.32"
	Stake 5	549	114	30	5.493	27°58'48.48"	86°46'24.97"
	Stake 6	580	39	25	5.462	27°58'56.13"	86°46'23.77"

	Stake 7	580	16	0	5.442	27°58'56.27"	86°46'33.44"

Table 11: Snow ablation data from stake measurements. The time frame covered by our survey is 113 days long. data are reported as cm of snow.

Ablation	Stake	Period	Lenght of stakepiece	Ice Depth 5 May	Ice Depth 23 Nov
-17	Stake3	From May 5 to November 23, 2012	202	265	282
-169	Stake5		180	155	324
-298	Stake6		193	153	451
-364	Stake7		193	159	523

The comparison between field measurements and calculated melt values present a good trend. The difference between measured ablation and calculated ablation is 80 m w.e., calculated melting is rapidly decreasing from middle April and from the ablation stakes, this situation is not so evident (Fig. 30).

It has to be considered that the ablation stakes have been positioned in winter season and the thickness of snow and the cold temperature didn't allow a good positioning of the stakes until the glacier surface. The rapid ablation at glacier surface has been also highlight by the fact that after May 28, no more field measurement were possible due to the falling down of the stakes.

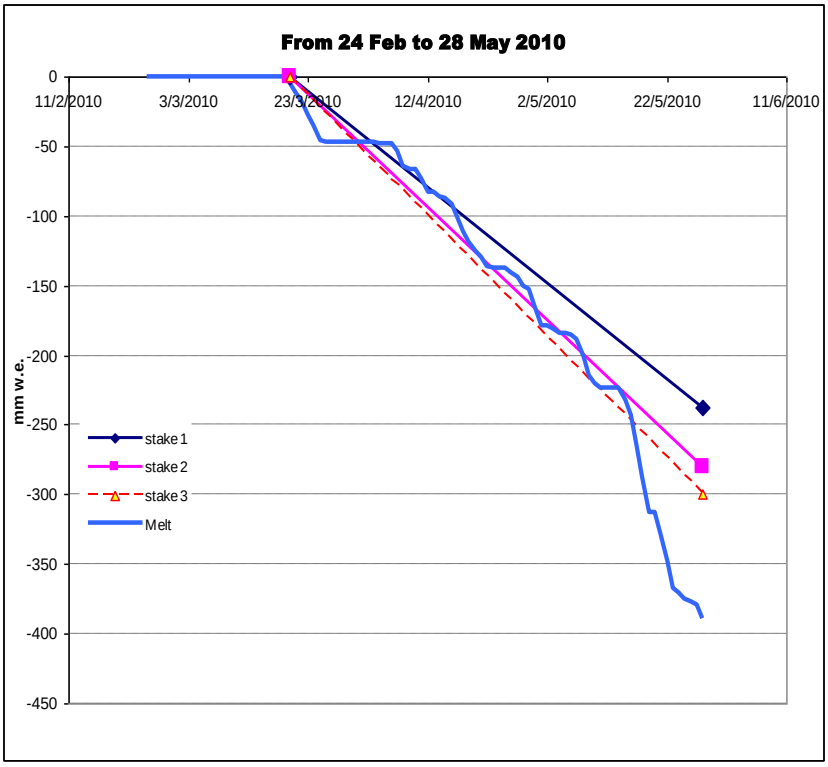

Figure 30: Comparison between field measurements during February-March 2010 and calculated melt values in the same period.

The comparison between field measurements and calculated melt values presents a good trend. The field measurements have been taken only one time after the positioning of the stakes (November), while calculated melting has been done hourly until October 2012. This fact didn't allow to compare the data at the same day, but figure 31, put in evidence a good trend between measured and calculated melt.

Moreover field measurement are available only from the stakes positioned more far from the station, at lower altitude. This aspect needs also to be considered in comparing the data, because good results are also related to the fact that ablation stakes and AWS measurement are very close.

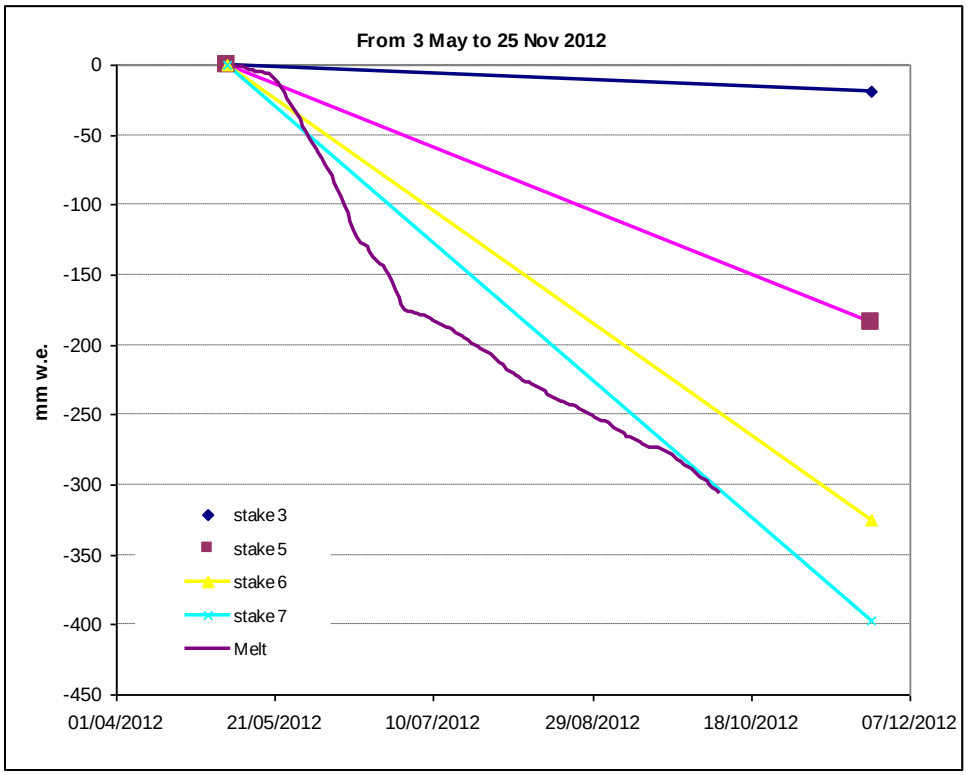

Figure 31:Comparison between field measurements during May-November 2012 and calculated melt values in the same period.

Filtering surface temperature (TS), net energy (RS), and latent heat flux (LE) data, the hours when melting (i.e.: TS>0 °C and RS>0 Wm^{-2}) and condensation (TS>0°C and LE>0 W m^{-2}) occurr have been identified . Considering these criteria, SWnet, LWnet, SH, LE, and RS have been averaged (Fig. 32).

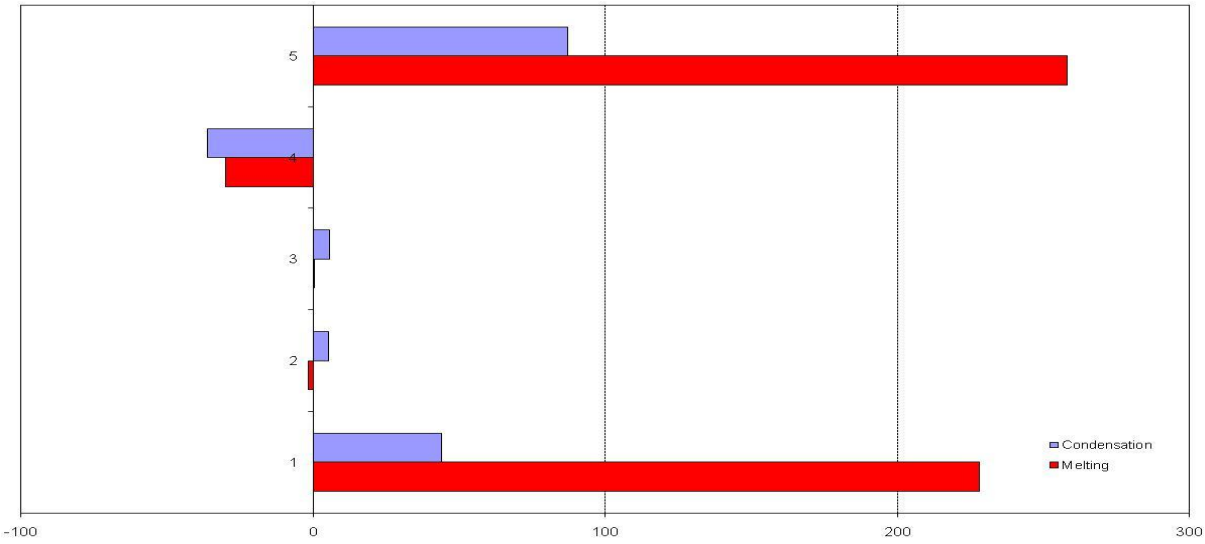

Figure 32: Components of the surface energy flux (from hourly mean values), averaged over time, when melting (red) and condensation (purple) conditions occurred. The units of measure for the x-axis are W m^{-2}

By analyzing mean values, net shortwave proves to be the parameter with the highest energy flux during both melting and condensation (with values of 258 and 87 W m^{-2} respectively), Rs has the similar behavior with mean values of 220 W m-2 during melting and 44 W m^{-2} during condensation; LE is higher during condensation (5 W m^{-2}) than during melting (-2 W m^{-2}). SH is a similar rend with a maximun during condensation (5 W m^{-2}) and a minimum during melting (0.5 W m^{-2}).

3.4 BC concentration and effect on the albedo reduction

In order to investigate any possible influence of BC in glacier albedo reduction and as a consequence in accelerating melting processes, daily mean concentrations of albedo at Changri Nup Glacier have been compared with daily mean value of atmospheric Black Carbon (BC) concentrations continuously monitored at NCO-P station (Fig. 33).

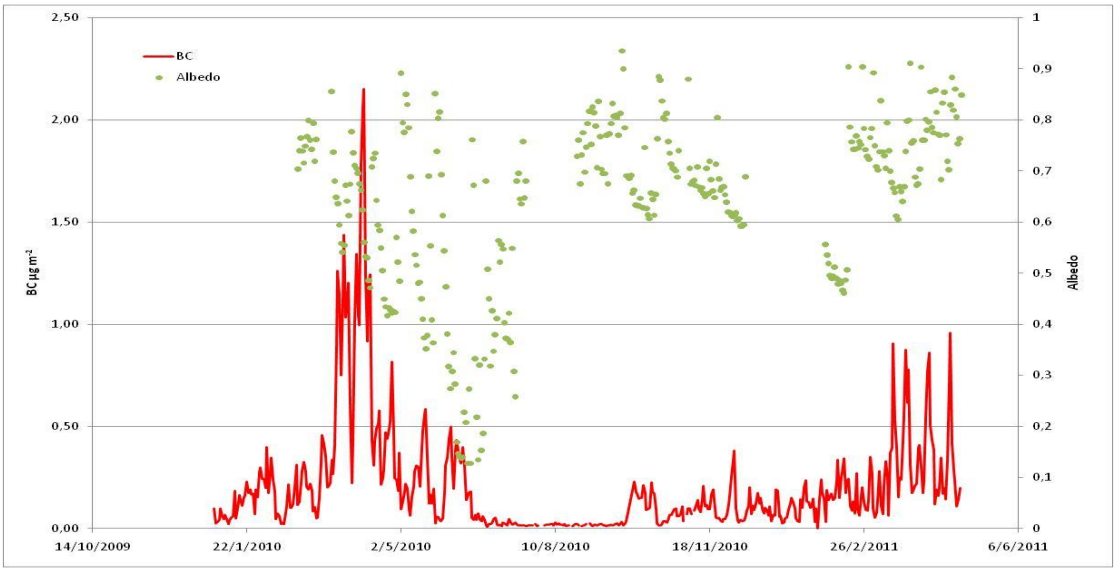

Figure 33: Daily mean albedo values measured at Changri Nup AWS and daily mean atmospheric BC concentration measured at NCO-P station in the period 2010-2012.

With the aim of have a more clear vision of the behavior of these two parameters and their relationship, data have been correlated calculating their respective weekly moving average (Fig. 34). This permits to better highlight the correlation between the high values of BC concentration measured during premonsoon season (April 2010) in the Changri Nup Humalayan area (NCO-P) and the consequent dramatic reduction of albedo values measured on the Glacier and starting from late pre-monsoon season up to monsoon season.

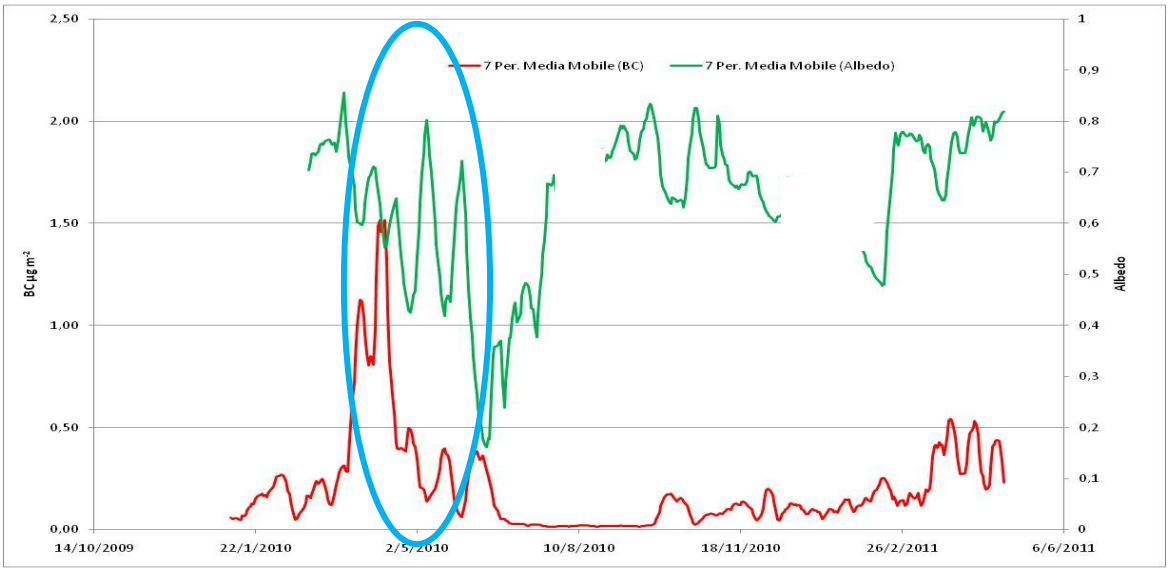

Figure 34: Moving average (7 Per.) of daily mean albedo values measured at ChangriNup AWS and daily mean atmospheric BC concentration measured at NCO-P station in the period 2010-2012.

To understand the influence of BC deposition in snow in the reduction of albedo, it has been needed to calculate the amount of BC deposition starting from BC atmospheric concentration. Therefore, total BC mass deposition flux per 30 minutes(1800 seconds) was calculated using assumption by Yasunari et al., 2010:

BC deposition=
[atmospheric BC] × (the minimal deposition velocity of1.0×10−4 ms−1) × (interval time=1800 s)

In this way, summating the BC flux for March–June 2010, it has been obtained the total deposition amount of BC of 394μg m^{-3}.

Usually, on a glacier, the 2-cm top layer (5-cm top layer in Aoki et al., 2000)of snow surface is more contaminated than the deeper part of the snow layer because the snow impurities are derived from dry depositions of atmospheric aerosols (Aoki et al., 2000, 2007; Tanikawa et al., 2009). In addition, Tanikawa et al. (2009) showed that the mass concentrations of snow impurities deposited in the surface layer of 2 cm were about 30–50 ppmw (part per million by weight) whereas that the concentrations in 2–10 cm were about 2–6 ppmw. This difference in characteristics between surface layer and lower snow layer were consistent for elemental carbon, organic carbon, and dust in their study. It indicates that the impurity concentration at the top 2-cm is much higher than that below 2 cm and the top snow layer is considered the key to assessment of albedo reductions (Yasunari et al., 2010).

For this reason, assuming that total BC of 394 μg m^{-3} is deposited on 2 cm of thickness of pure snow, without pre-existing od other contamination (e.g. dust), BC concentration in snow surface at Changri Nup, considering a measured snow density of 400 kgm−3, has been calculated as:

[BC concentration in snow] = BC dep / snow depth / snow density

Calculated amount of BC concentration in snow has been: 49 μg kg^{-1}, consistent with the concentration range of BCC in snow of 26.0–68.2 μg kg^{-1} due to snow density variations between 195–512 kg m^{-3} as reported in Yasunari et al., 2010 (Tab. 12).

Table 12: Comparison between estimated (a) and observed (b, c, d, e, f) BCCs in surface snow and ice core for locations reported in figure 35.

Site in Himalayan region	Altitude (m)	BCCsin snow and ice core (μg kg^{-1})
[a]NCO-P (lat. 27.958, lon. 86.815)	5079	26.0–68.2[e]
[b]Qiangyong Glacier (lat. 28.83, lon. 90.25)	5400	43.1
[b]Kangwure Glacier (lat. 28.47, lon. 85.82)	6000	21.8
[c]East Rongbuk Glacier (lat. 28.02, lon. 86.96)	6465	18.0
[d]East Rongbuk Glacier (lat. 28.02, lon. 86.96)	6500	20.3±9.2

a yasunarii work.
b The EC concentration data in snow sample by Xu et al. (2006).
c The BCC data in snow sample by Ming et al. (2009).
d The BCC data during 1995-2002 in an ice core by Ming et al. (2008). The BCC exceeded 50μg kg−1 in the summer of 2001.
e Estimated BCC in 2-cm surface snow with density variations of 195–512 kgm−3 at Yala Glacier

The percentage of the albedo reduction corresponded to the peak of atmospheric BC concentration deposited and measured at Changr iNup has been determined as:

(Min Albedo after [atmosph. Max BC] – natural snow albedo) / natural snow albedo

that permitted to obtain the value 4.29.

In order the put in relationship the estimated BCC in snow with the measured snow albedo reduction at Changri Nup, the obtained results have been compared with the correlation equation calculated by Ming at al., 2009 from available field and modeling data of BC concentration and % of albedo reduction of different worldwide glaciers (Fig. 35). As reported in figure 35, % of albedo reduction measured at Changri Nup related to BCC in snow estimated from atmospheric [BC] measured at NCO-P station are well correlated.

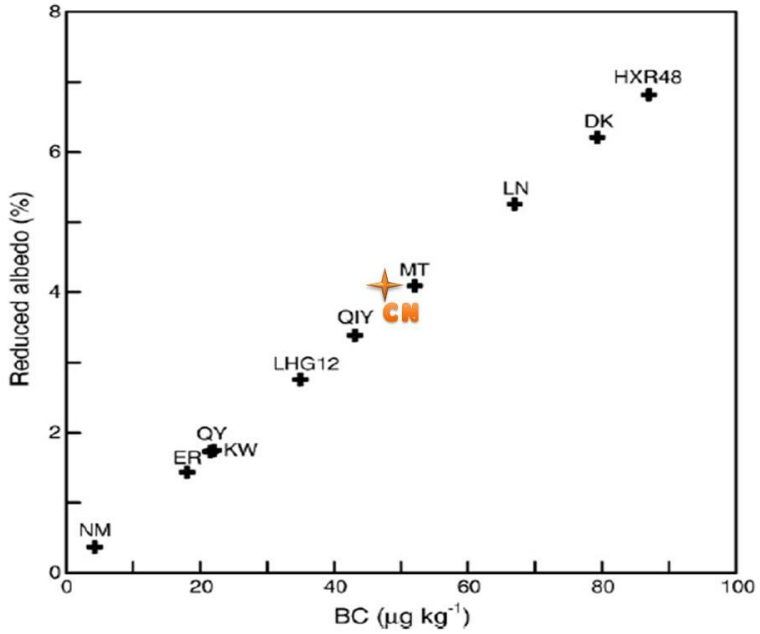

Figure 35: Albedo reduction vs BC concentration in snow (Ming tl al., 2009 modified). Orange indicator is related to ChangriNup glacier data.

In order to better verify the % of albedo reduction measured at Changri Nup with theoretical estimation of albedo reduction by Ming et al., 2009, the correlation equation:

$$y = 0.0757x + 0.575$$

has been applied considering as x value the BCC in snow estimated at Changri Nup glacier. Deriving % of albedo reduction has been 4.23, very close to the value measured at Changri Nup as reported in the table below:

Table 13: Estimated BCC in snow and % of albedo reduction deriving from Ming equation and measured at Changri Nup AWS.

BC deposition in snow (µg kg^{-1})	% Albedo reduction (from ChangriNup measurement)	% Albedo reduction (Calculated from Ming equation)
49	4.29	4.30

3.4 BC concentrations in snow

From 2010, at Changri Nup glacier started. Samples were collected during the field check by Nepalese local staff, monthly when possible.

Table 14 shows the number of samples, the location and the scarce availability of samples for the analysis due to problems occurred during the transportation from Nepal to France at LGGE, where BC concentration in snow have been determined with SP2 analysis (Fig. 36).

Table 14: Snow samples collected at Changri Nup in 2010

Sampling date	Comments	Bottle type
19/03/2010	stake 2	1 shott 500 ml empty
19/03/2010	stake 3	2 shotts 500 ml with 1 empty
10/05/2010	12.00 h 3 cm of snow 3 days before	6*tubes with 4 empty
28/05/2010	Fresh snow of today, snow level total from three days before, 10 cm	5* tubes
21/07/2010	fresh snow from today 10 cm snow level to ice 10 cm	4*tubes
08/08/2010	30 cm	4*tubes

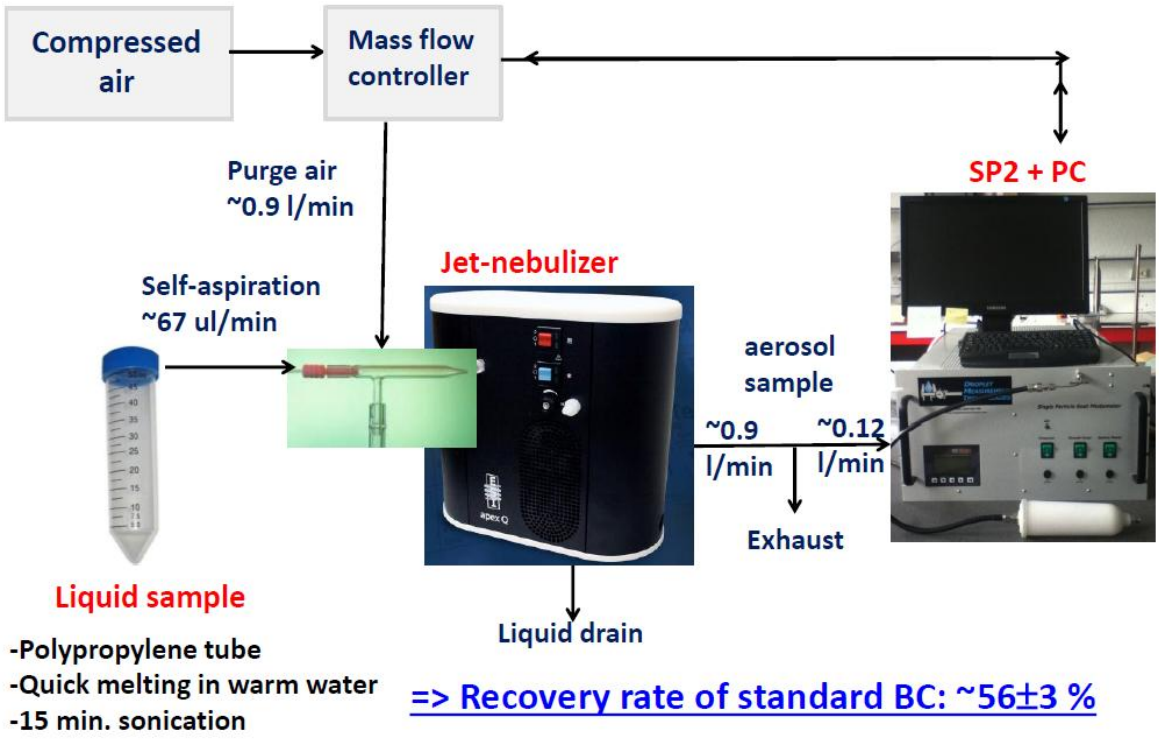

Figure 36: Analysis of BC concentration in snow through SP2.

The preliminary results of the characterization of snow samples collected at Changri Nup glacier (5,700 m asl) show higher concentration of BC due to the effect of aerosol dry deposition that allow to classify the snow as aged snow.

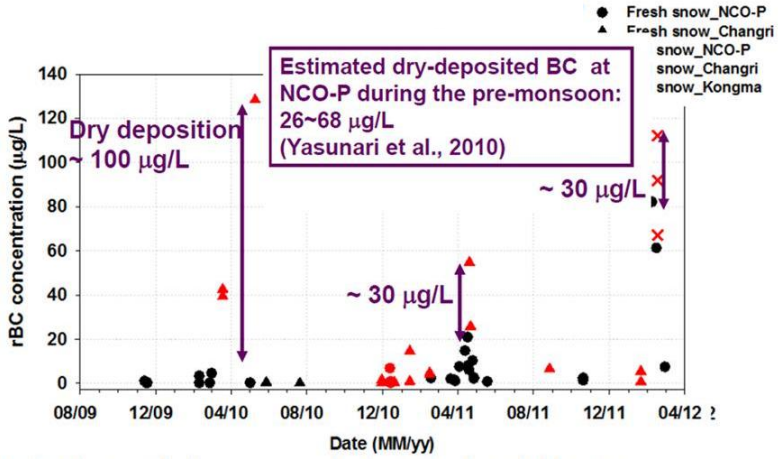

Figure 37 Preliminary results of snow samples analysis in Nepali sites (courtesy of LGGE, Grenoble)

Chemical analysis at Changri Nup glacier /Fug. 37), compared to the analysis carried out at Changir Nup show highest values compared to the samples collected at NCO-P because Changri Nup samples are related to aged snow, while at NCO-P, samples are representatives of fresh snow. For this reason SP2 results at NCO-P, comparable to the estimation of BC deposition in fresh snow calculated from atmospheric BC concentrations, are consistent and confirmed the estimation done by Yasunari et al,. 2010 for the premonsoon season.

Annual cycle is very similar to atmospheric BC in fresh and old snow, while BC in the older snow (Changri) tends to be higher then in fresh snow (Pyramid) during the same season, Field results confirmed that a strong dry deposition is present during premonsoon season.

Chapter 4

Discussion

Table 15 summarizes the features of the ChagriNup and the Forni glaciers. Glaciers' length is the same and the areas, even if similar for dimensions, highlight that Forni Glacier is a debris free glacier, while the ChangriNup shows a heavy debris coverage thus making it an actual debris covered glacier. In fact, only the 35% of the glacier surface is debris free. On this smaller sector we focused our attention and the field experiments were performed on this white area. Latitude and elevation ranges influence glacier micrometeorology and surface energy components. Contribution of SW radiation is higher in both sites, but in Himalaya, as expected it is higher than in the Alps.

Table 15: Comparison between CangriNup and Forni Glaciers: site characteristics, meteorological and energy balance data.

	ChangriNupGlacier	**Forni Glacier**
Coordinates	28° 00' N; 86° 48' E	46° 23' 56" N; 10° 35' 25" E
Elevation range (m a.s.l.)	5.000-5.700	2.600 – 3.670
Length (km)	3	3
Area (km^2)	7 *(65% debriscovered)*	12 Only medial moraines are present featuring continuous and uninterrupted debris coverage
AWS elevation (m a.s.l.)	5.700	2.631
net SW (W m^{-2})	84	68
net LW (W m^{-2})	-39	-38
SH (W m^{-2})	7	18
LE (W m^{-2})	-2	-5
RS (W m^{-2})	40	36
SW in (W m^{-2})	220	151
SW out (W m^{-2})	136	91
SW in extra (W m^{-2})	465	267
Air temperature °C	-4,6	-1,3
Snow albedo	0,75	0,85
Ice albedo	0,26	0,35

Net longwave radiation is similar, while latent and sensible heat fluxes are higher at the Forni glacier surface. As expected extraterrestrial shortwave radiation is higher at Changri Nup, and the difference between SWextra and SWin shows the impact of clouds and aerosols in absorbing part of the solar radiation reaching the Earth surface.

Average temperature is lower in the Himalayan site, while average snow/ice albedo are similar.

In both glaciers, the melting occurs in summer, the only season during which the combined effect of positive temperature (T>0 °C) and solar radiation allows melting processes. In Himalaya this period correspond to the monsoon season, during which not only T and SW affect glacier surface, but also liquid precipitation. In fact, in Himalaya, the upper limit where snow precipitation occur is located at around 6,000 m asl (RIF) and during the monsoon season, liquid precipitation events accelerate snow melting.

Figure 38 shows daily total liquid precipitation of Kala Patthar AWS, installed at 5,600 m asl close to Everest Base Camp. In monsoon season, total liquid precipitation reach amount of 15-25 mm even at above 5,000 m asl.

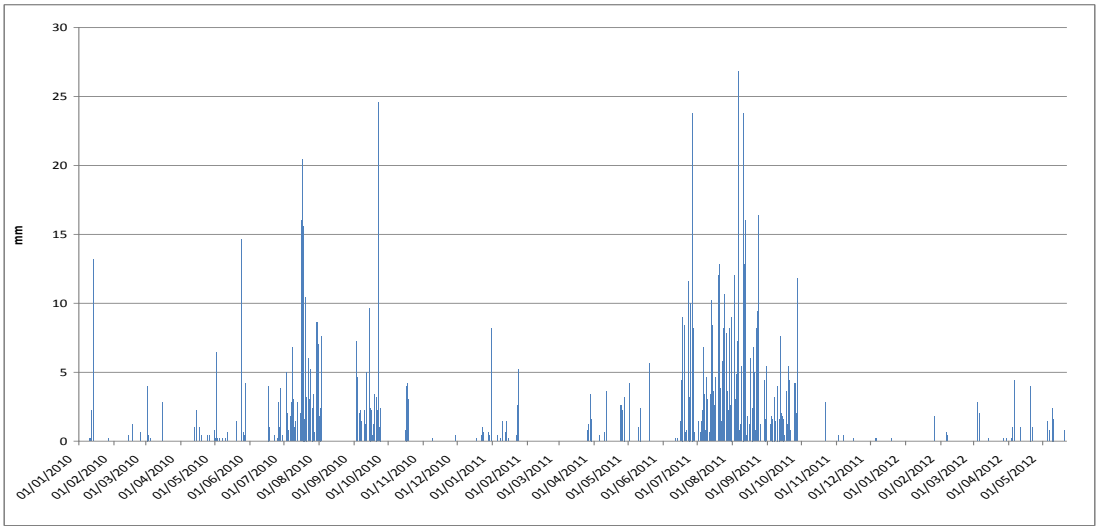

Figure 38:Lliquid precipitation at Kala Patther AWS in 2010-2012.

At the Forni Glacier liquid precipitation occur during summer season and they reach 30-40 cm thus surely affecting glacier melt rates. Rainfall are measured through a rain gauge located on the Forni AWS.

The components of the radiative balance at the melting surface of Forni and Changri glaciers were evaluated from AWSs data for a day with clear sky conditions. Downward longwave radiation (LW in), upward longwave (LW out), the net solar (SW in - SW out), net longwave (LW in - LW out) and net radiation (Rs) were calculated according to Hartmann (1994).

The diagram in figure 39 highlights in both sites the strong influence of the diurnal variation in insulation the surface energy balance. The incoming SW radiation reached high levels (close to 1000 Wm^{-2} in the Alpine site but also superior in the Himalayan glacier), which is typical of a glacier surface on days with few clouds, when the multiple reflections between clouds, snow-covered valley slopes and the glacier surface lead to a peak value comparable to the extraterrestrial irradiance.

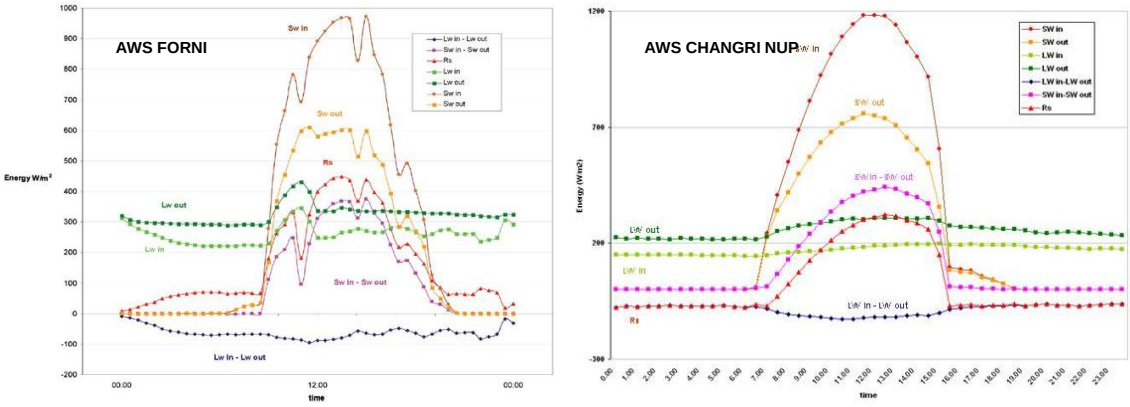

Figure 39.Components of the radiative balance at the melting surface of Forni (Citterio et al., 2007) and Changri Nup glaciers as measured on a day with clear sky conditions from the supraglacial AWSs. SW in= downward shortwave; SW out = upward shortwave; LW in = downward longwave, LW out = upward longwave; SW in - SW out = net solar; Lw in – LW out = net longwave; Rs = net radiation

Differences in precipitation intensity and occurrence and in radiation budget affect glacier melt which results different at the two studied glaciers. Table 16 shows a comparison between Changri Nup and Forni glaciers ice ablation seasons in the time window 2010-2012. The analysis is based on glacier albedo which permits to discriminate between exposed ice surface (lower albedo values) and snow covered surface (higher albedo values). Then it was possible not only to evaluate the temporal length of ice ablation season but also the occurrence of summer snow falls which could impact on magnitude and rates of glacier melting. Length of the ablation season is longer at the Alpine site than in the Himalaya, however number of snowfalls is similar (Tab.16).

Table 16: Comparison between CangriNup (a) and Forni (b) Glaciers: sites snow and ice days and snowfalls during the ice ablation seasons of 2010-2012

(a) CHANGRI NUP	snow		ice						
year	date	albedo	date	albedo	snowdays	tot days	tot snowdays	tot icedays	numsnowfalls
iceablationperiod of 2010			17/05/10	0,37		64	24	40	5
	20/05/10	0,69			3				
			23/05/10	0,36					
	24/05/10	0,85			1				
			01/06/10	0,38					
	17/06/10	0,76			8				
			19/06/13	0,33					
	26/06/13	0,68			2				
			29/06/10	0,32					
	04/07/10	0,56			10				
			14/07/10	0,31					
	19/7/10	**0,68**							
iceablationperiod of 2011			04/06/11	0,37		19	1	18	1
	07/06/13	0,48			1				
			08/06/11	0,39					
	23/6/11	**0,90**							
iceablationperiod of 2012			24/05/12	0,39		38	3	35	1
	18/06/12	0,74			25				
			21/06/12	0,34					
	1/7/12	**0,61**							

(b) FORNI	snow		ice						
year	date	albedo	date	albedo	snowdays	tot days	tot snowdays	tot icedays	numsnowfalls
iceablationperiod of 2010			29/6/10	0,39		88	16,5	71,5	6
	5/8/10	0,95			4				
			9/8/10	0,39					
	16/8/10	0,85			2,5				
			18/8/10	0,30					
	30/8/10	0,70			2,5				
			1/9/10	0,38					
	10/9/10	0,80			0,5				
			10/9/10	0,37					
	13/9/10	0,90			3				
			16/9/10	0,30					
	18/9/10	0,60			4				
			22/9/10	0,36					
	25/9/10	**0,80**							
iceablationperiod of 2011			14/6/11	0,37		115	18	97	3
	20/7/11	0,88			3				
			23/7/11	0,38					
	24/7/11 6.00	0,90			2				
			26/7/11	0,38					
			11/8/11	0,35					
	NO DATA								
			28/8/11	0,27					
	18/9/11	0,90			13				
			1/10/11	0,38					
	7/10/11	**0,9**							
iceablationperiod of 2012			16/6/12	0,30		119	8	111	2
	31/8/12	0,88			4				
			4/9/12	0,31					
	12/9/12	0,90			4				
			16/9/12	0,30					
	13/10/12	**0,8**							

Comparing the components of surface energy fluxes at Changi Nup (Fig. 40) and at Forni Glacier (Fig. 41), it is evident that in both sites RS and net SW play a fundamental role in determining glacier melting and condensation, and the contribution of net LW is similar in both glaciers for melting and condensation conditions. Sensible and latent heat fluxes play a minor role, with minor contribution at the Changri Nup then at the Forni glacier.

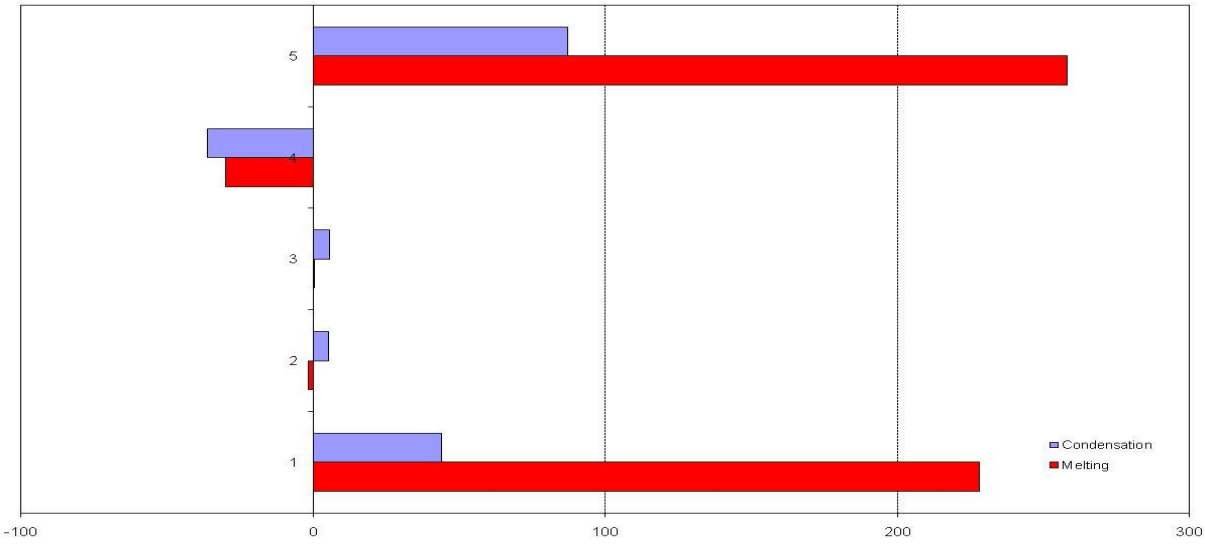

Figure 40: Components of the surface energy flux (from hourly mean values), averaged over time, when melting (red) and condensation (purple) conditions occurred. The units of measure for the x-axis are W m^{-2}

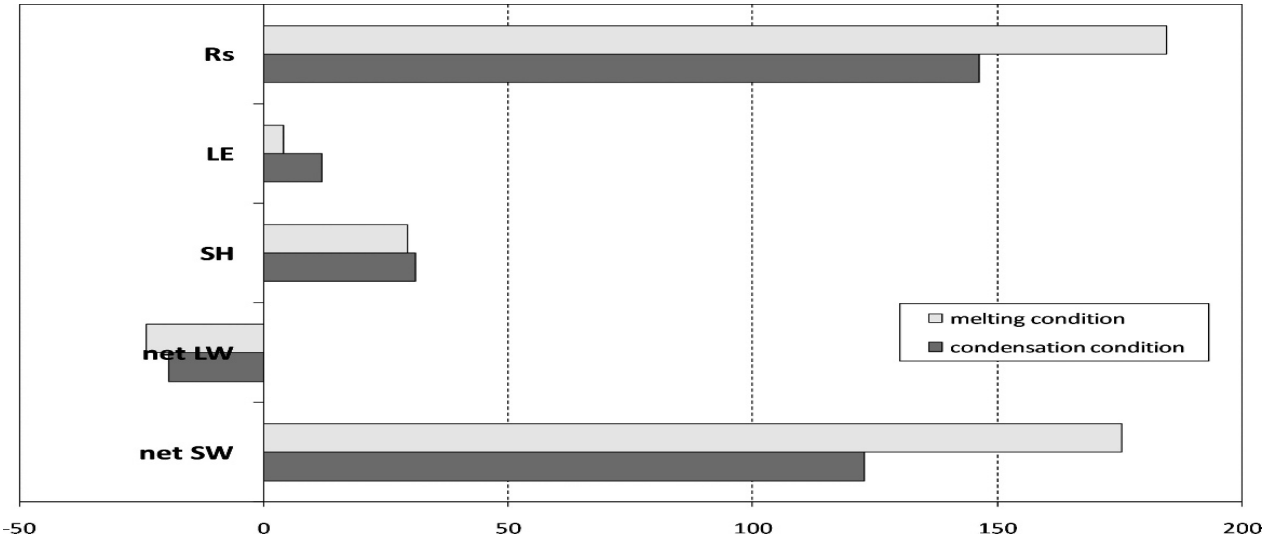

Figure 41: Components of the surface energy flux (from hourly mean values), averaged over time, when melting (i.e. about 31% of the time) (light gray) and condensation (i.e. about 24% of the time) W m^{-2} (Senese at al., 2012)

Moreover melting values obtained from the AWS data were also applied to evaluate the whole meltwater production at the Changri Nup debris free glacier. This evaluation was performed also with the aim to obtain data to be compared with the glacier runoff amount measured by an automatic hydrometer we have just installed at the debris free snout of the Changri Nup Glacier. From the next summer season we will have runoff data to describe glacier meltwater production then distribute ablation data will be fundamental to evaluate reliability and accuracy of hydrological investigations.

With this aim we downloaded the NASA DEM RSTM (Radar Shuttle Topography Mission) surveyed in 2001 and available for free at the NASA site. The DEM has a low spatial resolution (90 x 90 m) but it covers almost the whole Planet thus permitting to apply models for analysing environmental features variability. Among the other features, glacier melting can be distributed and analysed through this DEM. We downloaded DEM data describing Changri Nup area. Moreover though analysing recent satellite imagines (SPOT and Landsat) (Fig. 41) we also delimited the Changri Nup Glacier boundary glacier debris free area resulted about 0,99 km^2 wide (Fig. 42). By coupling DEM and glacier boundary data we calculated the glacier surface area distribution which is the fundamental input data to distribute glacier melt.

Figure 41:: Changri Nup glacier area estimated by analyzing SPOT Imagines.

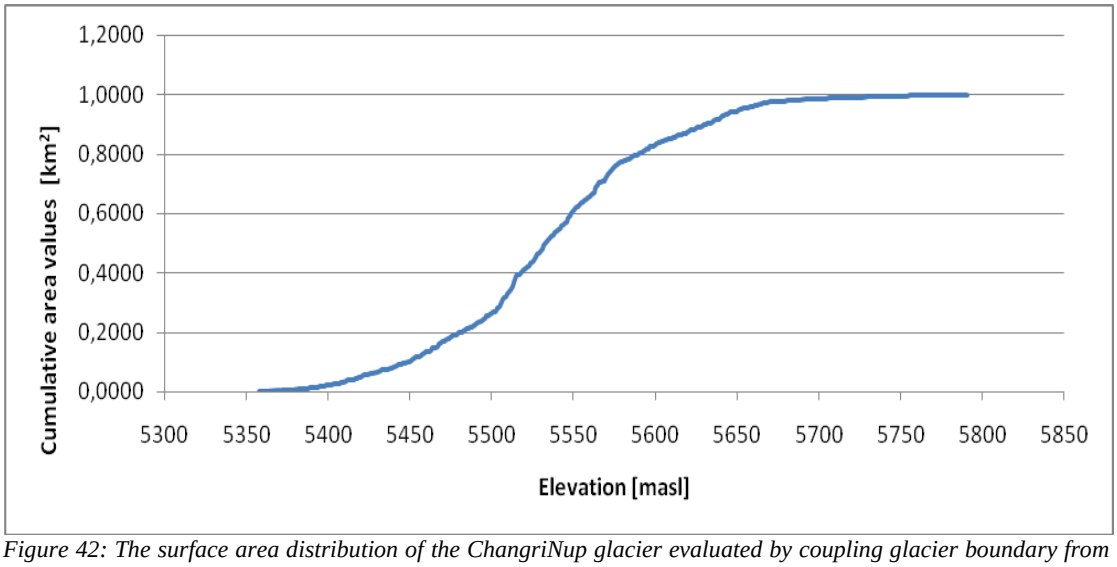

Figure 42: The surface area distribution of the ChangriNup glacier evaluated by coupling glacier boundary from SPOT with glacier DEM from SRTM NASA.

We distributed the glacier melt following a simple approach. We started from melt amount calculated in 2010, 2011 and 2012 from AWS data measured at 5700 m asl.

We applied a vertical ablation rate of 0,007 m w.e./m of elevation (see also Oerlemans, 2001). It means that ablation increases of 0,007m w.e. per an elevation decrease of 1 m. Then glacier zones located upper the AWS result with an ablation minor than the one we calculated at the AWS and glacier areas located lower the AWS have an ablation stronger. The glacier debris free area features an elevation range between 5358 m asl and 5791 m asl.

We divided the glacier area into 293 glacier belts and by a GIS software we evaluated their surface coverage. By applying the vertical melt rate we evaluated for each elevation belt the glacier melt and considering elevation belt area we computed the derived volume of meltwater. The total volume variation resulted to be -2609529,892 m^3w.e. in 2010 corresponding to -2,62 m of mean thickness variation. In 2011 the volume variation resulted to be-2095997,944 m^3w.e. corresponding to -2,02 mw.e. of mean thickness variation and in 2012 the volume change resulted -2728190,672 m^3 w.e. corresponding to -2,74 mw.e. of thickness variation.

Moreover through this simple modelling approach we also evaluated ELA (Equilibrium Line Altitude) of the Changri Nup Glacier. When melt amounts evaluated by applying the vertical gradient results equal to zero it means that ELA has been reached. It has been estimated at 6.000 masl in 2010 and 2012 as highlighted from the previous results showing a similarity in there two years, while in 2011 ELA was estimated at 5.850 m asl.

In summer 2012 (July-October) an atmospheric measurement campaign has been carried out at the Guasti Hut to measure atmospheric composition. In this period atmospheric BC concentrations have been measured continuously. Daily trend of BC concentrations highlight (Fig. 43) conditions sufficiently representative of the free troposphere background conditions. This consideration is due to the fact that daily average BC concentrations represent typical continental background conditions, non predominantly influenced by photochemical transport processes normally occurring at daily scale.
Applying the same methodology used to analyze Changri Nup data, daily atmospheric BC concentrations have been related to albedo values (Fig. 43).

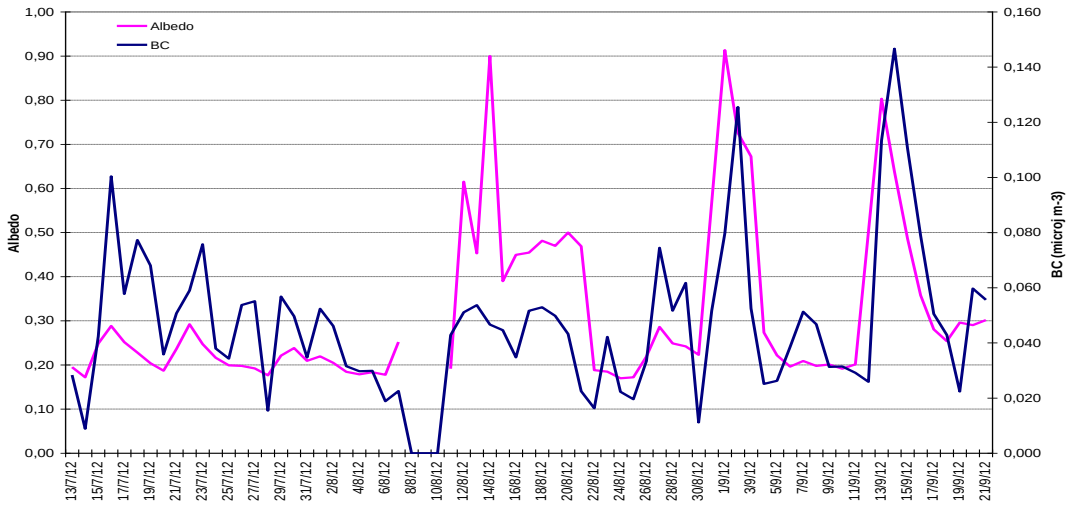

Figure 43: Daily mean albedo values measured at Forni Glacier AWS and daily mean atmospheric BC concentration measured at Guasti Hut in the 2012 summer campaign.

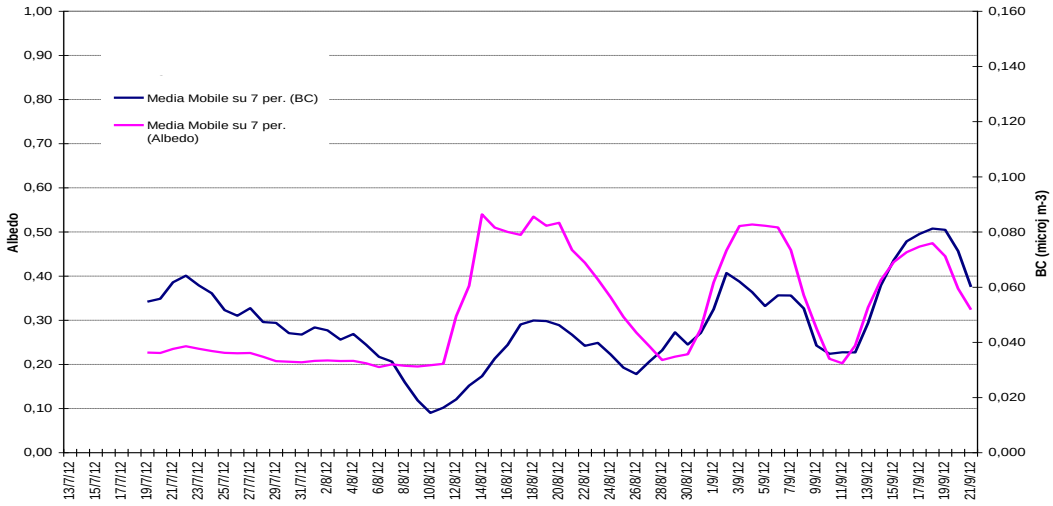

Figure: 44: Moving average (7 Per.) of daily mean albedo values measured at Forni Glacier AWS and daily mean atmospheric BC concentration measured at Guasti Hut in the 2012 summer campaign.

Using the moving average (7 per.) (Fig. 44) it is highlighted that, in this short summer campaign, it seems that there is a correspondence between trend of BC concentration and variation of albedo. In order to quantify the amount of BC deposition in snow, the method of Yasunari et al., 2012 has been applied for the period 13/07-22/09 2012. BC deposition in snow, considering a snow density of 200 kg $m^{-3}$and considering as depth of snow layer 0.02 m has been estimated as: 74 µg m^{-3}., corresponding to 18.5 µg kg^{-1} in snow and to an albedo reduction due to BC impact of 1.97%, using the correlation of Ming at al, 2009).

This estimated results is different from the average albedo reduction determined as difference between the natural snow albedo at Forni glacier and the average albedo in the period of BC measurement.

This result obtained for Forni Glacier is different from the results obtained at ChangiNup, where the percentage of albedo reduction correspondent to the BC deposition in snow calculated from the atmospheric observation at NCO-P station, and the albedo reduction effectively measured at the ChangriNup AWS, are very well correlated.

Both the results obtained in this work have to be consider as a preliminary analysis to be better verified through the analysis of BC concentration in snow measured from samples collected on the field.

However. Some considerations could be done: reduction of albedo estimated consider that the only factor determining this phenomenon is the presence of BC in snow, for this reasons, the difference obtained in the two sites underline that at Changri Nup, this assumption seems to be consistent with the field measurement, thus, the albedo reduction measured after the peak of BC concentrations could be effectively mostly determined by this factor. On the contrary, at Forni Glacier the situation seems to be different, and a possible cause could be that in this site the effect of BC deposition has a lower impact compare to other factors in affecting the reduction of albedo at glacier surface, particular because in the summer campaign BC concentrations was typical of background free troposphere conditions, while at Changri Nup and in Yasunari et al., 2010 considered BC concentration in the atmosphere were related to

the premonsoon season, period on which aereosol concentration are higher and comparable to the concentrations of a polluted site (ref).

In order to verify this hypothesis, more data on atmospheric BC and on BC in snow need to be collected and discussed.

BC concentrations and impact on melting processes are usually analyzed in surface snow or in the ice core, but, the impact of their deposition on the ice surface is another important issue to be studied.

In both sites samples for the chemical-physics analysis have been collected in order to identify the seasonal evolution of the debris fraction covering the glacial surface, not classified as fine debris. To collect the samples, surface debris has been removed in an area of 1 m^2 sampled snow have been transported to the laboratory analysis maintaining the temperature below zero, in order to preserve the material., without altering the organic substances, Analysis has been carried out by Roberto Azzoni and Andrea Zerboni from UNIMI.

In laboratory organic substances and organic carbon have been quantified. More repetitive samples have been observed through XRD ant at the electron microscope (SEM) in order to better understand their morphological characteristics (Fig. 45).

Each sediment sub-sample was submitted to a specific analysis and the analytical procedures are summarized as follows: (1) Grain-size analyses (Gale and Hoare, 1991) were performed after removing organics by hydrogen peroxide (130 vol) treatment; sediments were wet sieved (diameter from 1000 to 63 mm), then the finer fraction (63 mm) was determined by aerometer on the basis of Stokes's law. (2) Humified organic carbon was identified by means of the Walkley and Black (1934) method, using chromic acid to measure the oxidizable organic carbon (titration). (3) Total organic carbon (TOC) was estimated by loss on ignition (LOI; Heiri et al., 2001); samples were air-dried and organic matter was oxidized at 500–550°C to carbon dioxide and ash, then the weight lost during the reaction was measured by weighing the samples before and after heating. Additionally, we performed several XRD (X-Ray Diffraction Analysis) on randomly oriented powder from the bulk debris samples to investigate the mineralogical properties of the fine debris.

Moreover samples have been observed through at the electron microscope (SEM) in order to better understand their morphological characteristics (Fig. 15).

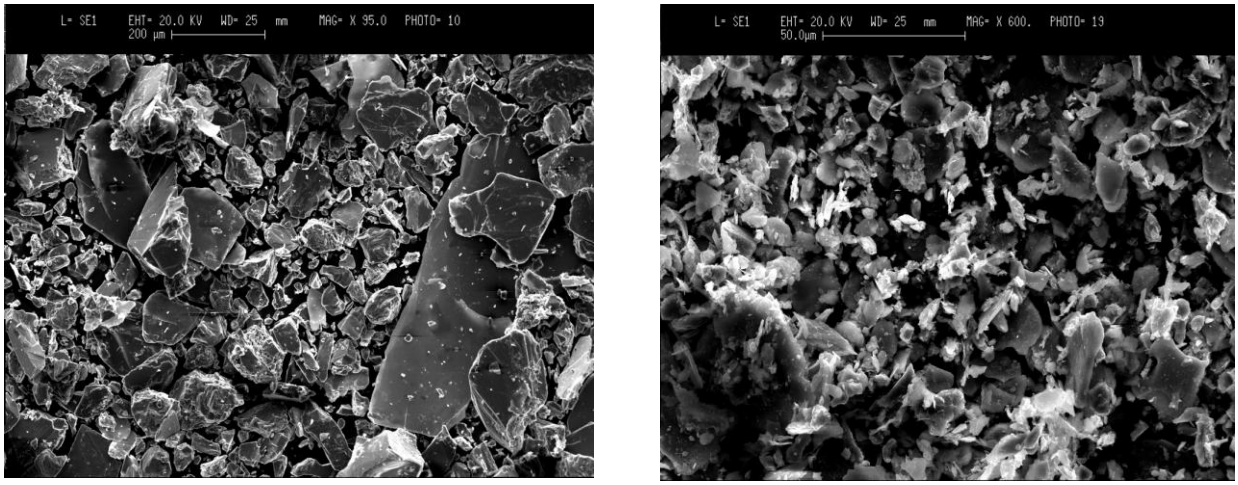

Figure 45: SEM analysis at ChangriNup (left image) and at Forni Glacier (right image)

Debris deposited in both sites is made up of similar granolometry fractions. Grain has high angular, underlining a minimal surface transport. EDS analysis show that mineral grain are compatible with the geological substrate, and in these preliminary work, no alloctonous contribution has been found (e.g. long range transport phenomena) (Fig. 45).

Figure 46 reveals an initial alteration stage of the mineral fraction, while poor and difficultly evident is the new formation of minerals due to the effect of the pedogenesis. An initial interaction between mineral and organic is present.

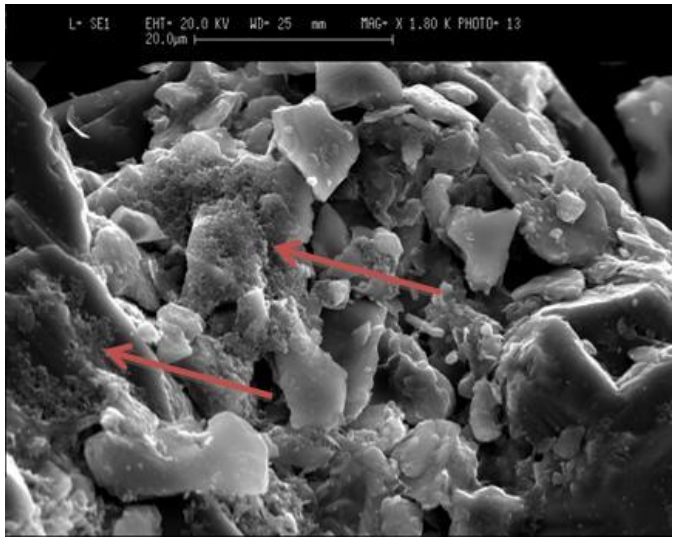

Figure 46: Mineral analysis at Changri Nup

Same analyses have been carried out at Forni Glacier for a longer period (Fig. 48). From the beginning and the end of the season, grain size fraction of the debris remain the same, but at SEM it is observed that at the end of the season mineral grain are organized in aggregate microscopic aggregates, probably related to the presence of organic matter that constitutes complexes between mineral and organic molecules. The origin from local rock substrate is also confirmed (Fig. 48).

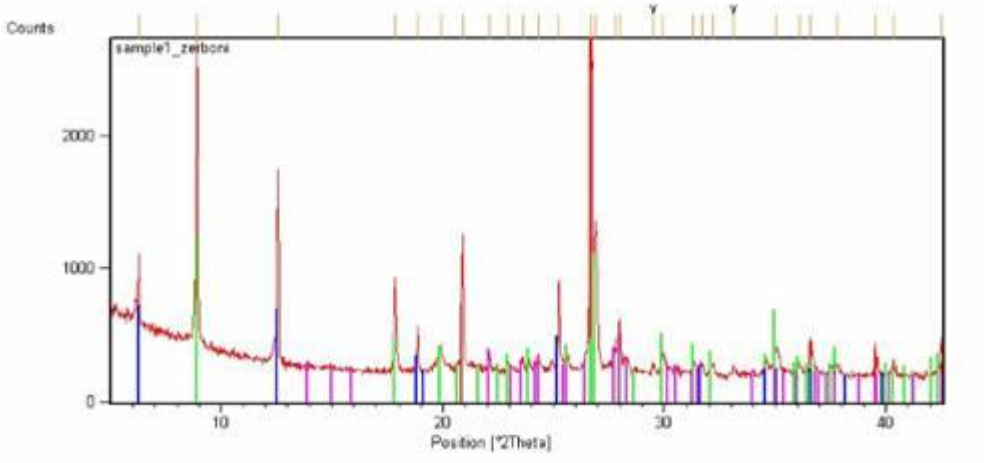

Figure 48: SEM analysis at Forni Glacier

Organic traces are present at a minimum level at the beginning of the season, while major concentration of organic substances at the end of the season if demonstrated by the bulk chemical analysis and a big increase is evident at SEM too.

There is a good interaction between organic and mineral fraction with clay mineral (probably newly formed) that cover the organic filaments (Fig. 49).

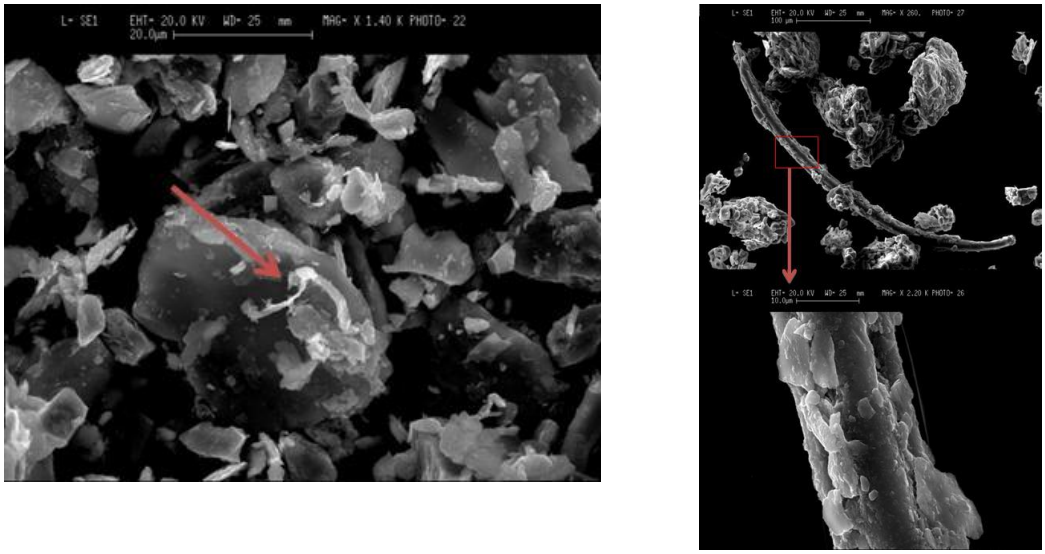

Figure 49: SEM analysis at Forni Glacier and presence of organic traces

Chapter 5

Conclusion

Himalyan and Alpine debris free glaciers are both subjected to the impact of climate variations which in the last decades are driving stronger melting processes thus impacting future water availability. In remote sites, and particularly in the Himalaya, the quantification of this melting amount is difficult due to the lack of permanent monitoring sites and long term reliable data.

The Himalayan situation allows to identify a clear regression of the larger glaciers, whose terminus tongues reach now the lowest levels (about 4.000 m asl), with a thinning rate ranging from 8 to 10 m below 4.400 m asl, Such loss varies 4 to 7 m between 4.400 and 5000 m asl and become higher up to 5.000 m asl (Bhertier at al., in press).

In the Alps too, regression processes are predominant. The Lombardy glaciers had lost c. 20% of their surface coverage in the time window 1992-2003 (Diolaiuti et al., 2012a) and the Aosta valley glaciers had reduced their surface area of about 1/4th over the last 30 years (time window 1975-2005, further details in Diolaiuti et al., 2012b). Moreover the glacier thinning rate is strong and stronger and during the last 6 years the Forni glacier tongue decreased its thickness of about 4-5 m per year at an elevation of 2700 m asl (Senese et al., 2012a; 2012b).

As reported in the figure below, mountain atmospheric structure and transport in mountain regions, in clear sky conditions and solar irradiance typical of a summer day, could be summarize as follows

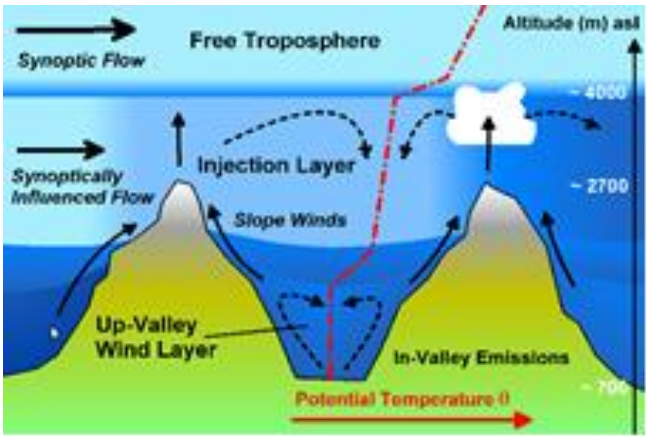

Figure 50: Atmospheric structure and transport process in mountain regions (Henne et al., 2004).

It has been recently put in evidence that the factors driving ablation, are not only related to the radiative forcing at glacier surface and climate conditions, but also to the effect of deposition of deposition of absorbing aerosol and dust at the glacier surface, varying the albedo and thus accelerating melting. The quantification of this effect is now been estimating and the study is still in progress.

These main aspects: surface and energy balance at glacier surface, and effect of BC deposition in albedo reduction have been experimentally evaluated in two glacial sites: the Changri Nup (5.500 masl) in the Nepal Himalaya and the Forni Glacier (2.600 m asl) in the Italian Alps.

In both sites the ablation season occur in summer season, during which the condition of temperature and solar radiation reaching glacial surface are favourable to drive melting processes. The two site, characterized by different latitude, elevation and climate regime, has similarity in indentifying the components mainly contributing to the melting, which are the positive temperature and the shortwave radiation, while in both cases sensible and heat fluxes have a minor effect. The ablation season at Forni Glacier is longer, while ay the Changri Nup the rainy season contributes to increase surface melting.

Close to both the supraglacial AWSs of Changri Nup and Forni glaciers, atmospheric BC concentrations have been monitored, The analysis of BC deposition in snow calculated from atmospheric data and the % of the albedo reduction has been more consistent with the estimation available in literature for Changri Nup site, where the highest amount of BC in the atmosphere during premonsoon season allows a consistent correlation with the % of albedo reduction measured and calculated. On the contrary at Forni Glacier, this correlation has been not so evident probably due to the lowest concentration of BC concentration in the period of the summer campaign and the fact that the deposition of other components such as fine debris, vegetation spores, yeasts and bacteria etc. could have a major effect in this case.

The importance of analyzing BC in snow is fundamental to understand the impact on glacier, completing the study related to their effect in the atmosphere and on climate. BC radiative forcing in the atmosphere is very high, moreover they have a cooling effect on the Earth surface, reducing the amount of the solar radiation reaching the Earth. Since BC are considered a short-lived climate pollutant (SLCP), their mitigation could have an immediate effect on climate and environment.

Field measurements on the glaciers are fundamental to con tribute to the understanding of water availability future scenarios, thus, the estimation of water loss needs to be validated by the positioning of hydrometric station in order to measure glacier water discharge, thus estimation at Changri Nup glacier will be compared to flow measurements.

Future step will foresee a more detailed analysis of these results, thanks also to the availability of long term dataset, moreover, in order to improve the knowledge of the effect of dust and aerosol deposition on glacier, more samples will be collected and analyzed.

Ringraziamenti

Questo progetto di tesi si è svolto nell'ambito del progetto Ev-K2-CNR/SHARE finanziato dal Ministero dell'Istruzione, dell'Università e della Ricerca attraverso il CNR e da Regione Lombardia attraverso la Fondazione Lombardia per l'Ambiente.

Ringrazio il Prof. Smiraglia e il Dott. Bonasoni per avermi dato l'opportunità di realizzare questo progetto di Dottorato e per l'importante contributo nell'analisi dei risultati e stesura della Tesi.

Un grazie di cuore alla Dott.ssa Diolaiuti per la l'insostituibile supporto durante tutte le fasi del lavoro e la grandissima disponibilità ogni qualvolta sia stato necessario.

Un ringraziamento particolare ad Agostino Da Polenza, per avermi permesso di portare avanti questo progetto e soprattutto per avermi dato l'opportunità di conoscere l'Everest, il K2, la Piramide e il fascino delle tante storie e tradizioni che questi bellissimi posti racchiudono.

Grazie a Gian Pietro Verza che dal 2004 mi ha insegnato a lavorare ad oltre 5.000 m di quota, non solo per l'insostituibile supporto nelle fasi di installazione e gestione della strumentazione utilizzata per questa tesi, ma soprattutto per aver fatto sembrare meno faticose le giornate e le lunghe salite anche quando, soprattutto all'inizio di quest'esperienza, non lo erano affatto!

Ringrazio tutto lo staff della Piramide per aver seguito tutte le attività di campo e aver contribuito al buon funzionamento del set up strumentale.

Grazie a tutte le persone che hanno contribuito in modo importante a questo lavoro di testi ed in particolare ad Antonella, Paolo C. ed Elisa B., ma anche a Paolo S. Angela, Tony, Daniele, Marcello, Roberta, Alberto, Carlo e Andrea.

Un ringraziamento particolare alla mia famiglia, in primis ai miei genitori che hanno supportato e sostenuto il mio percorso formativo, ad Alexey, per aver sopportato con incredibile pazienza la frenesia e lo stress di questo ultimo periodo, e soprattutto alla nostra piccola Alice, il regalo più bello.

References

Ageta, Y., Kadota, T. (1992). Predictions of changes of glacier mass balance in the Nepal Himalaya and Tibetan Plateau: A case study of air temperature increase for three glaciers. Ann. Glaciology, 16, 89–94.

Ahlmann W.H. (1948). Glaciological research on the North Atlantic coasts. Research Series 1, London: Royal Geographical Society, 66 pp.

Aizen, V.B., Aizen, E.M. (1994). Regime and mass-energy exchange of subtropical latitude glaciers under monsoon climatic conditions: Gongga Shan, Sichuan, China. Journal of Mountain Research and Development 14, 101–118

Aizen,V.B., Aizen, E.M., Nikitin, S.A. (2002). Glacier regime on the northern slope of the Himalaya (Xixibangma glaciers), Quaternary International, 97–98, 27–39.

Akhtar, M., Ahmad, N., Booij, M.J. (2008). The impact of climate change on the water resources of Hindukush–Karakorum–Himalaya region under different glacier coverage scenarios, Journal of Hydrology (2008) 355, 148-163

Ambach, W. (1963) Untersuchungen zum Energieumsatz in der Ablationzone des Gronlandischen Inlandeises. Meddelelser om Grønland, 174: 4–311.

Andreae, M.O. and Crutzen, P.J. (1997). Atmospheric Aerosols: Biogeochemical Sources and Role in Atmospheric Chemistry. Science 276 (5315): 1052–1058

Aoki, T., T. Aoki, M. Fukabori, A. Hachikubo, Y.Tachibana and F. Nishio. (2000). Effects of snow physical parameters on spectral albedo and bidirectional reflectance of snow surface. Journal of Geophysical Research , vol. 105, no. D8, 10219-10236

Aoki, T., H. Motoyoshi, Y. Kodama, T. J. Yasunari, K. Sugiura and H. Kobayashi. (2006). Atmospheric Aerosol Deposition on Snow Surfaces and Its Effect on Albedo. Sola , vol. 2, 13-16

Aoki, T., H. Motoyoshi, Y. Kodama, T.J. Yasunari and K. Sugiura. (2007). Variations of the snow physical parameters and their effects on albedo in Sapporo, Japan. Annals og Glaciology, 46, n. 1, 375-381

Bajracharya, B., K. Uddin, N. Chettri, B. Shrestha, and A. S. Siddiqui. (2010). Understanding land cover change using a harmonized classification system in the Himalayas: A case study from Sagarmatha National Park, Nepal. *Mountain Research and Development* 30 (2):143–156.

Barros, A. P. and Lang, T. (2003). Exploring Spatial Modes of Variability of Terrain-Atmosphere Interactions in the Himalayas During Monsoon Onset. Hydrosciences Report Series 03–001, Environmental Sciences and Engineering Program, Division of Engineering and Applied Sciences, Harvard University, 51, 2003b.

Bavay, M., Lehning, M., Jonas, T., and Lowe, H. (2009). Simulations of future snow cover and discharge in Alpine headwater catchments, Hydrol. Process., 23, 95–108, 10 doi:10.1002/hyp.7195.

Becker, A. & Bugmann, H. (1997). Predicting global change impacts on mountain hydrology and ecology: integrated catchment hydrology/altitudinal gradient studies. IGBP Report No. 43, IGBP Secretariat, Stockholm, Sweden

Beniston M. (2003). Climatic Change in mountain regions: a review of possible impacts. Climatic change, 59, 5–31

Berthier, E., Arnaud, Y. Kumar, R., Ahmad, S., Wagnon, P., Chevallier, P. (2007). Remote sensing estimates of glacier mass balances in the Himachal Pradesh (Western Himalaya, India), Rem. Sens. of Environ., 108, 327–338

Bintanja, R. and M.R. van den Broeke, 1996: The influence of clouds on the radiation budget of ice and snow surfaces in Antarctica and Greenland in summer. Int. J. Climatol., 16, 1281-1296.

Bird, R. E., and R. L. Hulstrom. (1981). Simplified Clear Sky Model for Direct and Diffuse Insolation on Horizontal Surfaces. Technical Report No. SERI/TR-642-761, Golden, CO: Solar Energy Research Institute http://www.nrel.gov/rredc/pdfs/761.pdf.

Bjornsson, H. (1972). Bæsigisarjo¨ kull, north Iceland. Results of glaciological investigations 1967–1968. Part II. The energy balance. Jo¨kull, 22: 44–59.

Bollasina, M., L. Bertolani, and G. Tartari, 2002: Meteorological observations in the Khumbu Valley, Nepal Himalayas, 1994-1999, Bulletin of Glaciological Research, 19, 1-11.

Bonasoni, P., P. Laj, A. Marinoni, M. Sprenger, F. Angelini, J. Arduini, U. Bonafè, F. Calzolari, T. Colombo, S. Decesari, C. Di Biagio, A. G. di Sarra, F. Evangelisti, R. Duchi, M. C. Facchini, S. Fuzzi, G. P. Gobbi, M. Maione, A. Panday, F. Roccato, K. Sellegri, H. Venzac, G. P. Verza, P. Villani, E. Vuillermoz & P. Cristofanelli. (2010). Atmospheric Brown Clouds in the Himalayas: first two years of continuous observations at the Nepal Climate Observatory at Pyramid (5079 m). In: Special Issue "Atmospheric Brown Clouds in the Himalayas" Atmospheric Chemistry and Physics, 10: 7515-7531.

Bonasoni, P.; Laj, P.; Angelini, F.; Arduini, J.; Bonafè, U.; Calzolari, F.; Cristofanelli, P.; et. al. (2008). The ABC-Pyramid Atmospheric Research Observatory in Himalaya for aerosol, ozone and halocarbon measurements. Science of the Total Environment, The Volume: 391, Issue: 2-3, pp. 252- 261

Bond, T., E.Bhardwaj, R. Dong, R. Jogani, S. Jung, C. Roden, D. G. Streets and NM. Trautmann (2007) Historical emissions of black and organic carbon aerosol from energy-related combustion, 1850–2000. GLOBAL BIOGEOCHEMICAL CYCLES, VOL. 21, GB2018, doi:10.1029/2006GB002840,

Boroneant, C., Plaut, G., Giorgi, F., Bi, X. (2006). Extreme precipitation over the Maritime Alps and associated weather regimes simulated by a regional climate model: Present-day and future climate scenarios, Theor. Appl. Climatol. 86, 81–99

Brock, B. W., Mihalcea, C., Kirkbride, M., Diolaiuti, G., Cutler, M., and Smiraglia, C. (2010). Meteorology and surface energy fluxes in the 2005–2007 ablation seasons at Miage debriscovered glacier, Mont Blanc Massif, Italian Alps. Journal of Geophysical Research, 115: D09106, doi:10.1029/2009JD013224.

Bultot, F., Gellens, D., Schadler, B., and Spreafico, M. (1994) Effects of climate change on snow accumulation and melting in the Broye catchment (Switzerland), Climate Change, Vol. 28, pp. 339-363.

Byers, A. (2005). Contemporary human impacts on alpine ecosystems in the Sagarmatha (Mt Everest) National Park, Khumbu, Nepal. *Annals of the Association of American Geographers* 95 (1):112–140

Capello, C. F. (1959–1960). Ricerche di microclimatologia sulla superficie glaciale del Miage. Bollettino del Comitato Glaciologico Italiano, 9(II serie, parte prima): 95–154.

Caroli, P. (2008). Visitor Survey—Sagarmatha National Park HKKH Partnership Project Working Paper. Kathmandu, Nepal: HKKH Partnership Project. http://hkkhpartnership.org; accessed on 14 April 2010.

Chalise, S. R., Kansakar, S. R., Rees, G., Croker, K., Zaidman, M. (2003). Management of water resources and low flow estimation for the Himalayan basins of Nepal, J. of Hydrol., 282, 25–35

Citterio, M., G. Diolaiuti, C. Smiraglia, G.P. Verza, E. Meraldi (2007). Initial results from the Automatic Weather Station (AWS) on the ablation tongue of Forni Glacier (Upper Valtellina, Italy). Geografia Fisica e Dinamica Quaternaria, 30: 141-151

Collins, R., Whitehead, P., Butterfield, D. (1999). Nitrogen leaching from catchments in the Middle Hills of Nepal: an application of the INCA model. Science of the Total Environment 228, 259-274

Daconto, G. and L. N. Sherpa. (2010). Applying scenario planning to park and tourism management in Sagarmatha National Park, Khumbu, Nepal. *Mountain Research and Development* 30 (2):103–112

De Ruyter De Wildt M., Oerlemans J. & Biornssonn H. (2003) – A calibrated mass balance model for Vatnajokull, Iceland. Jokull, 52(161), 1-20

Diaz H. F. & Bradley R.S. (1997). Temperature variations during the last century at high elevation sites. Climatic Change, 36, 253–279

Diolaiuti, G., Bocchiola, D., D'agata, C., Smiraglia, C., (2012b) Evidence of climate change impact upon glaciers' recession within the Italian alps: the case of Lombardy glaciers, Theoretical and Applied Climatology, 109(3-4), 429-445. DOI: 10.1007/s00704-012-0589-y.
http://www.springerlink.com/content/jp57023765r31436/

Diolaiuti, G., Bocchiola, D., Vagliasindi, M., D'agata, C., Smiraglia, C., (2012a)The 1975-2005 glacier changes in Aosta Valley (Italy) and the relations with

climate evolution, Progress in Physical Geography, Volume 36 Issue 6,764-785. DOI: 10.1177/0309133312456413

Diolaiuti G, Smiraglia C (2001b) A new method for sustainable ecotourism in protected mountain environment areas: the glacier trails in the Lombardy Alps. Geotema 14:42–45

Diolaiuti G, Smiraglia C (2010) Changing glaciers in a changing climate: how vanishing geomorphosites have been driving deep changes on mountain landscape and environment. Geomorph Relief Proc Environ 2:131–152

DNPWC [Department of National Park and Wildlife Conservation]. (2003). Sagarmatha National Park Buffer Zone (SNPBZ) Management Plan 2004–2008. Kathmandu, Nepal DNPWC.

Drogue, G., Pfister, L., Leviandier, T., El Idrissi, A., Iffly, J.-F., Matgen, P., Humbert, J., and Hoffmann, L. (2004). Simulating the spatio-temporal variability of streamflow response to climate change scenarios in a mesoscale basin, J. Hydrol., 293(1–4), 255–269

Dyurgerov, M.B., and M.F. Meier. (2005). Glaciers and the changing Earth system: A 2004 snapshot. Occasional Paper No. 58

Flanner M.G., Zender C.S., Hess P.G., Mahowald N.M., Painter T.H., Ramanathan V. & Rasch P.J. (2009). Springtime warming and reduced snow cover from carbonaceous particles. Atmospheric Chemistry and Physics, 9, 2481-2497.

Fukui Kotaro, Fujii Yoshiyuki, Mikhailov Nikolai, Ostanin Oleg, Iwahana Go (2007). The lower limit of mountain permafrost in the Russian Altai Mountains, Permafrost and Periglacial Processes, Volume 18 Issue 2, 129 – 136

Garavaglia V., G. Diolaiuti , C. Smiraglia, V. Pasquale, M. Pelfini (2012) Evaluating Tourist Perception of Environmental Changes as a Contribution to Managing Natural Resources in Glacierized Areas: A Case Study of the Forni Glacier (Stelvio National Park, Italian Alps). Environmental ManagementDOI 10.1007/s00267-012-9948-9

Greuell J.W., Knap W. & Smeets P. (1997). Elevational changes in meteorological variables along a midlatitude glacier during summer. Journal of Geophysical Research, 102 (D22), 25941-25954

Guglielmin M, Nardo A, Smiraglia C (1995) Lo spessore dei ghiacciai della Valfurva. Misurazioni tramite Sondaggi Elettrici Verticali. Neve e Valanghe 24:58–67

Hagg, W. & L. N. Braun (2005). The influence of glacier retreat on water yield from high mountain areas: Comparison of Alps and Central Asia. In: De Jong, C.; Ranzi, R.; Collins, D. (eds.) Climate and Hydrology in Mountain Areas, p263-275

Hannah, D.M., Kansakar, S.L., Gerrard, A.J., Rees, G. (2005). Flow regimes of Himalayan rivers of Nepal: nature and spatial patterns, Journal of Hydrology 308, 18–32

Hansen, J., and L. Nazarenko (2004) Soot climate forcing via snow and ice albedos. Proc. Natl. Acad. Sci. , 101, 423-428, doi:10.1073/pnas.2237157100.

Hartmann DL (1994) Global physical climatology. International geophysics 56, 411 pp

Henne, S., Furger, M., Nyeki, S., Steinbacher, M., Neininger, B., de Wekker, S. F. J., Dommen, J., Spichtinger, N., Stohl, A., and Prevot, A. S. H.: Quantification of topographic venting of boundary layer air to the free troposphere, Atmos. Chem. Phys., 4, 497–509, doi:10.5194/acp-4- 497-2004, 2004.

Hogg, I. G. G., Paren, J. G., and Timmis, R. J. (1982). Summer heat and ice balances on Hodges Glacier, South Georgia, Falkland Islands Dependencies. Journal of Glaciology, 28(99): 221–228

Hoinkes H.C. & Steinacker H. (1975). Hydrometeorological implications of the mass balance of Hintereisferner, 1952-53 to 1968-69. In Proceedings of the Snow and Ice Symposium, Moscow 1971, Wallingford: IAHS Publication 104, 144-49

Hoinkes H.C. & Untersteiner N. (1952). Wärmeumsatz und Ablation auf Alpengletschern I. Vernagtferner (Oetztaler Alpen), August 1950. Geografiska Annaler, 34 (1-2), 99-158

Hoinkes H.C. (1955). Measurements of ablation and heat balance on alpine glaciers. Journal of Glaciology 2, 497-501

Immerzeel, W.W., Droogers, P. de Jong, Bierkens, M.F.P. (2009). Large-scale monitoring of snow cover and runoff simulation in Himalayan river basins using remote sensing, Remote Sensing of Environment 113 (2009) 40–49

IPCC (2007). Climate Change 2007: The Physical Science Basis. Contribution of Working Group I to the Fourth Assessment Report of the Intergovernmental Panel on Climate Change [Solomon, S., D. Qin, M. Manning, Z. Chen, M. Marquis, K.B. Averyt, M. Tignor and H.L. Miller (eds.)]. Cambridge University Press, Cambridge, United Kingdom and New York, NY, USA, 996 pp.

Irvine-Fynn, T., Bridge, J., Hodson A., 2010. Rapid quantification of cryoconite: granule geometry and in situ supraglacial extents, using examples from Svalbard and Greenland. Journal of Glaciology. 56 (196), 297-308.

Ishikawa N., Owens I.F. & Sturman A.P. (1992). Heat balance studies characteristics during fine periods on the lower parts of the Franz Josef Glacier, South Westland, New Zeland. International Journal of Climatology, 12, 397-410.

Jacobsen J, Steen K (2007) Use of landscape perception methods in tourism studies: a review of photo-based research approaches. Tour Geogr 9(3):234–253

Kang, B. and J. A. Ramírez (2007) The Response of Streamflow to weather variability under climate change conditions in the Colorado Rockies. Journal of Hydrologic Engineering. doi: 10.1061/(ASCE)1084-0699 (2007)12:1(63)

Kapos V., et al. (2000). Developing a Map of the World's Mountain Forests. In: Price M. F. & Butt N. eds., Forests in a Sustainable Mountain Environment, CAB International, Wallingford.

Kaspari S., M. Schwikowski, M. Gysel, T.H. Painter. *In press*. Spatial and seasonal variations in black carbon concentrations in snow and ice in the Solu-Khumbu, Nepal.

Klok E.J. & Oerlemans J. (2002). Model study of the spatial distribution of the energy and mass balance of Morteratschgletscher, Switzerland. Journal of Glaciology, 48(163), 505-518

Klok E.J. & Oerlemans J. (2004). Modelled climate sensitivity of the mass balance of Morteratschgletscher and its dependence on albedo parameterization. International Journal of Climatology, 24, 231-245

Lau, K. M., Kim, M. K., and Kim, K. M.: Asian summer monsoon anomalies induced by aerosol direct forcing: the role of theTibetan Plateau, Clim. Dynam., 26(7–8), 855–864, 2006.

Lau, K. M., Ramanathan, V.,Wu, G.-X., Li, Z., Tsay, S. C., Hsu, C., Sikka, R., Holben, B., Lu., D., Tartari, G., Chin, M., Koudelova Atmos. Chem. Phys., 10, 6603–6615, 2010 www.atmos-chem-phys.net/10/6603/2010/

T. J. Yasunari et al.: NCO-P data and snow albedo changes over Himalayan glaciers 6615 P., Chen, H., Ma, Y., Huang, J., Taniguchi, K., and Zhang, R.:The Joint Aerosol-Monsoon Experiment - A new challenge for monsoon climate research, B. Am. Meteorol. Soc., 89(3), 369–383, doi:10.1175/BAMS-89-3-369, 2008.

Lau, K. M., Kim, M. K., and Kim, K. M.: Enhanced surface warming and snow melt in the Himalayas and Tibetan Plateau induced by the EHP effect, Environ. Res. Lett., 5, 025204,doi:10.1088/1748-9326/5/2/025204, 2010.

Marinoni, A., P. Cristofanelli, P. Laj, R. Duchi, F. Calzolari, S. Decesari, K. Sellegri, E. Vuillermoz, G.P. Verza, P. Villani & P. Bonasoni. (2010). Aerosol mass and black carbon concentrations, a two year record at NCO-P (5079 m, Southern Himalayas). In: Special Issue "Atmospheric Brown Clouds in the Himalayas" Atmospheric Chemistry and Physics, 10: 8551-8562

McConnell, J. R., Edwards, R., Kok, G. L., Flanner, M. G., Zender, C. S., Saltzman, E. S., Banta, J. R., Pasteris, D. R., Carter, M. M., and Kahl, J. D. W.: 20th-century industrial black carbon emissions altered arctic climate forcing, Science, 317, 1381-1384, 10.1126/science.1144856, 2007.

Meybeck M., et al. (2001). A New Typology for Mountains and other Relief Classes: An Application to Global Continental Water Resources and Population Distribution. Mount. Res. Dev. 21, 34–45

Ming, J., Cachier, H., Xiao, C., Qin, D., Kang, S., Hou, S., Xu, J., 2008. Black carbon record based on a shallow Himalayan ice core and its climatic implications. Atmos. Chem. Phys. 8, 1343–1352.

Ming J., C. Xiao, H. Cahier, D, Qin, X. Qin, Z. Li, J. Pu (2009). Black Carbon (BC) in the snow of glaciers in west China and its potential effects on albedos. Atmospheric Research 92, 114–123

Munro D.S. & Davies J.A. (1978) - On fitting the log-linear model towind speed and temperature profiles over a melting glacier. Boundary-Layer Meteorology, 15, 423-437

Munro D.S. (1989) - Surface roughness and bulk heat transfer on a glacier:comparison with eddy correlation. Journal of Glaciology, 35, 343-348

Nepal, S. K. (2008). Tourism-induced rural energy consumption in the Annapurna region of Nepal. *Tourism Management* 29:89–100

Oerlemans, J. (1996): Modelling the response of valley glaciers to climatic change. In ERCA Volume 2 (ed.: C Boutron), Les Editions de Physique, 91-123

Oerlemans J. & Grisogono B. (2002). Glacier winds and parameterization of the related surface heat fluxes. Tellus, 54A: 440-452.

Oerlemans J. (2010). The Microclimate of Valley Glaciers. Institute for Marine and Atmospheric Research Utrecth, Utrecth University, The Netherlands, pp. 138.

Oerlemans, J. (2005). The microclimate of glaciers. Lecture notes from Karthaus summer school 2005, Utrecth University.

Oerlemans, J., (2000) Analysis of a 3 year meteorological record from the ablation zone of Morteratschgletscher, Switzerland: energy and mass balance. Journal of Glaciology, 46(155): 571–579.

Oerlemans, J., (2001). Glaciers and Climate Change. Lisse: Balkema, 115 pp.

Oerlemans, J., (2009). Retreating alpine glaciers: increased melt rates due to accumulation of dust (Vadret da Morteratsch, Switzerland). Journal of Glaciology, 55(192): 729–736

Oerlemans, J., and Klok, E. J., (2002). Energy balance of a glacier surface: analysis of automatic weather station data from the Morteratschgletscher, Switzerland. Arctic, Antarctic, and Alpine Research, 34(4): 477–485.

Oerlemans, J., and Vugts, H. F. (1993). A meteorological experiment in the melting zone of the Greenland Ice Sheet. Bulletin of the American Meteorological Society, 74(3): 355–365.

Oerlemans, J., Bjornsson, H., Kuhn, M., Obleitner, F., Palsson, F., Smeets, P., Vugts, H. F. and De Wolde, J. (1999). Glaciometeorological investigations on Vatnajo¨ kull, Iceland, summer 1996. Boundary-Layer Meteorology, 92: 3–26

Ohata T., Zhongyuan B. & Limgfu D. (1989) - Heat balance study on Glacier No. 1 at head of Urumqi River, Tianshan Mountains, China. Journal of Glaciology and Geocryology, 11, 298-310.

Pandey, M. and B. Basnet. (1987). Chronic Bronchitis and Cor Pulmonale in Nepal. A Scientific Epidemiological Study Monograph. Kathmandu, Nepal Mrigendra Medical Trust.

Pelfini M, Gobbi M (2005) The ecological value of Forni Glacier as a possible new geomorphosite: new data from arthropods communities. Geogr Fis Din Quat 28(2):211–217

Pelfini M (1996) Surface area reduction and rise of the equilibrium line on the Ortles-Cevedale Group (Lombardy, Italy) from the Little Ice Age to present. Riv Geogr Ital 103:63–71

Pelfini M (1987) Contributo alla conoscenza delle variazioni oloceniche del Ghiacciaio dei Forni. Nat Bresc Ann Mus Civ Sci Nat 24:237–257

Polesello, S., Comi, M., Guzzella, L., Marinoni, A., Pecci, M., Roscioli, C., Smiraglia, C., Tartari, G., Teti, P.,Valsecchi, S., Vuillermoz, E. (2007). Chemical composition of fresh snow in the Himalaya and Karakoram, Develop. In Earth Surf. Proc., 10, 251-262

Ramanathan V., and G. Carmichael,.2008. Global and Regional climate change due to Black Carbon. Nature geoscience, Vol 1:221-227

Rees, H.G., Holmes, M.G.R., Fry, M.J., Young, A.R., Pitson, D.G., Kansakar, S.R. (2006). An integrated water resource management tool for the Himalayan region, Environmental Modelling & Software 21, 1001-1012

Reinwarth O. & Escher-Vetter H. (1999). Mass balance of Vernagtferner, Austria, from 1964/65 to 1996/97: results for three sections and the entire glacier. Geografiska Annaler, 81A, 743-51.

Robock, A., et al. (2003). Evaluation of the North American Land Data Assimilation System over the southern Great Plains during the warm season, J. Geophys. Res., 108(D22), 8846, doi:10.1029/2002JD003245.

Salerno, F., E. Buraschi, G. Bruccoleri, G. Tartari, and C. Smiraglia. (2008). Glacier surface-area changes in Sagarmatha National Park, Nepal, in the second half of the 20th century, by comparison of historical maps. Journal of Glaciology 54 (187):738–752.

Salerno, F., E. Cuccillato, P. Caroli, B. Bajracharya, E. C. Manfredi, G. Viviano, S. Thakuri, B. Flury, M. Basani, F. Giannino, and D. Panzeri. (2010). Experience with a hard and soft participatory modeling framework for social-ecological system management in Mount Everest (Nepal) and K2 (Pakistan) protected areas. Mountain Research and Development 30 (2):80–93.

Schneeberger K., M. Schwank, C. Stamm, P. de Rosnayd C. Mätzler and H. Flühler. (2004). Topsoil Structure Influencing Soil Water Retrieval by Microwave Radiometry. Vadose Zone Journal.2004; 3: 1169-1179

Senese A., Diolaiuti D., Mihalcea C. & Smiraglia C. (2012). Energy and mass balance of Forni Glacier (Stelvio National Park, Italian Alps) from a 4-year meteorological data record. Arctic, Antarctic, Alpine Research, 44 (1), 122-134.

Senese A.,DiolaiutiI G., G P Verza & Smiraglia C (2012) - Surface energy budget and melt amount for the years 2009 and 2010 at the Forni glacier (Italian Alps, Lombardy). Geogr. Fis. Dinam. Quat., 35, 69-77, DOI 10.4461/GFDQ.2012.35.7

Senese A., Diolaiuti G., Mihalcea C. & Smiraglia C. (2012) – Energy and mass balance of Forni Glacier (Stelvio National Park, Italian Alps) from a 4-year meteorological data record. Arctic, Antarctic, Alpine Research, 44 (1), 122-134.

Smiraglia C., C. Mayer, C. Mihalcea, G. Diolaiuti, M. Belò & G. Vassena. (2007). Ongoing variations of Himalayan and Karakoram glaciers as witnesses of global changes: recent studies of selected glaciers. In: Baudo, R., G. Tartari & E. Vuillermoz (Eds.). Mountains witnesses of global changes research in the Himalaya and Karakoram; SHARE-Asia project, Developments in Earth Surface Processes, 10: 235-247

Smiraglia, C. (1989) The medial moraines of Ghiacciaio dei Forni, Valtellina, Italy: morphology and sedimentology. Journal of Glaciology, 35(119): 81–84.

Smiraglia C (1984) Le ‘‘tavole di ghiacciaio’’ della Vedretta dei Forni (Gruppo Ortles-Cevedale). Osservazioni morfologiche. Natura- Societa` Italiana Scienze Naturali 75:91–100

Smiraglia C (1985) Il Ghiacciaio dei Forni (Gruppo Ortles-Cevedale) e la sua storia recente. Bollettino Annuario del Comitato Scientifico Centrale del CAI 83:28–84

Ueno, K. and Pokhrel, A. P.: Intra-seasonal variation of surface air temperature in Nepal Himalayas, Mausam, 53, 281–288, 2002.

UNEP [United Nations Environment Programme]–WCMC [World Conservation Monitoring Centre] 2008. Sagarmatha National Park, Nepal. In*:* McGinley, M. and C. J. Cleveland. editors. Encyclopedia of Earth. Washington, DC Environmental Information Coalition, National Council for Science and the Environment.

Van De Wal R.S.W., Oerlemans J. & Van Der Hage J.C. (1991) – A study of ablation variations on the tongue of Hintereisferner, Austria. Journal of Glaciology, 38, 319-324.

Vincent C., Kappenberger G., Valla F., Bauder A., Funk M. & Le Meur E. (2004) - Ice ablation as evidence of climate change in the Alps over the 20th century. Journal of Geophysical Research, 109, D10104, doi:10.1029/2003JD003857.

Wallace, J.M. and P.V. Hobbs. (2006). Atmospheric Science: An Introductory Survey. 2nd Edn, Academic Press, London and San Diego.

Wathne B.M., Battarbee R.W., Johannessen M., Mosello R., Patrick S., Raddum G.G., Rosseland B.O., Lien L., Tait D., Massabuau J.C., et al. and Istituto Italiano Di

Idrobiologia V.P. (1993) – The AL:PE projects, first results and further plans. Mem. Ist. ital. Idrobiol. 52: 341-354.

Wendler G. & Weller G. (1974) - Heat-balance study on Mc-Call Glacier, Brooks Range, Alaska: a contribution to the International Hydrological decade. Journal of Glaciology, 13, 13-26.

Wiscombe W.J. & Warren S.G. (1980b) - *A model for spectral albedo of snow. I. Snow Containing Atmospheric Aerosols*. Journal of the Atmospheric Sciences, 37, 2734-2745.

Whiteman D. (2000) - Mountain Meteorology. Oxford University Press, 355 pp.

Yadav, R. R., Singh, J. (2002). Tree-Ring-Based Spring Temperature Patterns over the Past Four Centuries in Western Himalaya, Quaternary Research 57, 299–305

Yasunari, T.J., P. Bonasoni, P. Laj, K. Fujita, E. Vuillermoz, A. Marinoni, P. Cristofanelli, R. Duchi, G. Tartari & K.M. Lau. (2010). Estimated impact of black carbon deposition during pre-monsoon season from Nepal Climate Observatory-Pyramid data and snow albedo changes over Himalayan glaciers. In: Special Issue "Atmospheric brown cloud in the Himalayas" Atmospheric Chemistry and Physics, 10: 6603-6615.